Diverse Coordination Motifs Leading to Supramolecular Architectures

A Thesis Submitted for the Degree of DOCTOR OF PHILOSOPHY

By Mukara Ramathulasamma



School of Chemistry

University of Hyderabad

Hyderabad

India

500046

September, 2022

Dedicated to
My Beloved Father

CONTENTS

	Page No.
Declaration	i
Certificate	ii
Acknowledgements	iii
Synopsis	v
Chapter 1. A General Outline on Metal-Organic Materials:	Introduction, Synthetic
Methods, Applications and Motivation of Present Work	
1.1. Introduction	1
1.2. Synthesis	3
1.2.1. Solvothermal Synthesis	4
1.2.2. Ionothermal Synthesis	5
1.2.3. Microwave-assisted Synthesis	6
1.2.4. Mechanochemical Synthesis	7
1.2.5. Electrochemical Synthesis	8
1.2.6. Sonochemical Synthesis	9
1.2.7. Post-synthetic modification (PSM)	9
1.3. Applications	11
1.3.1. Gas Absorption and Separation	11
1.3.2. Catalysis	13
1.3.3. Sensing	15
1.3.4. Proton conducting and magnetic materials	16
1.4. Motivation for the present thesis work	17
1.5. References	18
Chapter 2. Metallo-macrocycles from a library of flexible li	nkers: 1D cobalt (II
coordination polymers and a supramolecular pipe	
2.1. Introduction	26
2.2. Experimental	28

2.2.1. Materials and Physical Methods	28	
2.2.2. Characterization	28	
2.2.3. Synthesis	28	
2.2.4. Single Crystal X-ray Structure Determination of the		
Compounds 1–3	29	
2.3. Results and Discussion	30	
2.3.1. Description of Crystal Structures	30	
2.3.2. Electronic Spectra of Compounds 1–3	35	
2.3.3. PXRD and Thermogravimetric Analysis (TGA)	36	
2.4. Conclusion	38	
2.5. References	40	
Chapter 3. A 'two-in-one' crystal having two different dimensi	onality in the extended	
structures: A series of cadmium(II) coordination polymers from V-	shaped organic linkers	
3.1. Introduction	44	
3.2. Experimental	46	
3.2.1. Materials and Physical Methods	46	
3.2.2. Characterization	46	
3.2.3. Synthesis	47	
3.2.4. Single Crystal X-ray Structure Determination of the		
Compounds 1–3	48	
3.3. Result and Discussion	49	
3.3.1. Synthesis	49	
3.3.2. Description of Crystal Structures	49	
3.3.3. Powder X-ray Diffraction (PXRD) Patterns of the		
Compounds 1–3	57	
3.3.4. Thermogravimetric Analysis (TGA) Curves of the		
Compounds 1–3	57	
3.3.5. Electronic Spectra (DRS) of Compounds 1–3	58	
3.3.6. Gas Adsorption Analysis	59	
3.4. Conclusions and future scope	61	
3.5. References 63		

Chapter 4.	Diverse co	oordinati	on architec	tures based	d on a flexible m	nultidentate	carb	oxylate
ligand and	l N-donor	linkers:	synthesis,	structure,	supramolecular	chemistry	and	related
properties								

4.1. Introduction	67
4.2. Experimental	68
4.2.1. Materials and Physical Methods	68
4.2.2. Characterization	68
4.2.3. Synthesis	69
4.2.4. Single Crystal X-ray Structure Determination of the	
Compounds 1–3	70
4.3. Result and Discussion	70
4.3.1. Synthesis	70
4.3.2. Description of crystal structures	71
4.3.3. PXRD and Thermogravimetric Analysis (TGA)	75
4.3.4. Electronic Spectra of Compounds 1, 2 and 3	76
4.3.5. Gas Adsorption Analysis	77
4.4. Conclusions and Future Scope	79
4.5. References	81
Chapter 5. Coordination polymers from angular dicarboxylate-	and imidazol-ligands
synthesis, structure and supramolecular chemistry	
5.1. Introduction	85
5.2. Experimental	87
5.2.1. Materials and Physical Methods	87
5.2.2. Characterization	87
5.2.3. Synthesis	87
5.2.4. Single Crystal X-ray Structure Determination of the	
Compounds 1–4	89
5.3. Result and Discussion	89
5.3.1. Synthesis	89
5.3.2. Description of Crystal Structures	89
5.3.3. PXRD and Thermogravimetric Analysis (TGA)	95
5.3.4. Electronic Properties	97

5.4. Conclusion	98
5.5. References	100
Concluding Remarks and Future Scope	102
List of Publications	104
Posters and Presentations	105

DECLARATION

I, Mukara Ramathulasamma hereby declare that the matter embodied in the thesis "Diverse Coordination Motifs Leading to Supramolecular Architectures" is the result of my investigation carried out in School of Chemistry, University of Hyderabad, Hyderabad, India, under the supervision of Prof. Samar K. Das.

In keeping with the general practice of reporting scientific observations, due acknowledgements have been made wherever the work described is based on the findings of other investigators. Any omission, which might have occurred by oversight or error, is regretted. This research work is free from plagiarism. I hereby agree that my thesis can be deposited in Shodhganga/INFLIBNET. A report on plagiarism statistics from the University Library is enclosed.

Mukara Ramathulasamma

(12CHPH06)

S|CD M Prof. Samar K. Das | 5/09/2022

(Supervisor)

Prof. Samar K. Das School of Chemistry University of Hyderabad Vyderabad-500 046., INDIA. skdas@uohyd.ac.in



CERTIFICATE

This is to certify that the thesis entitled "Diverse Coordination Motifs Leading to Supramolecular Architectures" submitted by Mrs.Mukara Ramathulasamma bearing registration number 12CHPH06 in partial fulfillment of the requirements for award of Doctor of Philosophy in the School of Chemistry is a bonafide work carried out by her under my supervision and guidance.

This thesis is free from plagiarism and has not been submitted previously in part or in full to this or any other University or Institution for award of any degree or diploma.

Parts of this thesis have been published in the following publications:

- Paulami Manna, Mukara Ramathulasamma, Suresh Bommakanti, Samar K. Das, Polyhedron, 2018, 151, 394-400 (Chapter 2).
- Mukara Ramathulasamma, Suresh Bommakanti, Samar K. Das, Polyhedron, 2021, 210, Article No. 115508 (Chapter 3).
- 3. **Mukara Ramathulasamma**, Suresh Bommakanti and Samar K. Das*, Under review in *Polyhedron* (Chapter 4)
- 4. Mukara Ramathulasamma and Samar K. Das*, (to be communicated) (Chapter 5).

She has also participated in oral/poster presentations in the following conferences:

- 1. Poster presentation in CPCE-2020, Virtual National Conference-and NIT-Jamshedpur, India.
- 2. Oral presentation in CHEMFEST-2017, SoC, UoH, Hyderabad, India.

Further the student has passed the following courses towards fulfilment of coursework requirement for Ph.D.:

	Course	Title	Credits	Pass/Fail
1.	CY-801	Research Proposal	3	Pass
2.	CY-806	Instrumental Methods B	3	Pass
3.	CY-810	Basic Concepts in Coordination Chemistry	3	Pass
4.	CY-820	Main Group and Inner Transition Elements	3	Pass

Prof. Samar K. Das

Supervisor) 15/00/7/1

Dean

School of Chemistry

Prof. Samar K. Das

School of Chemistry
University of Hyderabad
''vderabad-500 046., INDIA.
skdas@uohyd.ac.in

P.O. Central University
Gachibowli, Hyderabad-500 046.

School of Chemistry

Acknowledgements

It is a great pleasure to take this opportunity to express my gratitude towards all the people who rendered their help and support during my research work.

It is with high regards and profound respect I wish to express my deep sense of gratitude to Prof. Samar K. Das, my supervisor. I owe it to him for his inspiring guidance, keen interest and encouragement throughout my thesis work. He has always been approachable, helpful and extremely patient. It has been a great privilege to obtain the opportunity to associate with him.

I acknowledge my sincere regards to Prof. Ashwini Kumar Nangia, Dean, School of Chemistry, for providing the facilities need for research. I extend my sincere thanks to former Deans and all the faculty members, School of Chemistry for co-operation on various aspects.

I consider myself prized enough to have polite and well-mannered lab seniors Dr. Supriya, Dr. Tamany, Dr. Ramababu, Dr. Durga Prasad, Dr. Srinivasas, Dr. Monima, Dr. Kishore, Dr. Sridevi, Dr. Krishna. I am grateful to my seniors Dr. T. Bharat Kumar and Dr. Paulami Manna for their guidance on my work from the first day to till the end. I wish to thank my labmates, Dr. Ramakrishna, Dr. Suresh, Dr. Sateesh, Pradeep, Olivia and my juniors Dr. Subhabrata, Dr. Chandani, Dr. Tanmaya Kumar, Joycy, Olivia, Hema, Debu Jana, Athira Ravi, Parvathi, Gopika, Rameshwari, Florance, for their love and support. I am also thankful to Dr. Joyashish, Dr. Suranjana, Dr. Girijesh, Dr. N. Veerareddy, Dr. K. Pratap, Dr. K. Sathish Kumar, Dr. M. Pradeep Kumar, Dr. Rajendar and Dr. Pinki for enriching the lab atmosphere with their support. A special token of thank to Raju Mekala, Ashan, Suman and Manaswitha for their pleasant presence.

I am also lucky enough to have the support of many School of Chemistry friends and colleagues, specially, Dr. Narendrababu, Dr. Swapna.

I am indeed fortunate to have friends in my life over the years like Dr. Suresh, Dr. Sateesh.

I also thank all the non-teaching staff/instrument operators of the School of Chemistry for their assistance on various occasions. I thank DST funded National Single Crystal X-ray Diffraction Facility, UGC/ UPE for providing the basic requirements, UGC and IoE for the financial support.

Looking back finally I kneel down to my Family: grandmother, M Rangamma and my parents; Mr. M. Venkateswara Rao and Mrs. M. Santhamma, my in-laws; Mr. Gopa Raju and Mrs. Revathi, Babai and pinny; Prof. K. Venkatarjun and K. Seetha, whom I adore most for

their love, blessing and confidence on me in building the very platform of my life. Also I express my love to my younger brother and sister; Neageswara Rao and Nagalakshmi, for their immeasurable affection. I feel fortunate to have my wonderful husband, B. Veerama Raju, with his imperative support from all the respect and my lovely babies, Yashaswi and Jhanavi, for their cheering environment in home.

And at last but not the least, those who are distant but close to my soul, accompanying me time to time when I am facing the odd, make me laugh, sharing my grief and cherishing my joy, will always be remembered by me.

Ramathulasamma

University of Hyderabad August, 2019.

SYNOPSIS

Architectures" consists of five chapters followed by concluding remarks and future scope. The titles of the chapters are named as: (1) A General Outline on Metal—Organic Materials: Introduction, Synthetic Methods, Applications and Motivation of Present Work, (2) Metallo-macrocycles from a Library of Flexible Linkers: 1D Cobalt (II) Coordination Polymers and a Supramolecular Pipe, (3) A 'Two-In-One' Crystal Having Two Different Dimensionality in the Extended Structures: A Series of Cadmium(II) Coordination Polymers from V-shaped Organic Linkers, (4) Diverse coordination architectures based on a flexible multidentate carboxylate ligand and N-donor linkers: synthesis, structure, supramolecular chemistry and related properties (5) Coordination Polymers from Angular Dicarboxylate- and Imidazol-Ligands: Synthesis, Structure and Supramolecular Chemistry

Each chapter is sub-divided into three parts. The first chapter *i.e.*, Introduction, consists of (a) Design, (b) Applications, and (c) Motivation of the present work. All other chapters (Chapter 2–5) consist of (a) Experimental Section, (b) Results and Discussion, and (c) Conclusions. The compounds, presented in this thesis work, are generally characterized by powder X-ray diffraction (PXRD) studies, IR spectral studies, CHNS analyses, thermogravimetric analysis (TGA) and solid-state UV-visible spectroscopy (UV-DRS), and of course unambiguously characterized by single crystal X-ray diffraction (SCXRD) studies.

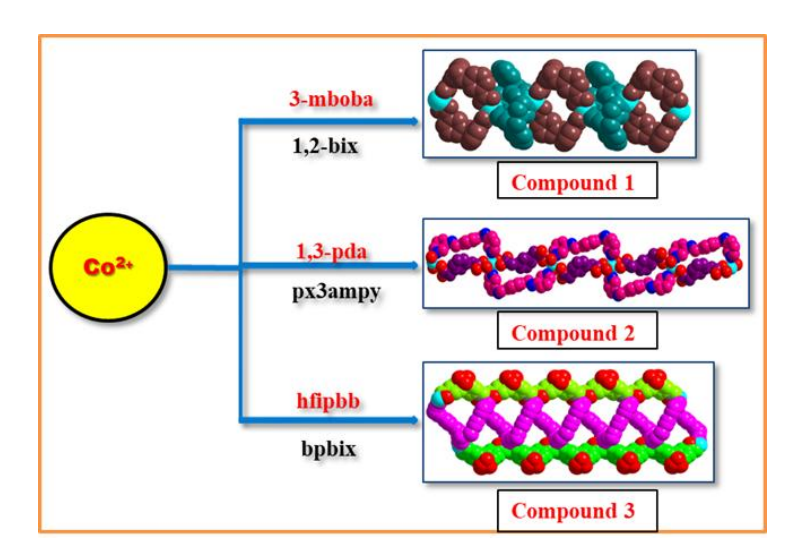
Chapter 1

A General Outline on Metal-Organic Materials: Introduction, Design, Applications and Motivation of the Present Work

This chapter starts with more basic knowledge about metal-organic materials (MOMs) and the relevant research progress has been discussed mainly under four sections: (1) a brief introduction, history and the evolution of these functional materials; (2) the design and synthesis of inorganic-organic hybrid materials by different methodologies/strategies, such as, solvothermal, ionothermal, microwave-assisted synthesis, mechanochemical, electrochemical synthesis, sonochemical and Post-synthetic modification (PSM) and; (3) the potential applications of metal-organic coordination polymers in the fields of gas

absorption and separation, catalysis, sensing and biomedicine; and (4) the motivation to study the crystal engineering leading to metal-organic coordination polymers, based on flexible and rigid ligands. The main objectives of the thesis work are then conversed briefly.

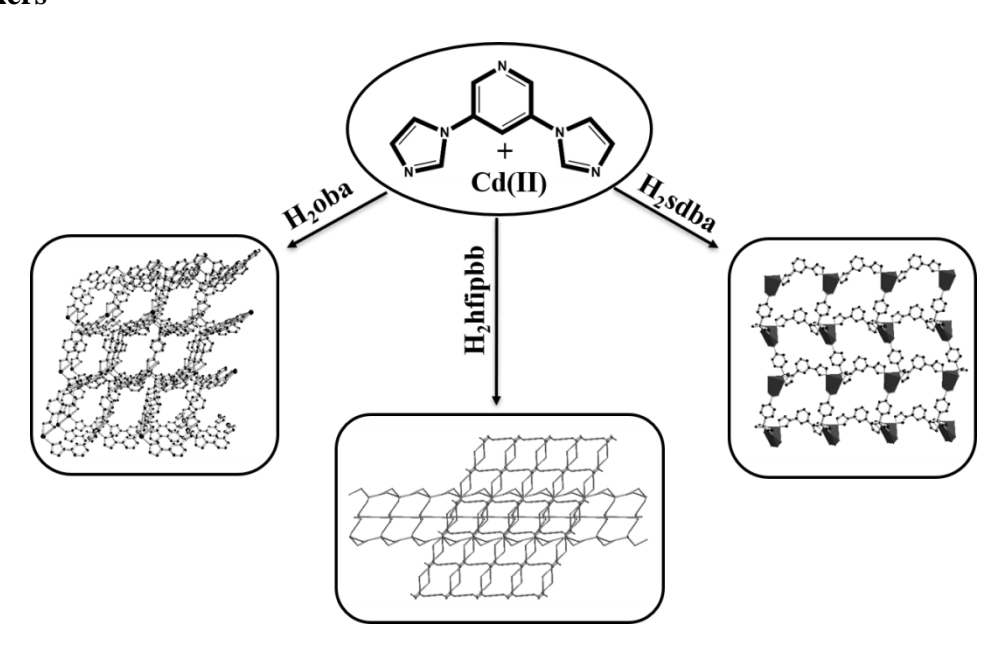
Chapter 2
Metallo-macrocycles from a Library of Flexible Linkers: 1D Cobalt(II) Coordination Polymers and a Supramolecular Pipe



This chapter includes three cobalt(II) coordination polymers containing compounds $\{Co(3-mboba)(1,2-bix)_2\}_n$ $\{Co_2(1,3-pda)(px3ampy)(H_2O)_2\}_n$ (1),(2), $\{Co_2(hfipbb)_2(bpbix)_2\}_n$ (3), that are formed from three different bent carboxylic acids [3,3'-methylenebis(oxy)dibenzoic acid (3-H₂mboba), 2,2'-(1,3 phenylene)diacetic acid (1,3-H₂pda) and 4,4'-(perfluoropropane-2,2-diyl)dibenzoic acid (H₂hfipbb)] as primary ligands and three different {N,N}-donor linkers [1,2-bis((1H-imidazol-1 dipyridin-3-amine yl)methyl)benzene(1,2-bix), N,N'-(1,4-phenylenebis(methylene)) (px3ampy) and 4,4'-bis((1H-imidazol-1-yl)methyl)biphenyl (bpbix)] as secondary ligands, under hydrothermal conditions. Compounds 1-3 are characterized by single crystal X-ray diffraction analysis, IR spectroscopy, thermogravimetric (TG) and elemental analysis. Single crystal X-ray crystallography shows that diverse metallo-macrocycles are formed in compounds 1, 2 and 3. In the crystal structure of compound 1, two different metallomacrocyles, 28-membered metal-acid {Co₂(3-mboba)₂} ring and 24-membered metal-Nlinker $\{Co_2(1,2-bix)_2\}$ ring, are formed. The alternative arrangement of these macrocylic rings leads to the formation of 1D chainlike coordination polymer (compound 1). In the crystal of compound 2, a 25-membered macrocycle ring {Co(1,3-pda)(px3ampy)} is formed from one dicarboxylic acid lignad and one {N,N}ligand, which further undergoes coordination with itself resulting in the formation of 1D chain. The {Co₃(hfipbb)(bpbix)₂} metallomacrocycle, observed in the crystal structure of compound 3, is more diversified in the sense that it is relatively bigger in size and this trinuclear metallo-macrocycle is formed by one dicaryboxylic acid ligand and two {N,N} donor linkers, but not in a plane. Interestingly, the inter-linking of these non-planar macrocycles results in the construction of a supramolecular pipe.

Chapter 3

A 'Two-In-One' Crystal Having Two Different Dimensionality in the Extended Structures: A Series of Cadmium(II) Coordination Polymers from V-shaped Organic Linkers

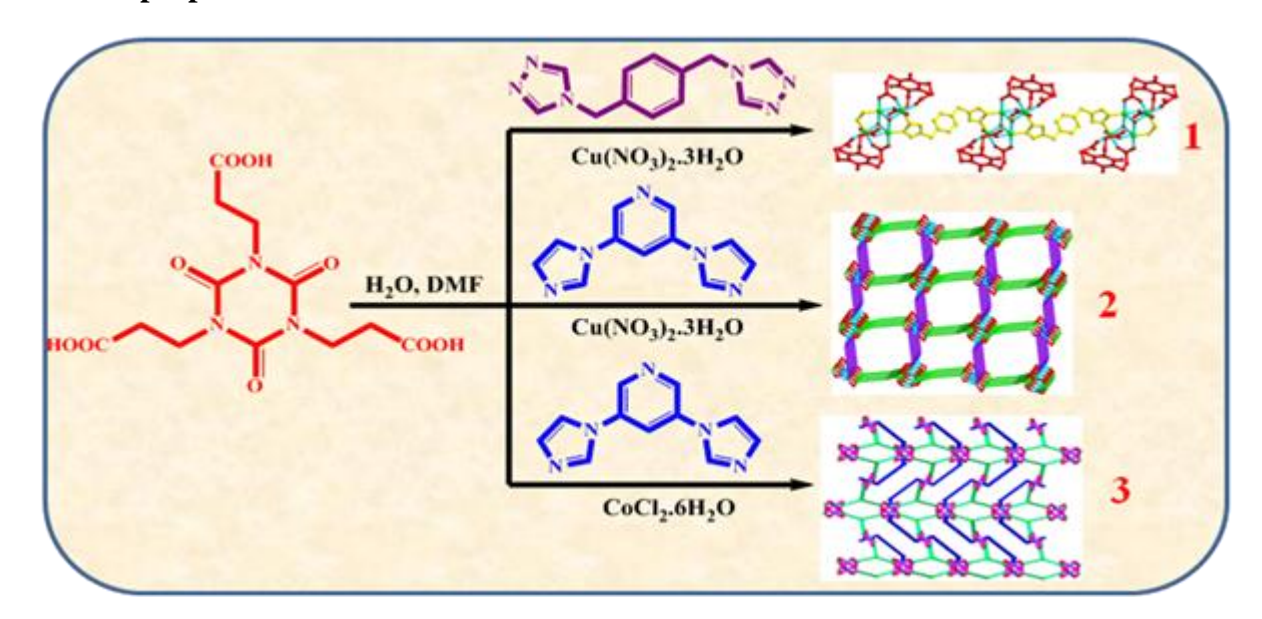


In this chapter, three Cd(II) containing coordination polymers, formulated as $\{Cd(oba)(biip)\}_n \cdot nH_2O$ (1), $\{Cd(sdba)(biip)\}_n \cdot n5H_2O$ (2) and $\{[Cd_{1.5}(hfipbb)_2(biip)_{1.5}(H_2O)][Cd(hfipbb)(biip)]\}_n \cdot n2H_2O$ (3), have been described that were synthesized by using ditopic V-shaped ligands *i.e.*, H_2oba (4,4'-oxydibenzoic acid), H_2sdba (4,4'-thiodibenzoic acid), $H_2hfipbb$ {4,4'-(perfluoropropane-2,2-diyl)dibenzoic acid} and an auxiliary linker, biip {3,5-di(1H-imidazol-1-yl)pyridine} under solvothermal conditions. Compounds 1–3 are unambiguously characterized by single crystal X-ray

diffraction analysis, IR spectroscopy, thermogravimetric (TG) and elemental analyses. Compound 1 contains a 3D framework, formed by the connectivity of $\{CdO_4N_2\}$ secondary building unit (SBU) with the organic linkers, whereas compound 2 is a 2D coordination polymer. Interestingly, unlike compounds 1 and 2, compound 3 possesses a distinctive structural feature having two crystallographically independent polymeric motifs (polymers, A and B) having two different dimensionality within the same crystal, *i.e.*, coordination polymer A (CP-A) that forms a one-dimensional motif and coordination polymer B (CP-B), which has a two-dimensional structure.

Chapter 4

Diverse coordination architectures based on a flexible multidentate carboxylate ligand and N-donor linkers: synthesis, structure, supramolecular chemistry and related properties



This chapter describes three new metal-organic framework (MOF) containing compounds, namely $\{Cu_2(tci)(btx)_{0.5}(\mu_3\text{-OH})(H_2O)\}_n$ (1), $\{Cu_{1.5}(tci)(biip)\}_n$ (2), $\{Co_{1.5}(tci)(biip)\}_n$ (3) $[H_3tci=tris(2\text{-carboxyethyl})isocyanurate, btx=1,4\text{-bis}(triazol-1\text{-yl-methyl})benzene, biip = 3,5\text{-bis}(imidazole-1\text{-yl})pyridine] have been successfully synthesized through the assembly of metal ions <math>[Cu(II)$ ion for compounds 1 and 2, Co(II) for compound 3] with H_3tci and two different N-donor ligands under solvothermal conditions. All compounds were characterized by IR spectroscopy, elemental and thermogravimetric (TG) analyses, powder X-ray diffraction (PXRD) studies and finally, the structures of all compounds

were unambiguously determined by single-crystal X-ray diffraction (SCXRD) technique. Compound **1** is a 1D coordination polymer, constructed by the connectivity of copper tetramer as a secondary building unit (SBU) with the H₃tci and btx ligands. Whereas the crystal structure of compound **2** possesses two different SBUs *i.e.*, paddlewheel and square involving Cu(II). The connectivity of these two SBUs results in the formation of 2D layers which are further pillared by biip ligand to result in a 3D structure. In the case of compound **3**, both Co1 and Co2 exhibit distorted octahedral geometry in their SBUs. Further, the connectivity of these SBUs with tci³⁻ and biip ligands results in the formation of a 3D framework.

Chapter 5

Coordination Polymers from Angular Dicarboxylate- and Imidazol-Ligands: Synthesis, Structure and Supramolecular Chemistry

$$\{(Co)(ADA)_2(biip)\}_n \text{ (4)} \qquad \begin{array}{c} Co(II) \\ \hline H_2ADA \end{array}$$

$$\{Co(ADC)(biip)(H_2O)\}_n \text{ (3)} \qquad \begin{array}{c} Co(II) \\ \hline H_2ADC \end{array}$$

$$\begin{array}{c} Cu(II) \\ \hline H_2ADA \end{array}$$

$$\begin{array}{c} Cu(II) \\ \hline H_2ADA \end{array}$$

$$\begin{array}{c} Co(II) \\ \hline H_2SDBA \end{array}$$

$$\{[(Co)(sdba)(biip)]_2\}_n \cdot 6nH_2O \text{ (2)}$$

This chapter has depicted four coordination polymers- / metal-organic frameworkscontaining four compounds, formulated $\{Cu_2(ADA)_2(biip)\}_n.4nH_2O$ as (1), $\{[(Co)(sdba)(biip)]_2\}_n.4nH_2O$ $\{Co(ADC)(biip)(H_2O)\}_n$ (2),**(3)** and $\{(Co)(ADAH)_2(biip)\}_n$ (4), have been synthesized by using flexible as well as rigid 1,3-adamantanediacetic acid; $H_2ADA =$ H₂ADC adamantanedicarboxylic acid; H₂sdba (4,4'-thiodibenzoic acid) and an secondary linker, biip {3,5-di(1H-imidazol-1- yl)pyridine} under solvothermal conditions. Compounds 1-4 have been well characterised by IR spectroscopy, single crystal X-ray diffraction analysis, thermogravimetric (TG) and elemental analyses. Compound 1 is 3D structure, formed by the connectivity of two different 2D- and 1D-metal-acid chains through the biip linkers. In the crystal structure of compound 2, one dimensional square wave-like chains are formed by the coordination of Co(II) with sdba²⁻ ligands and these chains are further connected by the biip ligand, leading to the formation of a 2D structure. The crystal structure of compound **3** consists of 2D sheets, constructed by the connectivity of Co(II) with N,N-linker and dicarboxylate ligand. In the crystal structure of compound **4**, two altered metallo-macrocyles, 20-membered metal—acid {Co₂(ADA)₂} ring and another 20-membered metal-N-linker {Co₂(biip)₂} ring, are formed, and these macrocylic-rings are arranged alternatively, leading to the formation of a new 1D extended coordination polymer. The related supramolecular chemistry has been discussed for all four compounds.

Concluding Remarks and Future Scope

The last section of this thesis describes summary of the whole thesis work and future scope of this work. The MOFs containing compounds, synthesized and characterized in this thesis work, can be explored for important applications, *e.g.*, energy related applications — this application part will mainly be discussed in the future scope of this thesis.

Introduction to Metal-Organic Framework (MOF) Materials: Fabrication, Applicability and Inspiration of Current Work

Fundamentally, coordination polymers (CPs) and Metal-organic frameworks (MOFs) are fascinating and promising class of organic-inorganic crystalline micro-/meso-porous hybrid materials with a huge range of potential applications. These materials have unique properties and ensnared substantial attention because of their aesthetically pleasing structures, unique characteristics of ultrahigh porosity, large surface area and tunable pore sizes. This chapter begins with more basic knowledge about metal-organic materials (MOMs) and gives a brief summary on synthetic techniques and applications, finally concludes with the motivation of the present work.

1.1. Introduction

Coordination Polymers (CPs), a tale addition set of periodic architectures, in which inorganic metal entities (**d**- and/or **f**-block metal ions/clusters) are associated by the organic linkers (multi-dentate organic ligands) through strong coordination bonds. CPs can be existent in one-dimension (x-direction) such as chains/ladders/loops etc., in two-dimensions (x and y-directions) as bilayers/sheets etc. or in three-dimension (3D) (x, y and z-direction) by the coordination bonds depending on the directions. MOFs are generally classified as a subcategory of porous crystalline 3D CP networks, built from metal nodes bridged by organic linkers. Being synonymously termed as porous coordination polymers (PCPs)¹ or porous coordination networks (PCNs)², they have been emerging as a notable class of a porous crystalline compounds.³ The metal ions/metal clusters acting as a nodes (SBUs) consist of transition metals, inner transition metals, whereas the organic ligands, such as carboxylates, phosphates, sulfonates, nitrogenous ligands, e.g., azolates (imidazole, triazoles, tetrazoles), pyridine derivatives, mixed ligand systems, terminal aromatic chelating ligands, *etc.* act as the linkers (organic building units).

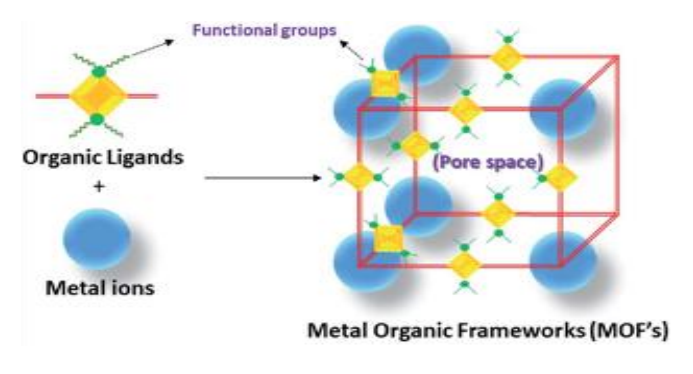


Figure 1.1. General Scheme of constructing a MOF.

Copious amount of work done on MOFs in recent years which projected them as attractive materials in various fields due to their unique, adjustable chemical and physical properties. A general scheme of constructing a MOF is shown in Figure 1.1. Though there are numerous MOF synthetic procedures presented in literature, solvothermal route (patented by Yaghi and his group⁴) has been found to be one of the widely used and efficient methods. Metal—organic frameworks (MOFs) have become the front-runner among advanced materials. CPs and MOFs have been researched with ever-increasing hop since their discovery early in the 1990s.⁵

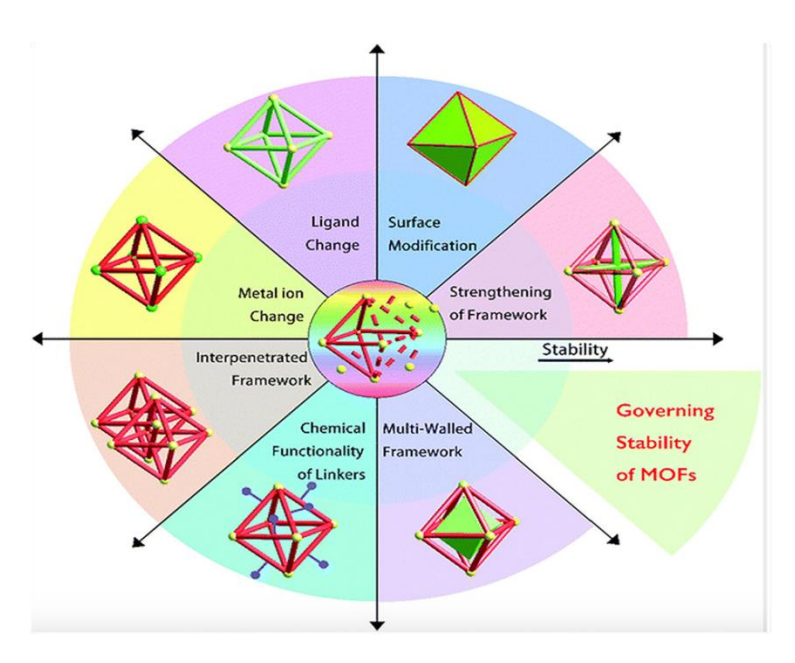


Figure 1.2. Schematic drawing of several strategies to govern the stability of MOFs.⁶

These materials have fascinated substantial attention, because of their (i) aesthetically pleasing structures, (ii) extremely high porosity and (iii) BET surface area up to 7×10^3 m²/g, ⁷ (iv) tuneable pores (size and/or shape), (v) flexible internal surface and (vi) optical nature. The above descriptions project MOFs as one of the best class of functional materials e.g. drug delivery, ⁸ gas storage ^{9,10} and separation, ¹¹ proton conductivity, ^{12,13} catalysis, ^{14,15} adsorption of ions, ¹⁶ and as sensors. ^{17,18} There are several factors to govern the stability of MOFs as shown in Figure 1.2. The chemical and structural characteristic of ligands (primary and secondary) has been found to be playing vital role in fabricating targeted functional CPs/MOFs. Following properties of ligands can alter the geometry and properties of MOF,

- distance between binding sites influences spacing between metal nodes,
- ligand flexibility and rigidity

- they can attribute multifunctional behaviour to MOF
- orientation of binding sites and variable binding modes alter geometry and functionality of the MOF.

Several MOFs endure reversible structural transformation in response to external stimuli, such as, change in temperature, guest adsorption, mechanical pressure, light irradiation and also nature of the metal, termed as simply flexible MOFs/dynamic MOFs. Generally, dynamic/flexible MOFs tend to undergo structural changes on removal of guest (in general solvent)molecules, but, on gaseous guest adsorption at high pressure, it retains its porous structure, ¹⁹ for example MOF-5, ^{20,21} MIL-8, ²² SNU-M10; ²³ these exhibit breathing effect through adsorption and desorption. On the other hand there are a few rigid MOF systems which hold their framework structure intact on reversible guest adsorption and desorption, and they can be utilized as molecular sieves. ²⁴ It was observed that, presence of water on open metal site enhances the CO₂ absorption ability of the MOF e.g. {(Cu)₃(btc)₂(H₂O)} [HKUST-1] with paddlewheel Cu₂(COO') nodes bridged by btc³⁻ linkers revealed to have enhanced CO₂ absorption ability which was attributed to the presence of 4% water. ²⁵ Studies have also revealed that grafting of Arylamine, ²⁶ alkylamine, ²⁷ hydroxyl²⁸ groups on to porous framework surface during ligation of linker to open metal center, enhances not only the CO₂ absorption ability but also its selectivity.

1.2. Synthesis

Several methodologies have been developed for synthesis of MOFs (Figure 1.3). Synthetic methodologies are majorly divided into two groups: conventional and alternative methods²⁹. In the conventional synthetic method, reactions are carried out using traditional electronic heating or without heating. Since the MOFs are made by metal ion/metal clusters and organic ligands through coordination bonds, there are several parameters *viz.* solvent type, pH, concentration of metal ion in addition to procedural parameters like time, pressure, temperature of reaction mixture, *etc* affect the MOF structure in simple conventional synthesis. The choice of the solvent, which is difficult for the synthesis of a MOF with better characteristics, is important. The synthesis of a MOF containing compound depends on different factors, e.g., redox potential, reactivity, stability constant and solubility of the concerned reactants.

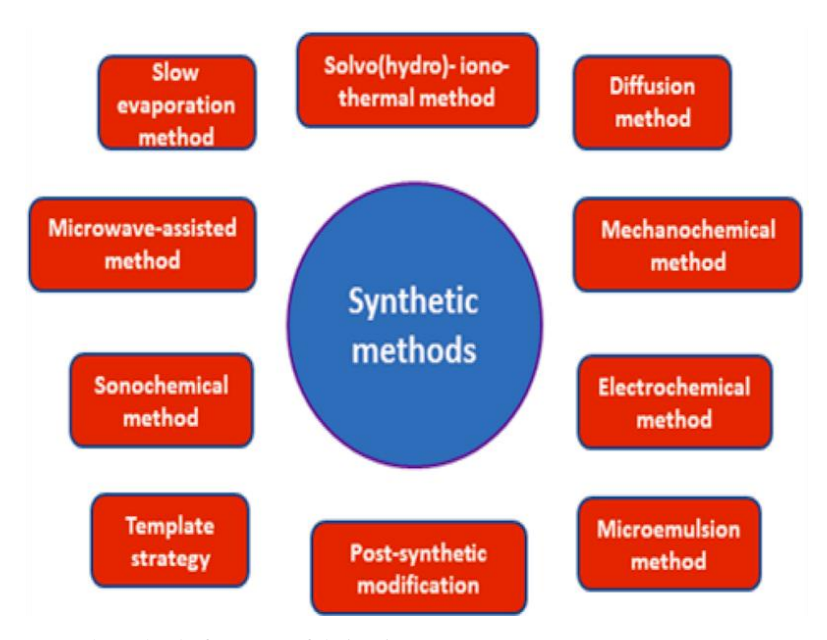


Figure 1.3. General methods for MOF fabrication.

1.2.1. Solvothermal Synthesis

Solvothermal method is a common recurrently procedure to accelerate the innovation of novel coordination polymers and MOFs. This is a conventional synthetic method, carried out in a closed reaction vessel (teflon-lined autoclave). The reaction is performed generally at temperatures higher than boiling point of respective solvent systems (in the range of 80–260 ^oC) and under auto-generated pressure. Syntheses were water is used as solvent, and then it is called hydrothermal synthesis. In the beginning, this method was used for the synthesis of zeolites, but later on it is widely adopted for synthesis of the MOFs/CPs. Yaghi and coworkers³⁰ utilised reticular chemistry to synthesize ZIF-8 MOFs in hydro/solvo-thermal synthesis by linker functionalisation, examining the structure direction and crystal growth control. These factors are important for the reticular MOF synthesis from metal centres and linkers.31 Afterwards, other research groups analyzed various other factors, like, Howarth et al^{32} recognized that the hydrothermal process demands for the mixing of metal salts in solvents followed by a heating period to improve MOF crystal structures. Certain factors in the reaction, like, pH, temperature & pressure, concentration of reaction mixture, time period, including solubility of reagents, etc play significant role on the crystallization process during the synthesis of MOFs/CPs. Among these factors, synthesis temperature, concentration of the reactants and pH of the solution are particularly important. DMF (dimethyl formamide), DEF (diethyl formamide), acetonitrile, acetone, methanol, ethanol are some of the most often used solvents solvo/hydrothermal method. In common, the temperature of the process is determined by the time with which the crystallization process happens. Removal of solvent

molecules, which is usually a complex process, is achieved by vaccum drying/washing with several solvents like, methanol, ethanol and followed by ether. The major advantage of this method is higher yield of the products. This technique controls the shape distribution, crystallinity of MOF material, and size of the MOF. Table 1.1 has listed some known MOFs that are synthesized by solvothermal synthesis method.

Table 1.1. List of some of the well-known MOFs/CPs synthesized by solvothermal method.

MOF	Precursors	Remarks	Ref
ZIF-8	Zn(NO ₃) ₂ , 2-methylimidazole, tea	1340 m ² /g surface area thermally stable	33
NH ₂ -UiO-66	ZrCl ₄ , 2-aminoterephthalic acid	CO ₂ reduction	34
HKUST-1	Trimesic acid, Cu(NO ₃) ₂ .2.5H ₂ O	Removal of dye	35
MIL-125(Ti)	Terephthalic acid, titanium isopropoxide	High surface area, storage capacity of H ₂	36
MOF-5 [(Zn ₄ O(BDC) ₃) _n]	Zn(NO ₃) ₂ .4H ₂ O, Terephthalic acid	Methane storage	37

1.2.2. Ionothermal synthesis

The ionothermal synthesis is the conventional synthetic process. This technique uses ionic liquids/deep eutectic solvents rather than organic solvents at room temperature in the production of MOFs/CPs. Cooper *et al.* reported a new method, referred to as ionothermal method to synthesize zeolites and porous materials in 2004. In 2008, Bu *et al.* invented the preparation of a series of MOFs using the ionic liquids as solvent/template. In this technique ILs/DESs serve as (i) solvents, (ii) structure directing agents and (iii) environment-friendly reagents; moreover, in this method, both anion and cation complexes function as charge-compensating templates. The ionothermal synthesis can be well thought-out as a subclass of solventmal technique. ILs attract excellent reagents because of their high thermal stability, low vapour pressure, nonflammability, non-volatilaty and high solubility for organic solvents. The majority of the ionothermal methods for MOFs' synthesis include ionic liquids which are acquired from1-alkyl-3- methylimidazolium.

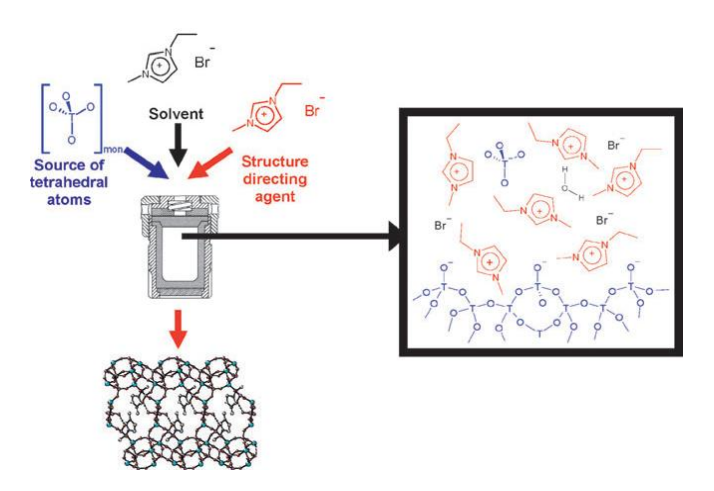


Figure 1.4. Schematic representations of synthesis of a tetrahedral (zeotype) framework under ionothermal condition.

The ionic liquid, 1-ethyl-3-methylimidazolium ([EMIM] Br) bromide is used as a solvent in the synthesis of a 3D MOF, $\{[EMIM][In_3(\mu_3-OH)_2L_2.2H_2O]\}_n$ based on 1,2,4,5-benzenetetracarboxylate (L).⁴¹ The inorganic chain $[In_3(\mu_3-OH)_2]_n$ in the polymer, is formed by the connectivity of pentagonal In(1) and octahedral In(2) with the μ_3 -OH groups. These $[In_3(\mu_3-OH)_2]_n$ inorganic chains are further connected by ligand L along with a axis, leading to the formation of 3D framework anion.

1.2.3. Microwave-assisted synthesis

Microwave (MW) synthesis methods have been used for the synthesis of nano-porous inorganic and organic materials, including MOFs as well as metal cluster containing compounds. The main advantage of this method is the short reaction time. For example, Cr-MIL-100 was the first MOF^{42} synthesized under microwave irradiation within 4 hours at 220 °C with 44% yield, which can be obtained by conventional hydrothermal method in 4 days at 220 °C. The benefits of this method are (i) tiny particle size distribution, (ii) swift crystallization, (iii) phase selectivity, (iv) facile morphology control, (v) high yield and (vi) low cost. Normally, MOFs can be produced swiftly by MW irradiation, whereas in conventional way, heating solvent (by electrical means) increases the crystal nucleation rate. Schlesinger and his co-workers⁴³ prepared the microwave-assisted synthesis of HKUST-1 (within a short time of 30 minutes) with formula $[Cu_3(BTC)_2(H_2O)_3]$ (BTC³⁻ = 1,3,5-benzenetricarboxylate) having BET surface area up to 1499 m²g⁻¹ and a specific pore volume of 0.79 m²g⁻¹. As revealed in Figure 1.5.,

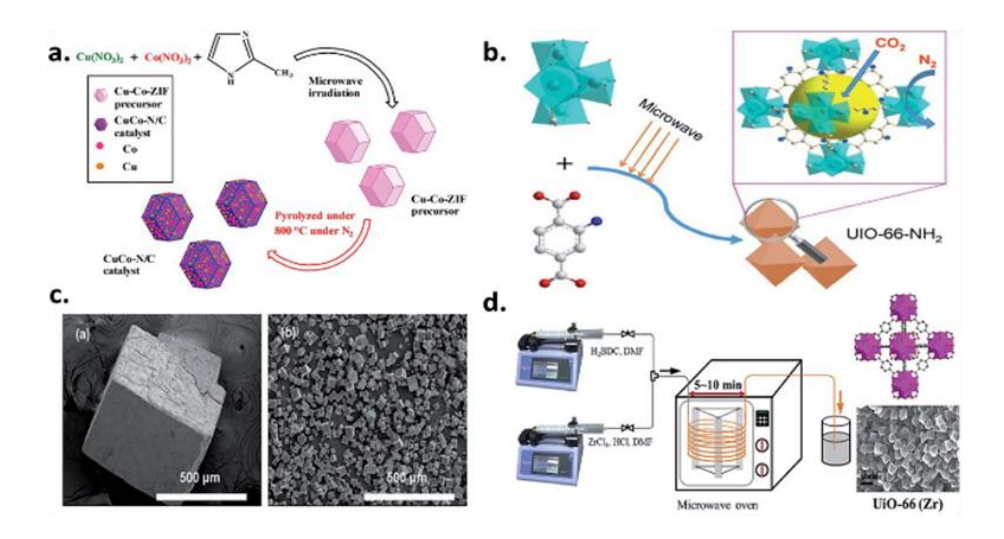


Figure 1.5.(a) Schematic representation for the synthesis of MOFs using microwaves and catalyst, CuCo– N/C; (b) UiO-66-NH₂ MOFs with better adsorption capacity; (c) SEM images of MOF- and (d) synthesis of UiO-66-based MOFs in large-quantity by microwave process.

Uio-66-based MOFs with diverse properties can afterwards be tailored using functionalized process and a wide range of prospects can be explored, for example, the crystallisation time for UiO-66-NH₂ MOFs was shortened by Huang*etal*⁴⁴ employing the microwave heating within 30 min with improved crystallinity. A good thermal stability up to a temperature of 400 °C along with good adsorption capacity and selectivity were achieved. IRMOF-1 was synthesized by microwave-assisted method; it exhibited higher quality of crystals and better CO₂ adsorption property when compared to other synthesis methods, e.g., solvo(hydro)thermal, mechanochemical methods *etc*.

.

1.2.4. Mechanochemical Synthesis

Mechanochemical approach, normally engages the mechanical force to breakage of intramolecular bonds for completion of chemical reaction. This technique is an environmentally friendly, economical and simple without using any organic solvents, which are frequently harmful, carcinogenic and toxic. In this process, organic linkers and metal oxides are used many times instead of metal salts to avoid other by-products except water. After grinding in a mortar pestle or in a mechanical ball mill, the solid mixture is heated compassionately to evaporate water or other volatile molecules for the production of MOFs. Mechanochemical synthesis was first reported by Pichon and his team⁴⁵ in 2006. Depending on solvent, this method is divided into three types for the synthesis of MOFs: (i) neat or dry

solvents for the production of MOFs, (ii) liquid-assisted grinding (LAG)—in this method, a catalytic amount of liquid is added for increasing mobility of reagents of mechanochemical reactions, (iii) ion-and-liquid assisted grinding (ILAG) — a process in which a catalytic amount of liquid with traces of salt are generally added into the solid reaction mixture; this process is very well-organized, especially for the construction of pillared-layered MOFs. ⁴⁶ Mechanochemical synthesis is an attractive method for the production of 1D, 2D and 3D coordination polymers. ⁴⁷ The drawback of this method is mainly the separation of amorphous by-products which are not suitable for single-crystal X-ray studies.

1.2.5. Electrochemical synthesis

Electrochemical synthesis was first reported by researchers at BASF⁴⁸ in 2005 for the production of MOFs using Zn, Cu, Mg, Co as cathode materials and 1,3,5-H₃BTC, 1,2,3-H₃BTC, H₂BDC and H₂BDC-(OH)₂ as ligands. In electrochemical technique, two electrodes including a glass reactor are involved, known as galvanic cells. Metal ions were used in the place of metal salts in this technique and these metal ions are provided through anodic dissolution as a metal source into the reaction mixture consisting of organic ligands and electrolytes. Numerous MOFs, HKUST-1, ZIF-8, ZIF-100(Al), MIL-53(Al), NH₂-MIL-53(Al) were synthesized by anodic dissolution in an electrochemical cell, as reported by Gascon *et al.*⁴⁹ The main advantages of this process are: (i) it takes shorter reaction time,(ii) reactions take place very fast under milder conditions, (iii) anions associated with metal cation in metal salts can be avoided, (iv) it controls the reaction rate, and (v) high temperature is not needed.

Table 1.2. List of some known MOFs synthesized by electrochemical method

Metal Organic Frameworks (MOFs)	Comments	Ref
MOF-199	Fast synthesis	50
DMOF-1–Zn	Fast synthesis	51
$[Cu_3(BTC)_2(H_2O)_3]_n$	high-quality crystals	52
MOF-5	Novel with flower-like morphology	53

The major drawback in electrochemical mode of synthesis is regular involvement of organic solvents to dissolve the organic building blocks in the construction of MOFs. Table 1.2 has listed a series of MOFs that have been synthesized by the electrochemical method.

1.2.6. Sonochemical synthesis

The source of sonochemical process is ultrasonic radiation (20 kHz-10 MHz) used for the production of MOFs within the short reaction time. This is usually rapid, economical, and easily reproducible and can be done in homogeneous manner. This method accelerates nucleations which reduce the particle size and crystallization time of the constructed MOFs. The bubbles/foams are formed when the reaction mixture is introduced into a horn-type Pyrex reactor fitted with a sonicator under high temperature (\approx 5000K) and pressure (\approx 1000 bar) without any external cooling, which endorse chemical reactions into the formation of nuclei abruptly leading to crystallization. A MOF [Zn₃(BTC)₂], was first synthesized in the sonochemical method by Qiu*et al.*⁵⁴ by using zinc acetate and trimesic acid at room temperature. High quality crystals of MOF-5⁵⁵ and MOF-177⁵⁶ are produced by this method (sizes: 5–25 µm and 5–20 µm, respectively) in the presence of 1-methyl-2-pyrrolidone (NMP) as a solvent. Representative MOFs that are synthesized by sonochemical method have been listed in Table 1.3.

Table 1.3. List of some known MOFs synthesized by sonochemical method.

Metal Organic Frameworks (MOFs)	Comments	Ref
$[Zn_3(BTC)_2]$	sensing	57
MOF-177	Short reaction time	54
HKUST-1	rapid synthesis at room temperature	58
IRMOF-9 and -10	CO ₂ adsorption	59
[Ln(BTC)(H_2O)] (Ln = Ce, Tb, Y)	Short reaction time	60

1.2.7. Post-synthetic modification (PSM)

Post-synthetic modification (PSM) is a powerful technique that involves single-crystal to single-crystal (sc-sc) transformations with modification of the side groups in pores or on exterior of MOF structures. Designing and obtaining the desired MOFs/CPs with PSM process occur through functionalisation of MOFs, metal-ligand exchange, *etc.*; it results in improved surface area, high crystallinity, porosity, thermal and chemical stabilities, ^{61,62} compared to parent MOFs. The ligand functional groups, metal ions, and inner free space are the main sites that are available for functionalisation of desired structures. Three different types of PSMs can be possible: covalent PSM, dative PSM and de-protected PSM as shown in Figure 1.6. Covalent PSM route is used for the hybridisation of MOFs to obtain a post

synthetically modified MOF with desired properties, e.g., porosity, catalysis, *etc.* PSP (post-synthetic polymerisation) was first conducted by Wang and co-workers⁶³ on UiO-66-NH₂ in 2015. In this process, methacrylic anhydride was introduced on amine group of UiO-66-NH₂

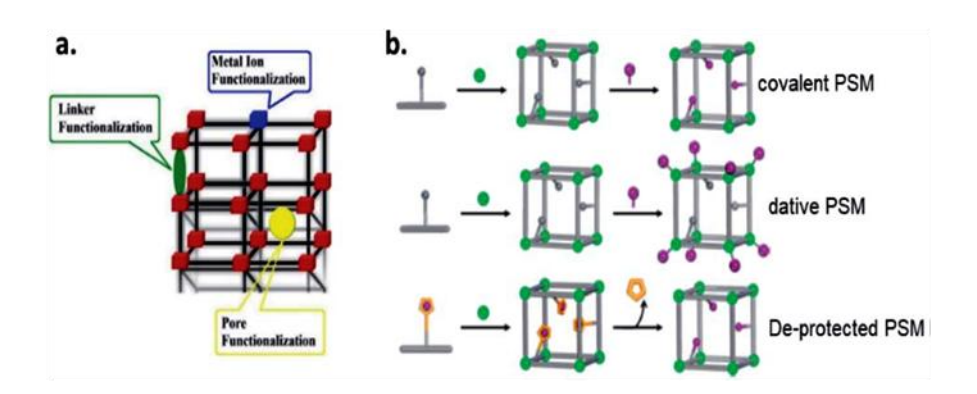


Figure 1.6. (a) Different constituent parts of MOFs which are targeted for functionalization and (b) different approaches for PSM; covalent, dative, and de-protected PSM.

to result in MOF, UiO-66-NH₂-Met containing methacrylamide. The de-protected PSM approach uses functional groups on the ligands as de-protected; after successful de-protected PSM, these functional groups on ligands get converted to new functional groups, which can inherit different characteristics in comparison to those of the parent MOFs. The technique rivets the elimination of intricacy in MOFs resulting in large cavities, sometimes also called the protection, complexation and de-protection.⁶⁴ De-protection and protection processes open new and more possibilities for the "unlock" of confined functionalities for construction of active coordinating fragments on MOFs, which are very useful in metal-organic catalysis. 65 On the other hand, the metal sources to the MOFs trusses with organic linkers, resulting in the formation of dative bond. Post-synthetic exchange (PSE), called as build block replacement (BBR), includes (i) solvent-assisted linker exchange (SALE), (ii) nonbonding ligand replacement, and (iii) transmetalation using SC-SC-transformations. SALE is a widely used process for adjusting the functionality of MOFs involving a systematic preferred solvent and the concerned MOF's crystals. 66 A complete replacement of organic ligands can take place during the SALE process. This adds different functionalities to the resulting MOF. BBR reactions are observed only on the outer surface of MOF crystals; the relevant technique involves the heterogeneous substitute of metal ion or linkers by breaking and forming chemical bonds within the original MOF, resulting in the functionalization of the pore or nodes. This in turn achieves the desired functional properties such as selective gas

adsorption, catalysis, redox activity and ionic conductivity. PSE is an easier and more efficient technique for the synthesis of MOFs, which cannot be performed directly under solvothermal conditions. When UiO-66⁶⁷ solid is added to an aqueous solution of 2,3-dithiocatechine-1,4-benzenedicarboxylic acid (tcat-H₂bdc) for at 85 °C for 24 h by PSE process, it results in the linker exchange to form thio-catechol material, UiO-66-TCAT as a yellow microcrystalline powder. Replacing metal ions or ligands in MOFs by solid-solid PSE involves exchange between two different MOFs. Whereas in the case of solid-liquid PSE, the process involves the exchange in a solution containing a ligand or a metal ion in the presence of synthesized MOF. Post-synthetic transmetallation involves breaking of coordinate covalent bonds between the organic ligands and metal ions beside the formation of new bonds with the incoming metal ions. Kim *et al.* has reported that the metal ions present in MIL-53 (Al)–Br and that in MIL-53 (Fe)–Br MOFs can be exchanged under mild conditions using water as a solvent.⁶⁸

1.3. Applications

CPs/MOFs, owing to their pores with alterable sizes, shapes and functional surfaces along with their highly crystalline nature and thermal stability, have been evolving as well proven class of candidates for material chemistry applications. They are found to play significant role mainly in sensing, catalysis, toxic gas and metal ion scrubbers *etc*.

1.3.1. Gas absorption and separation

Several well-known porous materials, *viz.* zeolites and activated carbons were extensively studied for their gas storage capabilities. In this regard, MOFs have afforded edge over other materials for gas storage effectively. Gas storage and separation were closely related to assorted features in human activities, such as environmental fortification, energy consumption and industrial fabrication. Hydrogen and methane has been evolving as couple of the high energy density and clean energy options for sustainable future, but their efficient storage is one of the primary challenges needs to be addressed. Besides, Trapping and/or removing toxic gases (i.e. NH₃, H₂S, NO_x and SO₂ *etc.*) and volatile organic compounds (i.e. benzene *etc.*) from industrial gaseous waste is important considering clean environmental reasons. On the other hand, purification of gasses and separation of gaseous mixtures (e.g. CO₂/CH₄, CO₂/N₂ *etc.*) is proved to be one of the vital steps in chemical industries.

CO₂ is a main greenhouse gas. Human society is depending on the exploitation of fossil fuels, which on burning releases CO₂ in to the atmosphere in high concentration and leads to global warming as well as water acidification. MOFs have been reported to be useful for reducing

CO₂ intensity in the atmosphere. MOF-210 is known to have the highest surface area of 10450 m²g⁻¹ which was showing comparatively good CO₂ uptake (up to 2400 mg. g⁻¹ (74.2 wt%) at 50 bar and 298 K),⁶⁹ which is higher than the amounts adsorbed by MIL-101(Cr) or MOF-177 (56.9 wt% and 60 wt%, respectively).⁷⁰ MOF-200 also exhibits similar property compared to MOF-210 under similar conditions. MOF-74-Mg (a magnesium analogue of MOF-74) the observed to show reasonably good CO₂ adsorption, 228 and 180 cm³g⁻¹ respectively at 273 K and 1 bar. The outstanding performance by MOF-74-Mg was ascribed to the enhanced ionic character of Mg-O bond.⁷¹ Other well-known MOFs, which show significantly highest CO₂ uptake, include MOF-5 (58 wt% at 10 bar and 273K), NU-100 (69.8 wt% at 40 bar and 298K), the HKUST-1 (19.8 wt% at 1 bar and 298K), *etc*.

The amine incorporation into the MOFs facilitates the introduction of additional metal ions into the MOFs. In the industry, the technique used for CO₂ separation has the amine scrubbing arrangement that suffers from high regeneration energy due to the presence of large portions of water in their compositions; the other relevant problem is amine degradation of amine groups and corrosion of equipment. Moreover, amine incorporated MOFs found be good candidates for CO_2 separation. For example, mmen (N, N'-dimethylethylenediamine) incorporated $[Mg_2(dobpdc)]_n$ (dobpdc⁴⁻ = 4,4'-dioxido-3,3'-biphenyldicarboxylate) led to formation of [mmen-Mg₂(dobpdc)], which showed an outstanding CO₂ adsorption ability at low pressures and at conditions relevant CO₂ removal from air (8.1 wt% (2.0 mmol/g) at 25 °C and 0.39 mbar) and flue gas (12.1 wt% (3.14 mmol/g) at 40 °C and 0.15 bar). 72 Bio-MOF-11, $[Co_2(ad)_2(CH_3CO_2)_2]$ (DMF)₂ (H_2O)_{0.5} (ad = adeninate), framework with pores trapping molecules with pyrimidine and amino functionalities was not only showing high CO2 adsorption capacity (~6 mmol.g⁻¹ at 273 K) but also better selectivity towards CO₂ over N₂ (273 K (81:1) and 298 K (75:1)). 73 Yaghi and co-workers derived six analogous MOFs by functionalization of linker (in IRMOF-74-III) containing primary amine and produced MOFs with varying functionalities (IRMOF-74-III-CH₃, IRMOF-74-III-NH₂, IRMOF-74-III-CH₂NHBoc, IRMOF-74-III-CH₂NMeBoc, IRMOF-74-III-CH₂NH₂, and IRMOF-74-III-CH₂NHMe). The CO₂ uptake of 3.2 mmol/g (at 800 Torr and 298 K) was observed for IRMOF-74-III-CH₂NH₂. ⁷⁴ Similarly, UiO-67(Zr)-(COOH)₂ (UiO-66 with functinalized ligand), found to exhibiting good selectivity of 56 towards CO₂ at 1 bar and 303K from the mixture of 15/85 CO₂/N₂. Likewise, BUT-10 and BUT-11 functionalized by UiO-67 demonstrated high CO₂ absorption (50.6 and 53.5 cm³/g, respectively) and the selective separation over N_2 (18.6 and 31.5 for a mixture of CO_2/N_2 (15/85)) and CH_4 (5.1 and 9.0 for a mixture of CO_2/CH_4 (10/90)). ^{75,76}

Methane sorption study on MOFs was firstly demonstrated by Noro *et al.*⁷⁷ Methane absorption of 16 wt% (at 35 bar) in PCN-14 having BET surface area of 1753 m²g⁻¹,was reported by Zhou.⁷⁸ Interestingly, toxic gases like CO and NO are also separated from gaseous mixtures by using MOF materials. This separation phenomenon explained in terms of open metal center and CO dipole interaction. The capturing the NO gas by MOFs, Cu-SIP-3⁷⁹ and Zn(TCNQ-TCNQ)(bpy)⁸⁰ have been demonstrated. The nonporous nature of these MOFs adsorb selectively the NO gas (~9 molecules/formula unit at 1 bar) above gate-opening pressure and these MOFs cannot adsorb gases like Ar, N₂, CO₂. In 2010, Allen and co-workers explained the reason for this performance of the above two MOFs. In 2014, D. Yan *et al.* synthesized a new organic linker m-H₄TCPB (1,2,4,5-tetrakis(3-carboxyphenyl)-benzene) and its first MOF (Cu-m-TCPB), which can uptake 24.4 cm³g⁻¹ H₂ and 2.3 cm³g⁻¹ N₂ at 77K and 1 atm. It has been reported to possess uptake capacity of 23.3 cm³g⁻¹ acetylene, 23 cm³g⁻¹ CO₂ and 7.3 cm³g⁻¹ at 273 K atmosphere.⁸¹

1.3.2. Catalysis

MOFs, (owing to their robustness, larger surface areas, well organized pores and channels, linkers with multifunctional groups) have also penetrated their roots into heterogeneous catalysis as shown in Figure 1.7. MOFs have been used as catalyst or catalytic supports for the various chemical synthetic applications, e.g., epoxidation and sulfoxidation. MOFassisted catalytic reactions also includes C-C bond formation, like Suzuki Coupling, Heck reaction and Sonogashira coupling etc. 1,3-cycloaddition, transesterification, aerobic oxidation and the unsaturated organic compounds hydrogenation. MOFs have also been used for catalytic reactions due to the presence of Lewis acidic metal nodes, for instance, alkenes epoxidation with up to 99% selectivity was achieved using MnFe-MOF-74. 82,83 Post synthetically adapted MOFs, e.g., copper functionalized UiO-66, molybdenum complex with UiO-67,(Cr)NH₂-MIL-101,have been used for the epoxidation reactions (role: Lewis acidic sites).⁸⁴ In some other cases, nanoparticles of noble metals, such as gold and palladium were incorporated in the pores of MOF, to be used as catalyst for selective aerobic oxidation 85,86 of alcohols to aldehydes or ketones. Cu-based MOFs have been used in 1,3-dipolar cycloaddition reaction for the formation of five-membered ring compounds. UiO-66 and UiO-67 MOFs were used for transesterification, 87,88 Palladium nanoparticles incorporated-Zr-MOF-80889 has also been used as a heterogeneous catalyst for Heck reaction. Another such example is the catalytic hydrogenation of α , β -unsaturated aldehydes into unsaturated alcohols, by the encapsulated Pt nanoparticles in MIL-101(Fe,Cr). In another case, Ni nanoparticles encapsulated within MIL-120 were found to have a better catalytic performance towards gas-phase hydrogenation of benzene, than Ni/Al₂O₃. Cu-based MOFs, [Cu₃(btc)₂] HKUST-1and [Cu₃(btb)₂] MOF-14 demonstrated high catalytic activity toward CO oxidation at 105K, which is associated with the high adsorption of CO molecules on the open metal sites (Cu²⁺). 92

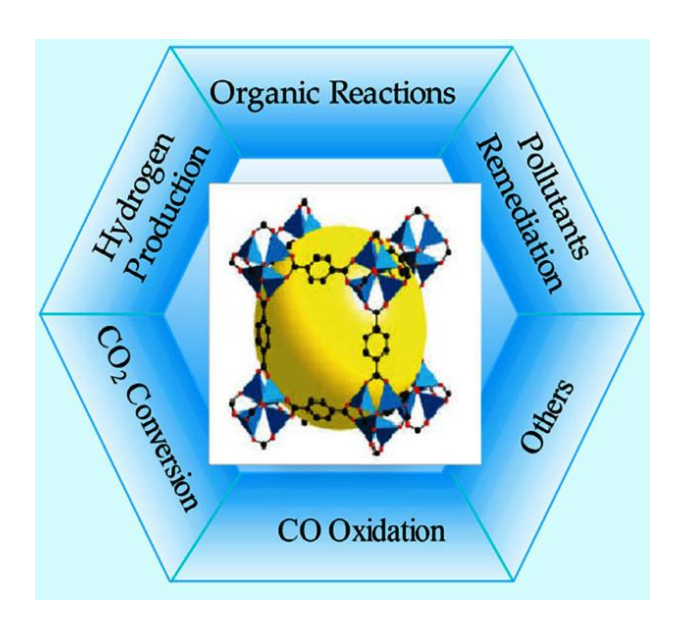


Figure 1.7. Versatile applications of MOFs in heterogeneous catalysis. 93

2D multifunctional MOFs are developed recently as catalysts of wonderful intrinsic reactivity and used as supporters for catalysts for diverse organic transformations. For example, 2D MOFs, based on tetrakis(4-carboxyphenyl)-porphyrin, exhibit exclusive photochemistry, high effectiveness in light-harvesting and illustrated catalytic activity in photooxidation reactions. MOFs also play an important role in the electrocatalytic activity for hydrogen evolution reaction (HER), oxygen evolution reaction (OER), carbon dioxide reduction reaction, *etc.* for example, Cu-MOF, Zn-BTC-MOF, and Cu-HKUST have been reported for electrochemical reduction of CO₂ recently in a standard three electrode set-up. Photo catalytic activity of MOFs can be realized by different mechanisms: parts of MOFs absorb light due to ligand-to-metal charge transfer (LMCT), metal-to-ligand charge transfer (MLCT), metal-to-metal charge transfer (MMCT), ligand-to-ligand charge transfer (LLCT). The dual excitation pathways work due to their porous nanostructures, controllable semiconductor properties and ability to incorporate co-catalyst, such as metals and metal

oxides. In the photocatalytic reduction, the core-shell HKUST-1@TiO₂, ⁹⁶ compared to parents HKUST-1 and TiO₂, proves photocatalytic reduction effectiveness of CO₂ to CH₄ (five times over that of TiO₂) and selectivity over hydrogen. Environmentally-friendly MOFs, their composites and mainly Fe-MOFs, are used in advanced oxidation processes (AOPs) as photo catalysts for the exclusion of organic materials from water and wastewater by oxidation through reactions with hydroxyl radicals. ^{97, 98}

1.3.3. Sensing

A huge number of MOFs have been found to be quite efficient materials in sensing various metal ions and gases because of their improved detective sensitivity owing to their structural features like high specific surface area, presence of open metal sites, tunable pores, and channels, all of which promote host-guest interactions and reversible uptake and release of small molecules, cations, anions, and biomolecules (owed to flexible porosity). Some MOFs are reported to be photo luminescent by absorbing UV-visible light because of the presence of guest molecules, which might interact and cause light shift in the emission spectrum. This can lead to changes in colour and intensity of the emitted light – a useful feature for studying fluorescence 'turn-on' and 'turn-off' routes. A stable magnesium-based MOF -[Mg(pdda)(dmf)] $(H_2pdda = 4,4'-(pyrazine-2,6-diyl)dibenzoic acid), containing non$ coordinating nitrogen atoms on the surface of the pores, has been found to display good coordinating selectivity for Eu³⁺ ions in aqueous solution, even at low concentration.⁹⁹ A bimetallic Eu-Tb (Ln-MOF) MOF demonstrated Pb⁺²selectivity because of the MOF being doped with different ratios of Eu/Tb. In this case, the colour of the Ln-MOF changed from green to red. The emission colour changes from red-orange to green in the presence of Pb²⁺, which was observed by naked eye. 101 Guest-dependent luminescent MOFs respond to the detection of volatile organic molecules and explosive materials by displaying changes in the emission spectrum. ¹⁰² As shown in Figure 1.8, the cationic MOF, [CuL₂(H₂O)_{0.5}](NO₃)₂¹⁰³ exhibits diverse colours in presence of different anions, such as SCN $^-$,Cl $^-$, B $^-$, Γ ,and N $_3$ $^-$.

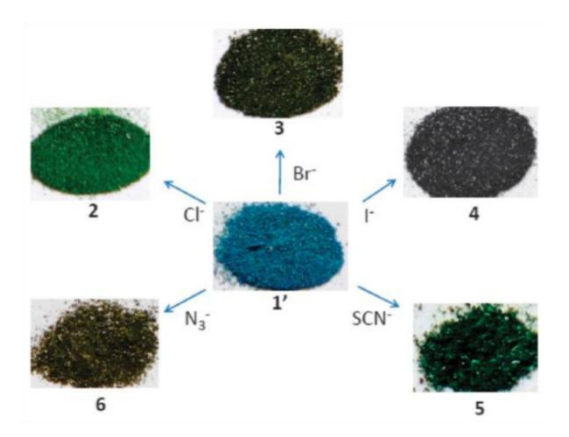


Figure 1.8. Change in colour due to the exchange of nitrate anions by other anions in $[CuL_2(H_2O)_{0.5}](NO_3)_2(1')$.

1.3.4. Proton conducting and magnetic materials

MOFs are also known to be excellent proton conducting materials because of the scope of presence of different types of proton carriers in their pores and channels. A study of such materials can provide information about the mechanistic pathways of proton conduction. Some of the proton conducting MOFs is also anionic in nature. Some MOFs can have protonated amines molecules or protonated solvent molecules as guests in the pores, or protonated functional groups already present on the ligands of the MOF. In one such report, $\{H[(N(CH_3)_4)_2][Gd_3(NIPA)_6]\}.3H_2O\ (H_2NIPA = 5-nitroisophthalic acid)\ MOF\ exhibited$ proton conductivity of 7.17×10^{-2} S.cm⁻¹, which is one of the highest values reported for MOF-based proton conductors. 104 Neutral MOF [Tb₄(TTHA)₂(H₂O)₄].7H₂O (H₆TTHA = 1,3,5-triazine-2,4,6-triamine hexaaceticacid), which is known to have extensive H-bonded networks among the carboxyl groups of the framework and the water molecules present inside the pores, exhibits proton conductivity of the order of 10^{-2} S.cm⁻¹ in the temperature range of 295–358 $K.^{105}$ The MOF $[Ln_2(CO_3)(ox)_2(H_2O)_2].3H_2O$ $(Ln^{III} = Ce, Pr, Nd, Tb)$ shows proton conductivity of the order of 10^{-3} S.cm⁻¹ at very low humidity (Figure 1.9). 106 The magnetic properties of MOFs can be tuned according to our needs by carefully varying the functional nodes, the organic linker molecules, or by introducing guest molecules in the pores. 107 The magnetic properties in a MOF are more commonly induced by the metal node, (either transition metal ions or lanthanides metal ions) and their specific ordering in the framework.

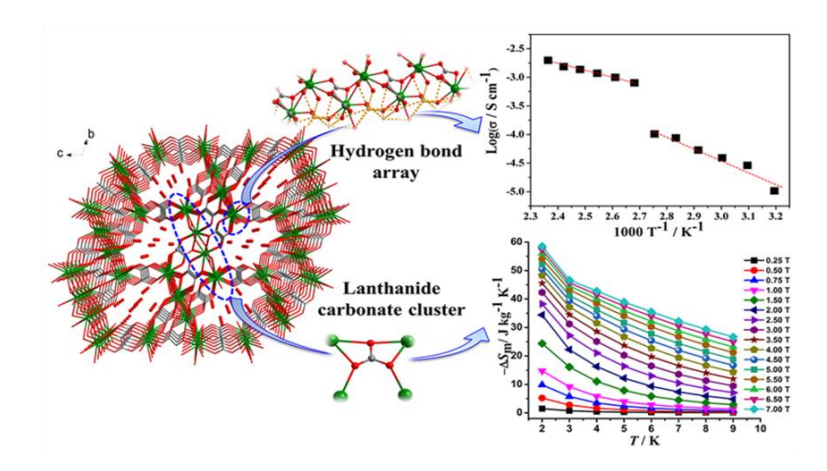


Figure 1.9. The three-dimensional framework of $\{[Gd_2(CO_3)(ox)_2(H_2O)_2].3H_2O,\}$, showing 1-D channels along theorystallographica-axis. The Arrhenius plot from proton conductivity of the compound (up right); plot showing the magnetocaloric effect of the compound (down right).

In two such MOFs - MOROF-1 and $[Cu_3(PTMTC)_2(py)_6(EtOH)_2(H_2O)]$ (H₃PTMTC = perchlorotriarylmethyltricarboxylic acid radical), the highly porous structure combined with the with bulk magnetic ordering, give rise to interesting materials. ¹⁰⁸ 3D MOFs like $[Cu_6(PTMHC)_2(4,4'-bipy)_3(H_2O)_{12}]$ and $[Cu_6(\alpha H-PTMHC)_2(4,4'-bipy)_3(EtOH)_6(H_2O)_6]$, are known to show ferromagnetic and weak antiferromagnetic interactions, respectively. ¹⁰⁹

1.4. Motivation for the present thesis work

As seen in the preceding sections, MOFs can be diverse types based on the types of ligands used in the respective concerned syntheses. Our group has been exploring MOFs based on flexible ligands for last several years. The literature studies, described above, inspired me to design and synthesize MOF containing compounds of diverse supramolecular architectures so that we can explore relevant supramolecular chemistry. We have seen that when we used the flexible ligands in MOFs' syntheses, it results in networks of diverse kinds. In the present thesis work, I have chosen diverse flexible ligands to achieve diverse secondary building units (SBUs)

and I have also chosen different N,N linkers that can further link the SBUs (formed from the flexible ligands) or that further join the 1D chains (formed from the SBUs) in the perpendicular direction resulting 2D-layers; or N,N linker can connect the 2D layers (formed from the SBUs) in the perpendicular direction forming in a 3D network.

For example, in the first working chapter (chapter 2), the flexible ligands include 3,3'methylenebis(oxy)dibenzoic acid (3-H₂mboba), 2,2'-(1,3 phenylene)diacetic acid (1,3-H₂pda) and 4,4'-(perfluoropropane-2,2-diyl)dibenzoic acid (H₂hfipbb) and the N,N-donor linkers, used. 1,2-bis((1H-imidazol-1yl)methyl)benzene(1,2-bix), N,N'-(1,4phenylenebis(methylene)) dipyridin-3-amine (px3ampy) and 4,4'-bis((1H-imidazol-1yl)methyl)biphenyl (bpbix). Cobalt(II) salt with respective flexible ligand-linkers combination, e.g., 3-H₂mboba-1,2-bix and so on result in coordination polymers of different sized- and shaped-metallomacrocycles, that have diverse supramolecular architectures. Likewise, other three working chapters are also the descriptions of MOF containing compounds that are synthesized from different modes of flexible ligands and N,N-linkers. We have described their supramolecular chemistry in details. All the compounds, described in this thesis, are unambiguously characterized by single crystal X-ray crystallography including routine spectral analysis and elemental analysis. Some of the MOFs have been characterized by gas adsorption studies.

References

- 1. (a) S.L. James, Chem. Soc. Rev. 32 (2003) 276;
 - (b) S. Kitagawa, R. Kitaura, S.-i. Noro, Angew. Chem., Int. Ed. 43 (2004) 2334;
 - (c) A.Y. Robin, K.M. Fromm, Coord. Chem. Rev. 250 (2006) 2127;
 - (d) J.R. Long, O.M. Yaghi, Chem. Soc. Rev. 38 (2009) 1213;
- 2. O.M. Yaghi, G. Li, H. Li, Nature. 378 (1995) 703.
- 3. (a) S. Kitagawa, R. Kitaura, S.-i. Noro, Angew. Chem., Int. Ed. 43 (2004) 2334;
 - (b) J.R. Long, O.M. Yaghi, Chem. Soc. Rev. 38 (2009) 1213;
 - (c) S.T. Meek, J.A. Greathouse, M.D. Allendorf, Adv. Mater. 23 (2011) 249.
- 4. O.M. Yaghi, US Pat.grant, 5648508, 1995.
- 5. (a) Y.-S. Ho, H -Z. Fu, Inorg. Chem. Commun. 73 (2016) 174;
 - (b) C.-C. Wang, Y.-S. Ho, Scientometrics. 109 (2016) 481;
 - (c) B.F. Hoskins, R. Robson, J. Am. Chem. Soc. 112 (1990) 1546;
 - (d) S.R. Batten, B. F. Hoskins, R. Robson, J. Am. Chem. Soc. 117 (1995) 5385;
 - (e) H. Li, M. Eddaoudi, M. O'Keeffe, O. M. Yaghi, Nature. 402 (1999) 276.
- 6. N. Li, J. Xu, R. Feng, T.L. Hu, X.H. Bu, Chem. Commun. 52 (2016) 8501.
- 7. H. Furukawa, K. E. Cordova, M. O'Keeffe, O. M. Yaghi, Science. 341 (2013) 1230444.
- 8. P. Horcajada, T. Chalati, C. Serre, B. Gillet, C. Sebrie, T. Baati, J.F. Eubank, D. Heurtaux, P. Clayette, C. Kreuz, J.S. Chang, Y.K. Hwang, V. Marsaud, P.N. Bories, L. Cynober, S. Gil, G. F´erey, P. Couvreur, R. Gref, Nat. Mater. 9 (2010) 172.
- 9. T.G. Glover, G.W. Peterson, B.J. Schindler, D. Britt, O. Yaghi, Chem. Eng. Sci. 66 (2011) 163.
- 10. A. Aijaz, N. Fujiwara, Q. Xu, J. Am. Chem. Soc. 136 (2014) 6790.
- 11. A. Chakraborty, S. Roy, M. Eswaramoorthy, T. K. Maji, J. Mater. Chem. A. 5 (2017) 8423.
- 12. D. Umeyama, S. Horike, M. Inukai, S. Kitagawa, J. Am. Chem. Soc. 135 (2013) 11345.
- 13. M. Sadakiyo, T. Yamada, H. Kitagawa, J. Am. Chem. Soc. 131 (2009) 9906.
- 14. S. Aguado, J. Canivet, D. Farrusseng, J. Mater. Chem. 21 (2011) 7582.
- 15. A. Dhakshinamoorthy, Z. Li, H. Garcia, Chem. Soc. Rev. 47 (2018) 8134.

- 16. Z.S. Hasankola, R. Rahimi, H. Shayegan, E. Moradi, V. Safarifard, Inorg. Chim. Acta. 501 (2019) 119264.
- 17. X. Fang, B. Zong, S. Mao, Nano-Micro. Lett. 10 (2018) 64.
- 18. J. Lei, R. Qian, P. Ling, L. Cui, H. Ju, TrAC, Trends Anal. Chem. 58 (2014) 71.
- 19. S.Horike, S. Shimomura, S. Kitagawa, Soft porous crystals. Nat. Chem. 1 (2009) 695.
- 20. L. Hamon, P.L. Llewellyn, T. Devic, A. Ghoufi, G. Clet, V. Guillerm, G.D. Pimgruber, G. Maurin, C. Serre, G. Driver, W. V. Beek, E. Jolimaitre, A. Vimont, M. Daturi, G. Ferey, J. Am. Chem. Soc. 131 (2009) 17490.
- 21. P. Llewellyn, S. Bourrelly, C. Serre, Y. Filinchuk, G. Férey, Angew. Chem., Int. Ed. 45 (2006) 7751.
- 22. C. Serre, C. Mellot, S. Surblé, N. Audebrand, Y. Filinchuk, G. Férey, Science. 315 (2007) 1828.
- 23. H. Choi, M. Suh, Angew. Chem., Int. Ed. 48 (2009) 6865.
- 24. M. Dincă, J. R. Long, J. Am. Chem. Soc. 127 (2005) 9376.
- 25. Z. Liang, M. Marshall, A. L. Chaffee, Energy and Fuels 23 (2009) 2785.
- 26. A. Millward, O. M. Yaghi, J. Am. Chem. Soc. 127 (2005) 17998.
- 27. A. Demessence, D. D'Alessandro, M. Foo, J. Long, J. Am. Chem. Soc. 131 (2009) 8784.
- C. Serre, S. Bourrelly, A. Vimont, N.A. Ramsahye, G. Maurin, P. Llewellyn, M. Daturi, Y. Filinchunk, O. Leynaud, P. Barnes, G. Ferey. Advanced Materials. 19 (2007) 2246.
- 29. (a) Y.-R. Lee, J. Kim, W.-S. Ahn, Korean. J. Chem. Eng. 30 (2013) 1667;
 - (b) Y. Sun, H.-C. Zhou, Sci. Technol. Adv. Mater. 16 (2015) 054202;
 - (c) C. Dey, T. Kundu, B. P. Biswal, A. Mallick, R. Banerjee, Acta Crystallogr B Struct Sci CrystEng Mater. 70 (2014) 3.
- 30. O. Yaghi, H. Li, J. Am. Chem. Soc., 117 (1995) 10401.
- 31. O.M. Yaghi, M. O'keeffe, N.W. Ockwig, H.K. Chae, M. Eddaoudi, J. Kim, Nature 423 (2003) 705.
- 32. A.J. Howarth, A.W. Peters, N.A. Vermeulen, T.C. Wang, J.T. Hupp, O.K. Farha, Chem. Mater. 29 (2017) 26.
- 33. V.V. Butova, A. P. Budnyk, E A. Bulanova, C. Lamberti, A.V. Soldatov, Solid State Sci. 69 (2017) 13.

- 34. A. Crake, K.C. Christoforidis, A. Gregg, B. Moss, A. Kafizas, C. Petit, Small. 15 (2019) 1805473.
- 35. F. Azad, M. Ghaedi, K. Dashtian, S. Hajati, V. Pezeshkpour, Ultrason. Sonochem. 31 (2016) 383.
- 36. C. Zlotea, D. Phanon, M. Mazaj, D. Heurtaux, V. Guillerm, C. Serre, P. Horcajada, T. Devic, E. Magnier, F. Cuevas, G. F´erey, P.L. Llewellyn, M. Latroche, Dalton Trans. 40 (2011) 4879.
- 37. M. Eddaoudi, J. Kim, N. Rosi, D. Vodak, J. Wachter, M. O'Keeffe, O.M. Yaghi, Science. 295 (2002) 469.
- 38. E.J. Keith. The Electrochemical Society Interface 2007.
- 39. P.K. Fatma, et al. Chem. Sus. Chem. 10 (2017) 2842.
- 40. T. P. Vaid, et al. International Union of Crystallography 4 (2017) 380.
- 41. W.-J. Ji, Q.-G. Zhai, S.-N. Li, Y.-C. Jiang, M.-C. Hu, Inorg. Chem. Commun. 28 (2013) 16.
- 42. S.H. Jhung, J. H. Lee, J.S. Chang, Bull. Korean Chem. Soc. 26 (2005) 880.
- 43. M. Schlesinger, S. Schulze, M. Hietschold, M. Mehring, Microporous Mesoporous Mater. 132 (2010) 121.
- 44. A. Huang, L. Wan, J. Caro, Mater. Res. Bull., 98 (2018) 308.
- 45. A. Pichon, A. Lazuen-Garay, S.L. James, CrystEngComm. 8 (2006) 211.
- 46. (a) T. Frišcic, D.G. Reid, I. Halasz, R.S. Stein, R.E. Dinnebier, M.J. Duer, Angew. Chem., Int. Ed. 49 (2010) 712;
 - (b) T. Frišcic, J. Mater. Chem. 20 (2010) 7599;
 - (c) P.J. Beldon, L. Fábián, R.S. Stein, A. Thirumurugan, A.K. Cheetham and T. Friši, Angew. Chem., Int. Ed. 49 (2010) 9640.
- 47. T. Frišcic, I. Halasz, P.J. Beldon, A.M. Belenguer, F. Adams, S.A.J. Kimber, V. Honkimäki, R.E. Dinneier, Nat. Chem. 5 (2012) 66.
- 48. U. Mueller, H. Puetter, M. Hesse, M. Wessel. Patent WO2005/049892.
- 49. A.M. Joaristi, J. Juan-Alcañiz, P. Serra-Crespo, F. Kapteijn, J. Gascon, Cryst. Growth Des. 12 (2012) 3489.
- 50. S. Mandegarzad, J.B. Raoof, S.R. Hosseini, R. Ojani, Appl. Surf. Sci., 436 (2018) 451.
- 51. S. Khazalpour, V. Safarifard, A. Morsali, D. Nematollahi, RSC Adv. 5 (2015) 36547.

- 52. T.R.C. Van Assche, N. Campagnol, T. Muselle, H. Terryn, J. Fransaer, J.F.M. Denayer, Microporous Mesoporous Mater. 224 (2016) 302.
- 53. H.M. Yang, X.L. Song, T.L. Yang, Z.H. Liang, C.M. Fan, X.G. Hao, RSC Adv. 4 (2014) 15720.
- 54. L.-G. Qiu, Z.-Q. Li, Y. Wu, W. Wang, T. Xu, X. Jiang, Chem. Comm. 31 (2008) 3642.
- 55. W.-J. Son, J. Kim, J. Kim, W.-S. Ahn, Chem. Commun. 47 (2008) 6336.
- 56. D.-W. Jung, D.-A. Yang, J. Kim, J. Kim, W.-S. Ahn, Dalton Trans. 39 (2010) 2883.
- 57. M. Ding, X. Cai, H.-L. Jiang, Chem. Sci. 10 (2019) 10209.
- 58. D. Tranchemontagne, J. Hunt, O.M. Yaghi, Tetrahedron. 64 (2008) 8553.
- 59. M. Schlesinger, S. Schulze, M. Hietschold, M. Mehring, Microporous Mesoporous Mater. 132 (2010) 121.
- 60. J. Kim, S.-T. Yang, S.B. Choi, J. Sim, J. Kim, W.-S. Ahn, J. Mater. Chem.21 (2011) 3070.
- 61. N.A. Khan, Md. M. Haque, S.H. Jhung, Eur. J. Inorg. Chem. 31 (2010) 4975.
- 62. A.E. Baumann, D.A. Burns, B. Liu, V.S. Thoi, Commun. Chem. 2 (2019) 1.
- 63. Y. Zhang, X. Feng, H. Li, Y. Chen, J. Zhao, S. Wang, L. Wang, B. Wang, Angew. Chem., Int. Ed. 54 (2015) 4259.
- 64. P.V. Dau, S.M. Cohen, Chem. Commun. 49 (2013) 6128.
- 65. A.S. Gupta, R.K. Deshpande, L. Liu, G.I.N. Waterhouse, S.G. Telfer, CrystEngComm 14 (2012) 5701.
- 66. W. Bury, D. Fairen-Jimenez, M.B. Lalonde, R.Q. Snurr, O.K. Farha, J.T. Hupp, Chem. Mater. 25 (2013) 739.
- 67. H. Fei, S.M. Cohen, J. Am. Chem. Soc. 137 (2015) 2191.
- 68. M. Kim, J.F. Cahill, Y. Su, K.A. Prather, S.M. Cohen, Chem. Sci. 3 (2012) 126.
- 69. H. Furukawa, N. Ko, Y.B. Go, N. Aratani, S.B. Choi, E. Choi, A.O. Yazaydin, R.Q. Snurr, M. O'Keeffe, J. Kim, O.M. Yaghi, Science. 329 (2010) 424.
- 70. (a) H. Furukawa, N. Ko, Y.B. Go, N. Aratani, S.B. Choi, E. Choi, A.O. Yazaydin, R.Q. Snurr, M. O'Keeffee, J. Kim, et al. Science. 329 (2010) 424;
 - (b) A.G. Wong-Foy, A.J. Matzger, O.M. Yaghi, J. Am. Chem. Soc. 128 (2006) 3494;
 - (c) G. Ferey, C. Mellot-Draznieks, C. Serre, F. Millange, J. Dutour, S. Surble, I. Margiolaki, Science. 309 (2005) 2040.
- 71. S.R. Caskey, A.G. Wong-Foy, A.J. Matzger, J. Am. Chem. Soc. 130 (2008) 10870.

- 72. T.M. McDonald, W.R. Lee, J.A. Mason, B.M. Wiers, C.S. Hong, J.R. Long, J. Am. Chem. Soc. 134 (2012) 7056.
- 73. J. An, S.J. Geib, N.L. Rosi, J. Am. Chem. Soc. 132 (2010) 38.
- 74. A.M. Fracaroli, H. Furukawa, M. Suzuki, M. Dodd, S. Okajima, F. Gandara, J.A. Reimer, O.M. Yaghi, J. Am. Chem. Soc. 136 (2014) 8863.
- 75. Q. Yang, S. Vaesen, F. Ragon, A.D. Wiersum, D. Wu, A. Lago, T. Devic, C. Martineau, F. Taulelle, P.L. Llewellyn, et al Angew. Chem., Int. Ed. 52 (2013) 10316.
- 76. B. Wang, H. Huang, X.-L. Lv, Y. Xie, M. Li, J.-R. Li, Inorg. Chem. 53 (2014) 9254.
- 77. S. Noro, S. Kitagawa, M. Kondo, K. Seki, Angew Chem Int Ed 39 (2000) 2081.
- 78. S. Ma, D. Sun, J.M. Simmons, C.D. Collier, D. Yuan, H.C. Zhou, J. Am. Chem. Soc. 130 (2008) 1012.
- 79. P.K. Allan, B. Xiao, S.J. Teat, J.W. Knight, R.E. Morris, J. Am. Chem. Soc. 132 (2010) 3605.
- 80. S. Shimomura, M. Higuchi, R. Matsuda, K. Yoneda, Y. Hijikata, Y. Kubota, Y. Mita, J. Kim, M. Takata, S. Kitagawa, Nat. Chem. 2(2010) 633.
- 81. D. Yan, B. Chen, Q. Duan, Inorg. Chem. Commun. 49 (2014) 34.
- 82. A.W. Stubbs, L. Braglia, E. Borfecchia, R.J. Meyer, Y. Roman-Leshkov, C. Lamberti, M. Dinca, ACS Catal. 8 (2018) 596.
- 83. K. Yuan, T. Song, D. Wang, Y. Zou, J.Li, X. Zhang, Z.Tang, W.Hu, Nanoscale. 10 (2018) 1591.
- 84. (a) K. Tabatabaeian, M.A. Zanjanchi, N.O. Mahmoodi, T. Eftekhari, S.M. Shafiei, J. Clust. Sci. 28 (2017) 949;
 - (b) M. Kaposi, M. Cokoja, C.H. Hutterer, S.A. Hauser, T. Kaposi, F. Klappenberger,A. Pöthig, J.V. Barth, W.A. Herrmanna, F.E. Kühn, Dalton Trans. 44 (2015) 15976;(c) J.Zhao, W. Wang, H. Tang, D. Ramella, Y. Luan, Mol. Catal. 456 (2018) 57.
- 85. S. Akbari, J. Mokhtari, Z. Mirjafari, RSC Adv. 7 (2017) 40881.
- 86. J.-S. Wang, F.-Z. Jin, H.-C. Ma, X.-B. Li, M.-Y. Liu, J.-L. Kan, G.-J. Chen, Y.-B. Dong, Inorg. Chem. 55 (2016) 6685.
- 87. X. Liu, W. Qi, Y. Wang, R. Su, Z. He, Eur. J. Inorg. Chem. 2018 4579.
- 88. W.T. Schumacher, M.J. Mathews, S.A. Larson, C.E. Lemmon, K.A. Campbell, B.T. Crabb, B.J.-A. Chicoine, L.G. Beauvais, M.C. Perry, Polyhedron 114 (2016) 422.
- 89. X. Yan, K. Wang, X. Xu, S. Wang, Q. Ning, W. Xiao, N. Zhang, Z. Chen, C. Chen, Inorg. Chem. 57 (2018) 8033.

- 90. M. Zhao, K. Yuan, Y. Wang, G. Li, J. Guo, L. Gu, W. Hu, H. Zhao, Z. Tang, Nature, 539 (2016) 76.
- 91. Y. Wan, C. Chen, W. Xiao, L. Jian, N. Zhang, Microporous Mesoporous Mater. 171 (2013) 9.
- 92. H. Noei, S. Amirjalayer, M. Müller, Z. Zhang, R. Schmid, M. Muhler, R.A. Fischer, Y. Wang, ChemCatChem 4 (2012) 755.
- 93. V.R. Remya, M. Kurian, Int Nano Lett 9 (2019) 17.
- 94. (a) M. Xu, S. Yuan, X.-Y. Chen, Y.-J. Chang, G. Day, Z.-Y. Gu, H.-C. Zhou, J. Am. Chem. Soc. 139 (2017) 8312;
 - (b) T. He, B. Ni, S. Zhang, Y. Gong, H. Wang, L. Gu, J. Zhuang, W. Hu, X. Wang, Small. 14 (2018) 1703929;
 - (c) Y. Xiao, W. Guo, H. Chen, H. Li, X. Xu, P. Wu, Y. Shen, B. Zheng, F. Huo, W.D. Wei, Mater. Chem. Front. 3 (2019) 1580.
- 95. (a) R. Hinogami, S. Yotsuhashi, M. Deguchi, Y. Zenitani, H. Hashiba, Y. Yamada, Ecs. Electrochem. Lett. 4 (2012) H17;
 - (b)R.S. Kumar, S.S. Kumar, M.AKulandainathan, Electrochem. Commun. 25 (2012) 70;
 - (c)X. Kang, Q. Zhu, X. Sun, J. Hu, J. Zhang, Z. Liu, B. Han, Chem. Sci. 7 (2016) 266;
 - (d) K. Zhao, Y. Liu, X. Quan, S. Chen, H. Yu, Acs Appl. Mater. Interfaces. 9 (2017) 5302.
- 96. R. Li, J. Hu, M. Deng, H. Wang, X. Wang, Y. Hu, H.-L. Jiang, J. Jiang, Q. Zhang, Y. Xie, et al., Adv. Mater. 26 (2014) 4783.
- 97. V.K. Sharma, M. Feng, J. Hazard. Mater. 372 (2019) 3.
- 98. G. Zhu, S. Wang, Z. Yu, L. Zhang, D. Wang, B. Pang, W. Sun, Res. Chem. Intermed. 45 (2019) 3777.
- 99. Y. Gao, X. Zhang, W. Sun, Z. Liu, Dalton Trans. 44 (2015) 1845.
- 100. J.-P. Ma, Y. Yu, Y.-B. Dong, Chem. Commun. 48 (2012) 2946.
- X. Zeng, Y. Zhang, J. Zhang, H. Hu, X. Wu, Z. Long, Z. Hou, Microchem. J. 134 (2017) 140.
- 102. (a) F.-Y. Yi, D. Chen, M.-K. Wu, L. Han, H.-L. Jiang, ChemPlusChem 81 (2016) 675;
 - (b) Z.-Q. Shi, N.-N. Ji, H.-L. Hu, Dalton Trans. 49 (2020) 12929;
 - (c) R. Kaur, A.K. Paul, A. Deep, Forensic Sci. Int. 242 (2014) 88.

- 103. J.-P. Ma, Y. Yu, Y.-B. Dong, Chem. Commun. 48 (2012) 2946.
- 104. X.-S. Xing, Z.-H. Fu, N.-N. Zhang, X.-Q. Yu, M.-S. Wang, G.-C. Guo, Chem. Commun. 55 (2019) 1241.
- L. Feng, H.-S. Wang, H.-L. Xu, W.-T. Huang, T.-Y. Zeng, Q.-R. Cheng, Z.-Q.
 Pan, H. Zhou, Chem. Commun. 55 (2019) 1762.
- Q. Tang, Y.-L. Yang, N. Zhang, Z. Liu, S.-H. Zhang, F.-S. Tang, J.-Y. Hu, Y. Z. Zheng, F.-P. Liang, Inorg. Chem. 57 (2018) 9020.
- 107. (a) M. Kurmoo, Chem. Soc. Rev. 38 (2009) 1153;
 - (b) E. Coronado, G.M. Espallargas, Chem. Soc. Rev. 42 (2013) 1525;
 - (c) C.N.R. Rao, S. Natarajan, R. Vaidhyanathan, Angew. Chem., Int. Ed. Engl. 43 (2004) 1466.
- 108. D. Maspoch, D. Ruiz-Molina, K. Wurst, N. Domingo, M. Cavallini, F. Biscarini, J. Tejada, C. Rovira, J. Veciana, Nat. Mater. 2 (2003) 190.
- N. Roques, D. Maspoch, F. Luis, A. Camón, K. Wurst, A. Datcu, C. Rovira,D. Ruiz-Molina, J. Veciana, J. Mater. Chem. 18 (2008) 98.

Metallo-macrocycles from a library of flexible linkers: 1D cobalt (II) coordination polymers and a supramolecular pipe

Three cobalt(II) coordination polymers containing compounds $\{Co(3-mboba)(1,2-bix)_2\}_n$ (1), $\{Co_2(1,3-mboba)(1,2-bix)_2\}_n$ (1), $\{Co_2(1,3-mboba)(1,2-bix)_2\}_n$ pda)(px3ampy)(H₂O)₂}_n (2), {Co₂(hfipbb)₂(bpbix)₂}_n (3), that are formed from three different bent carboxylic acids [3,3'-methylenebis(oxy)dibenzoic acid (3-H₂mboba), 2,2'-(1,3 phenylene)diacetic acid (1,3-H₂pda) and 4,4'-(perfluoropropane-2,2-diyl)dibenzoic acid (H₂hfipbb)] as primary ligands and three different {N,N}-donor linkers [1,2-bis((1H-imidazol-1 yl)methyl)benzene(1,2-bix), N,N'-(1,4phenylenebis(methylene)) dipyridin-3-amine 4,4'-bis((1H-imidazol-1-(px3ampy) and yl)methyl)biphenyl (bpbix)] as secondary ligands, have been synthesized under hydrothermal conditions. Compounds 1-3 are characterized by single crystal X-ray diffraction analysis, IR spectroscopy, thermogravimetric (TG) and elemental analysis. Single crystal X-ray crystallography shows that diverse metallo-macrocycles are formed in compounds 1, 2 and 3. In the crystal structure of compound 1, two different metallo-macrocyles, 28-membered metal-acid {Co₂(3-mboba)₂} ring and 24membered metal-N-linker {Co₂(1,2-bix)₂} ring, are formed. The alternative arrangement of these macrocylic rings leads to the formation of 1D chainlike coordination polymer (compound 1). In the crystal of compound 2, a 25-membered macrocycle ring {Co(1,3-pda)(px3ampy)} is formed from one dicarboxylic acid lignad and one {N,N}ligand, which further undergoes coordination with itself resulting in the formation of 1D chain. The {Co₃(hfipbb)(bpbix)₂} metallomacrocycle, observed in the crystal structure of compound 3, is more diversified in the sense that it is relatively bigger in size and this trinuclear metallo-macrocycle is formed by one dicaryboxylic acid ligand and two {N,N} donor linkers, but not in a plane. Interestingly, the inter-linking of these non-planar macrocycles results in the construction of a supramolecular pipe.

2.1. Introduction

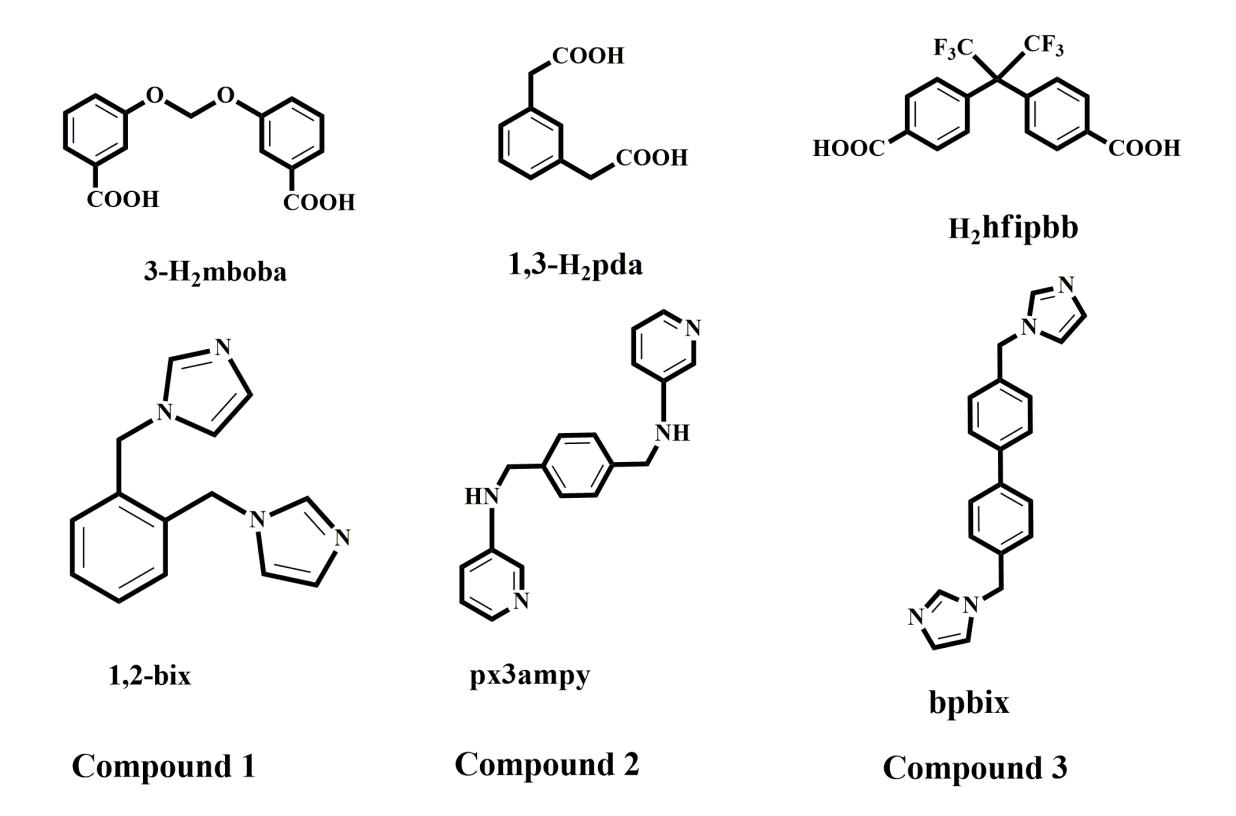
Metal-organic frameworks (MOFs) containing compounds, also known as coordination polymers (CPs), have been emerged as a novel class of functional materials. These are generally highly crystalline inorganic-organic hybrids, constructed by assembling metal ions with multidentate organic ligands *via* coordinate covalent bonds. MOFs / CPs have major potential applications, such as, molecular recognition¹, separation², gas storage³, drug delivery⁴, catalysis⁵, sensing⁶, proton conduction⁷, magnetism⁸ etc. The construction of these materials with interesting structures and excellent performance relays on the choice of the metal centers and ligands used. Synthetic strategies of the MOFs have been developed based on the direct assembly of the organic linker and metal nodes. MOFs containing mixed ligand systems include aliphatic or aromatic carboxylic acids and N-containing secondary linkers i.e., azide, imidazoles, triazole and pyridine derivatives.

The diverse macrocyclic rings-based MOFs have received attention due to the advantage of having two kinds of porosities i.e., one being provided by the macrocyclic ligand used for the construction of these materials and the other possibility being offered by the framework topology. Generally, these macrocyclic MOFs are prepared by employing predesigned macrocyclic ligands, for example, crown ethers, cyclodextrins (CDs), calixarenes, cucurbiturils (CBs) and pillararenes. On the other hand, in some cases, the multitopic ligand coordinates to the metal centers in such a way that they form matallomacrocyclic ring (the concerned metal ion is the part of the cyclic ring) or the *in-situ* formed organic macrocyclic ring encapsulates the metal ion (coordinate bond) at the center / cavity of the ring and the resulting supramolecular entity further coordinates to itself or to other metal ion used in the relevant synthesis, resulting in the formation of macrocyclic coordination polymers / MOFs. The size of the macrocyclic ring can be controlled / tuned either by increasing the length of the organic ligand or by increasing the number of components of macrocyclic ligand.

In this work, we have presented three new metallo-macrocyclic ligands-based coordination polymers based on a library (Scheme 1) of three different bent dicarboxylic acid (primary) ligands and three $\{N,N\}$ donor secondary ligands. The dicarboxylic acids are 3-H₂mboba (3,3'-methylenebis(oxy)dibenzoic acid), 1,3-pda (1,3 phenylenediaceticacid) and H₂hfipbb $\{4,4'$ -(hexa-fluoroisopropylidene)bis-(benzoicacid) $\{4,4'$ -(hexa-fluoroisopropylidene)bis-(benzoicacid) $\{4,4'$ -(bis(3-pyridylaminomethyl) benzene $\{4,4'$ -bis((1H-imidazol-1-px3ampy $\{1,4$ -(bis(3-pyridylaminomethyl) benzene $\{4,4'$ -bis((1H-imidazol-1-px3ampy $\{4,4'$ -bis((1H-imidazol-1-px3ampy

yl)methyl)biphenyl} as shown in Scheme 1. The Cambridge structural database search resulted that these ligands were extensively used in the construction of other coordination polymers with cobalt (II).¹³

Scheme 1. The dicarboxylic acids and {N,N} linkers used as ligands in this work.



The metallo-macrocyclic ligand-based coordination polymers, synthesized hydrothermally in this work, are formulated as $\{Co(3\text{-mboba})(1,2\text{-bix})_2\}_n$ (1), $\{Co_2(1,3\text{-pda})(px3ampy)(H_2O)_2\}_n$ (2) and $\{Co_2(hfipbb)_2(bpbix)_2\}_n$ (3). The structures of all three compounds 1, 2 and 3 are unambiguously established by single crystal X-ray diffraction (SCXRD) analysis, revealing that two of them (compounds 1 and 2) are one-dimentional coordination polymers of diverse topologies and compound 3 is a kind of supramolecular pipe of coordination polymers. Interestingly, in the crystal structure of compound 1, there exists two different types of macrocyclic rings, 28-membered metal-acid $\{Co_2(3\text{-mboba})_2\}$ ring and 24-membered metal-N-linker $\{Co_2(1,2\text{-bix})_2\}$ ring. On the other hand, in compounds 2 and 3, the macrocyclic rings are made up of mixed ligands i.e., $\{Co_2(1,3\text{-pda})(px3ampy)\}$ and $\{Co_3(hfipbb)(bpbix)_2\}$, respectively. Compounds 1, 2 and 3 are additionally characterized by routine spectral studies and elemental analysis including thermogravimetric and PXRD (powder X-ray diffraction) studies.

2.2. Experimental

2.2.1. Materials and physical methods

All the chemicals were received as reagent grade and used without any further purification. The ligands 3-H₂mboba¹⁴, 1,2-bix¹⁵, bpbix¹⁶ and px3ampy¹⁷ were prepared according to the literature procedures.

2.2.2. Characterization

Elemental analyses were determined by FLASH EA series 1112 CHNS analyzer. Infrared spectra of solid samples, obtained as KBr pellets, on a JASCO-5300 FT-IR spectrophotometer. Thermogravimetric analyses were carried out on a STA 409 PC analyzer and corresponding masses were analyzed by QMS 403 C mass analyzer, under the flow of N_2 gas with a heating rate of 5 °C min⁻¹, in the temperature range of 30–800 °C. Powder X-ray diffraction patterns were recorded on a Bruker D8-Advance diffractometer using graphite monochromatic CuK α 1 (1.5406 Å) and K α 2 (1.54439 Å) radiations. The electronic absorption (diffuse reflectance) spectra have been recorded on a Cary 100 Bio UV–visible spectrophotometer at room temperature.

2.2.3. Synthesis

Synthesis of $\{Co(3\text{-mboba})(1,2\text{-bix})\}_n(1)$

A mixture of CoCl₂·6H₂O (59.5 mg, 0.25 mmol), 3-mboba (72 mg, 0.25 mmol) and 1,2-bix (60 mg, 0.25 mmol) was dissolved in 10.0 ml of distilled water and stirred for 30 minutes. The pH of the reaction mixture was adjusted to 6.15 by adding 0.5 M NaOH solution and the resulting reaction mixture was placed in a 23 ml Teflon-lined stainless-steel autoclave, which was sealed and kept at 160 0 C for 3 days. The autoclave was allowed to cool to room temperature over 48 hours to obtain red block crystals of compound **1** in 65.5% yield (based on Co). Anal. Calcd for C₂₉H₂₄CoN₄O₆ (M_r =583.45): C, 59.75%; H, 4.15 %; N, 9.6%. Found: C, 59.48%; H, 4.25%; N, 9.53%. IR (KBr pellet, cm⁻¹): 3139, 3106, 1600, 1550, 1435, 1402, 1326, 1287, 1216, 1117, 1024, 986, 942, 805, 772, 663.

Synthesis of $\{Co_2(1,3-pda)(px3ampy)(H_2O)_2\}_n(2)$

A mixture of CoCl₂·6H₂O (59.5 mg, 0.25 mmol), px3ampy (72.5 mg, 0.25 mmol) and 1,3-H₂pda (48.5 mg, 0.25 mmol) was dissolved in 10.0 ml of distilled water and stirred for 30 minutes. The pH of the reaction mixture was adjusted to 6.76 by adding 0.5 M NaOH solution and the resulting reaction mixture was placed in a 23 ml Teflon-lined stainless-

steel autoclave, which was sealed and heated at $160~^{0}$ C for 3 days. The autoclave was allowed to cool to room temperature over 48 hours to obtain red block crystals of compound **2** in 45% yield (based on Co). Anal. Calcd for $C_{56}H_{60}Co_{2}N_{8}O_{12}$ (M_{r} =1154.98): C, 58.23%; H, 5.24 %; N, 9.7%. Found: C, 58.13%; H, 5.32%; N, 9.61%. IR (KBr pellet, cm⁻¹):3328, 3266, 3028, 1505, 1474, 1138, 1107, 1071, 1055, 988, 952, 777, 751, 699, 523.

Synthesis of $\{Co_2(hfipbb)_2(bpbix)_2\}_n$ (3):

A mixture of $CoCl_2.6H_2O$ (59.5 mg, 0.25 mmol), bpbix (78.5 mg, 0.25 mmol) and $H_2hfipbb$ (98·5 mg, 0.25 mmol) was dissolved in 10.0 ml of distilled water and stirred for 30 minutes. The pH of the reaction mixture was adjusted to 6.15 by adding 0.5 M NaOH solution and the resulting reaction mixture was placed in a 23 ml Teflon-lined stainless-steel autoclave, which was sealed and heated at 160 °C for 3 days. The autoclave was allowed to cool to room temperature over 48 hours to yield red block crystals of compound 3 in 65.5% (based on Co). Anal. Calcd for $C_{74}H_{52}Co_2F_{12}N_8O_8$ (M_r =1527.10): C, 58.20%; H, 3.43 %; N, 7.34%. Found: C, 58.32%; H, 3.36%; N, 7.45%. IR (KBr pellet, cm⁻¹): 3121, 2930, 1598, 1541, 1515, 1391, 1288, 1252, 1205, 1174, 1143, 1107, 1086, 1024, 973, 947, 854, 787, 746, 658.

2.2.4. Single Crystal X-ray Structure Determination of the Compounds 1–3

Single-crystals suitable for structural determination of all the compounds (1-3) were mounted on a three circle Bruker SMART APEX CCD area detector system under Mo-K α (λ = 0.71073 Å) graphite monochromatic X-ray beam. Crystal to detector distance was 60 mm with a collimator of 0.5 mm. The scans were recorded with a ω scan width of 0.30. Data reduction was performed by SAINTPLUS^{18a}; empirical absorption corrections were made using equivalent reflections performed by program SADABS.^{18b} Structure solution was done using SHELXS-97^{18c} and full-matrix least-squares refinement was performed using SHELL-97^{18d} for above compounds. All the non-hydrogen atoms were refined anisotropically. Hydrogen atoms on the C atoms were introduced on calculated positions and were included in the refinement riding on their respective parent atoms. Crystal data, structure refinement parameters for all the compounds (1-3) are summarized in Table 2.1. For the crystal structure of compound 3, the residual electron density related to the disordered DMF molecule was removed by using squeeze option in the PLATON tool with WINGX package. Alert level A is present due to this squeezing. C47 and C52 of

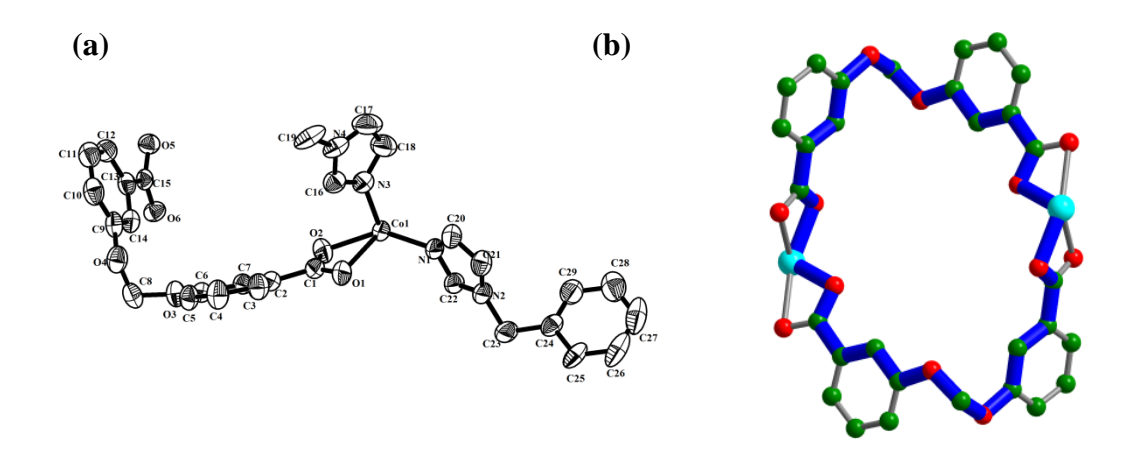
one of the benzene rings of bpbix linker (Alert level B) were treated with EADP instruction to remove ADP errors.

2.3 Results and Discussion

2.3.1. Description of Crystal structures

${Co(3-mboba)(1,2-bix)}_n(1)$

The result of the crystallographic analysis reveals that the compound 1 crystallises in triclinic space group P-1. The thermal ellipsoidal diagram of the compound 1 shows that the asymmetric unit consists of one Co(II) ion, one 3-mboba²⁻ ligand and one 1,2-bix ligand (Figure 2.1a). Overall, in the crystal structure, Co(II) metal centre is surrounded by four O atoms from two different 3-mboba ligands and two N atoms of imidazole ring from two different 1,2-bix linkers affording a octahedral coordination sphere around the Co(II) metal ion. All the Co – O bond distances are in the range of 2.089 – 2.319Å and the Co – N bond distances are 2.053Å and 2.084Å. 1,2-bix linker connects two Co(II) centres by the N atoms of the imidazole rings with a distance of 8.160Å. Both the carboxylate groups of the 3-mboba²⁻ ligand adopt the chelating bidentate (μ^1 - η^1 : η^1) coordination mode to connect the Co(II) metal centers with a separation of 9.62Å. The dihedral angle between the two -COOH groups of the 3-mboba²⁻ ligand is 89.63°. Interestingly, the connectivity of the Co(II) metal ions with 3-mboba²⁻ ligand and 1,2-bix linker results in the formation of two different macrocycle rings, i.e., 28-membered{Co₂(3-mboba)₂} ring (Figure 2.1b) and 24-membered $\{Co_2(1,2-bix)_2\}$ ring (Figure 2.1c). These two different macrocycles meet at the common Co(II) center, resulting the formation of a 1D chain, where {Co₂(3 $mboba)_2$ and $\{Co_2(1,2-bix)_2\}$ macrocycle rings are arranged alternatively (Figure 2.1d).



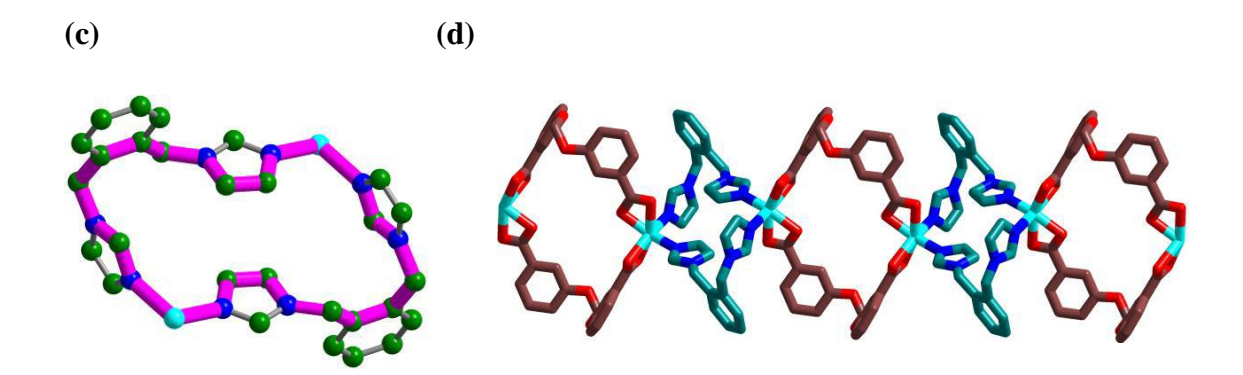


Figure 2. 1. Crystal structure of compound 1: (a) thermal ellipsoidal plot (hydrogen atoms are omitted due to clarity), (b) a sketch of $\{Co_2(3\text{-mboba})_2\}$ macrocycle ring, generated by connecting two Co(II) metal ions using two 3-mboba²⁻ as bridging ligands, (c) a structural drawing of $\{Co_2(1,2\text{-bix})_2\}$ macrocycle ring, generated by bridging two Co(II) centers using two 1,2-bix ligands and (d) 1D chain, formed by connecting these macrocycles in an alternative fashion.

${Co_2(1,3-pda)(px3ampy)(H_2O)_2}_n(2)$

Single crystal X-ray analysis reveals that the compound **2** is crystallized in triclinic space group P-I. The asymmetric unit of the compound **2** consists of two crystallographically independed Co(II) centers, one 1,3-pda²⁻ ligand (Scheme 1), one px3ampy linker (Scheme 1) and two water molecules (Figure 2.1a). Both the Co(II) metals are in almost perfect octahedral geometry where two equatorial positions are occupied by the two-oxygen atom from two different acid ligands and other two by two water molecules and the two-apical positions are occupied by the two N atoms from two px3ampy ligands. All the Co – O bond distances are in the range of 2.064 - 2.150Å and the Co – N bond distances are 2.154 and 2.163Å. Both the acid groups of the 1,3-pda²⁻ ligand adopt monodentate μ_1 - η^1 : η^0 coordination mode in *trans* conformation and connected to the Co(II) center to generate a 1D zig-zag single chain along the crystallographic a axis. Further, the px3ampyconnectivity with the metal centers results another 1D zig-zag single chain along the same axis (Figure 2.2b). The connectivity of both these two different chains (one is dicarboxylate **chain** and other one is N,N linker chain) through common Co(II) centers

(a)

C12

C13

C14

N3

C22

C21

C20

C23

C25

C28

C24

C25

C28

C25

C28

C25

C26

C27

C26

C27

C26

C27

C26

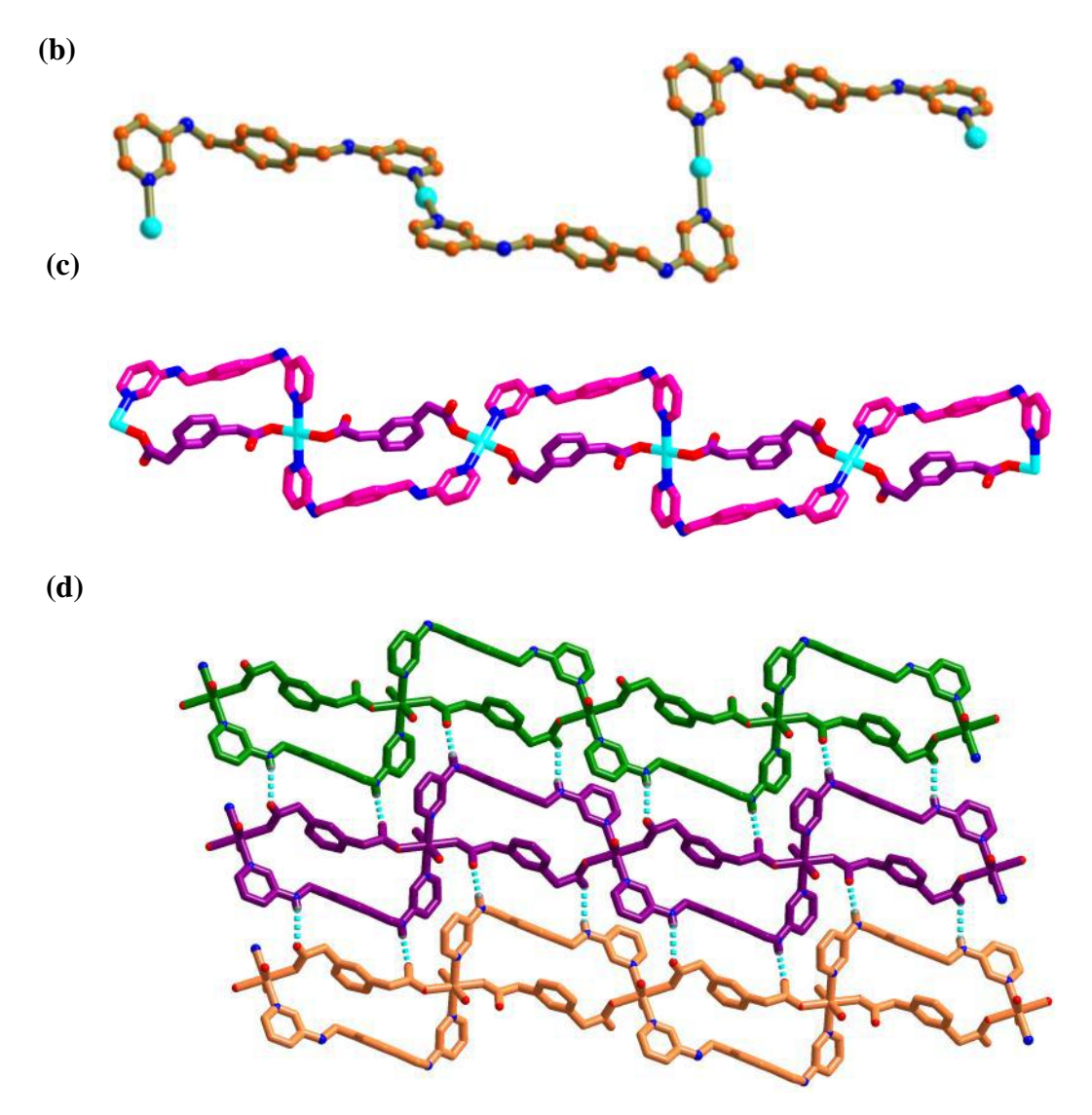
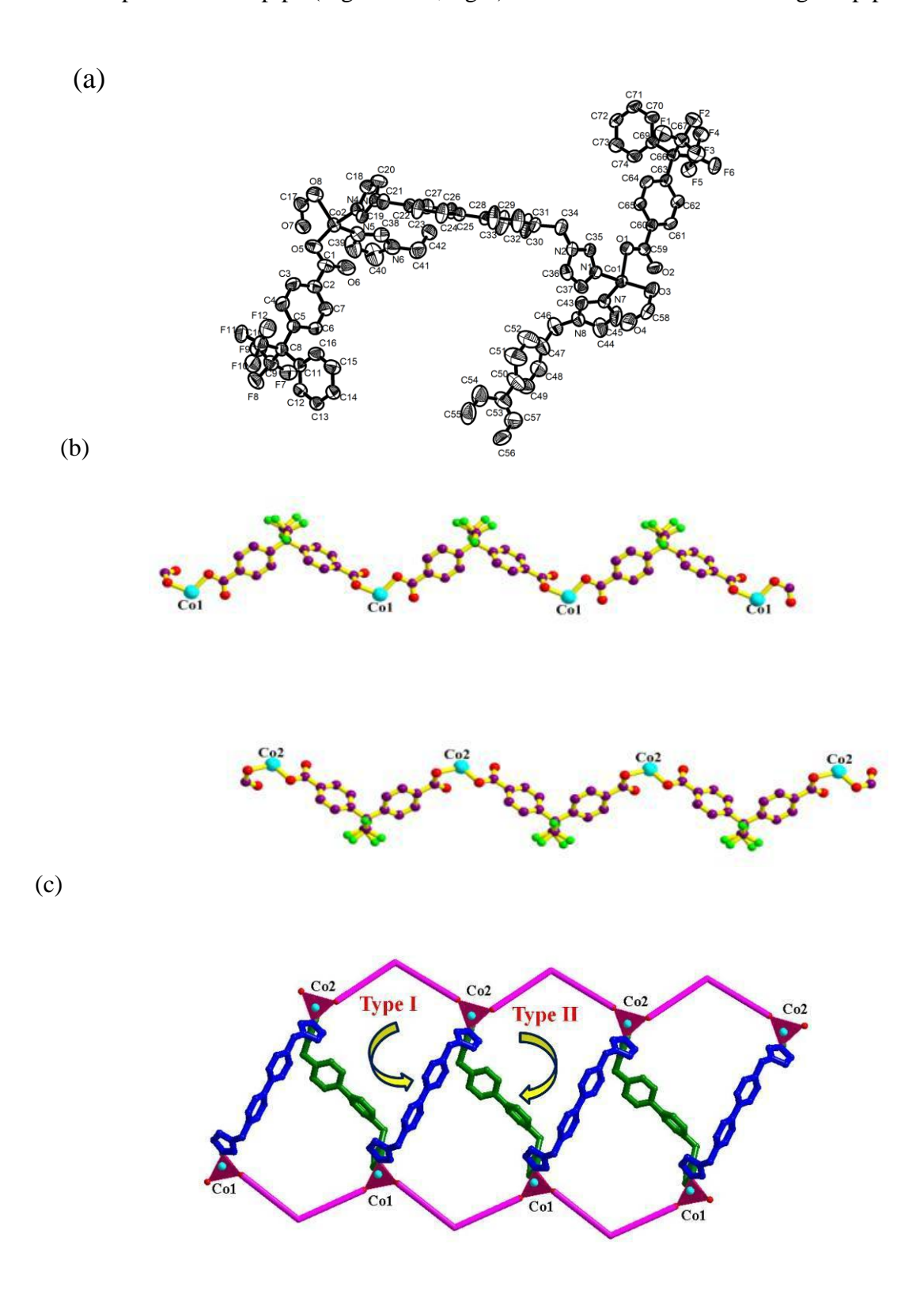


Figure 2. 2. Crystal structure of compound **2**: (a) thermal ellipsoidal diagram (hydrogen atoms are omitted due to clarity), (b) connectivity of the $\{Co(1,3-pda)(px3ampy)\}$ macrocycles leading to the formation of 1D chain, (c) connectivity of the $\{Co(1,3-pda)(px3ampy)\}$ macrocycles leading to the formation of 1D chain and (d) inter-chain N–H···O hydrogen bonding interactions (shown in cyan color).

results in the formation of a ladder-like chain (Figure 2.2c), in which each block/compartment is a 25-membered metallo-macrocycle ring $\{Co_2(1,3\text{-pda})(px3ampy)\}$. Additionally, the uncoordinated oxygen atom of the carboxylate groups in 1,3-pda²⁻ ligand of one chain participates in formation of the strong intermolecular H-bonding with the '-NH' groups of the px3ampy ligand of the other chain; this way, two different N-H···O hydrogen bonding $(N2 - H2N \cdots O2, d_N \dots_O = 2.930 \text{ Å} \text{ and } N3 - H3N \cdots O5, d_N \dots_O = 3.303 \text{ Å})$ interactions further extend the 1D chains to a 2D supramolecular network (Figure 2.2d).

${Co_2(hfipbb)_2(bpbix)_2}_n$ (3)

Compound 3 crystallizes in monoclinic space group $P2_1/c$ and the asymmetric unit is comprised with the two independent Co(II) metal ions, two hfipbb²⁻ ligands and two bpbix ligands (Figure 2.3a). Both the Co(II) ions are in distorted tetrahedral geometry coordinated by two oxygen atoms from two different hfipbb²⁻ ligands and two N atoms from two different bpbix ligands. The Co – O bond distances (1.972Å and 1.994Å) around Co1 metal ion are lesser than those around Co2 metal ion (2.043Å and 2.010Å), whereas, the Co – N bond distances around both the Co(II) ions are almost in the same range from 2.027 - 2.055 Å. The distortion parameter for tetrahedral geometry of Co1 and Co2 metal ion are 0.89 and 0.85 respectively, indicating that both the metal ions are in slight distortion in their tetrahedral geometry. Both the carboxylate groups of the hfipbb²- ligand adopt the monodentate μ_1 - η^1 : η^0 coordination mode to connect the Co(II) metal ions. The connectivity of the hfipbb²⁻ ligand with the crystallo-graphically independent metal ions, Co1(II) and Co2(II), leads to formation of two different metal acid chains (Figure 2.3b). The Co1 – Co1 and Co2 – Co2 distances are same (14.16Å) along both the Co-hfipbb² chains. All the phenyl rings of hfipbb²⁻ ligands, in both metal-acid chains are oriented in the same side of the axis, unlike the zigzag fashion. But, the orientation of the phenyl rings in Co1-hfipbb chain and Co2-hfipbb chain are not identical to each other. These two metal-acid chains are interconnected by the flexible bpbix linker (see Scheme 1) through Co(II) centers in a twisted manner. The bpbix linker adopts two conformations: (i) gauche conformation, closely to cis conformation (may be named as Type I), in which, the imidazole rings twist with respect to each other by an synclinal torsion angle of 59.21° (viewed through N3-C21-C34-N2) and the two phenyl ring are in almost same plane with a twisting angle 10.80° and (ii) closely to trans conformation (named as Type II) with a anticlinal torsion angle of 135.78° between the two imidazole rings followed by a considerable deviation between the planes of the two phenyl ring with a twisting angle 51.63°, as shown in Figure 2.3c. The imidazole rings of both types of bpbix ligands are connected to a Co1 metal ion (of the Co1-Hfipbb chain, in Figure 2.3d, down one) and the imidazole rings at the opposite side of these two linkers are connected to two different Co2 metal ions (of the Co2-Hfipbb chain, in Figure 2.3d, the upper chain) in a bifurcated manner and vice versa, thereby forming a {Co₃(hfipbb)(bpbix)₂} metallo-macrocycle. The resulting situation is the formation of a supramolecular pipe (Figure 2.3d) with the 47membered $\{Co_3(hfipbb)(bpbix)_2\}$ metallo-macrocycle as a building unit. The front view of the supramolecular pipe (Figure 2.3d, right) shows the internal hole along the pipe.



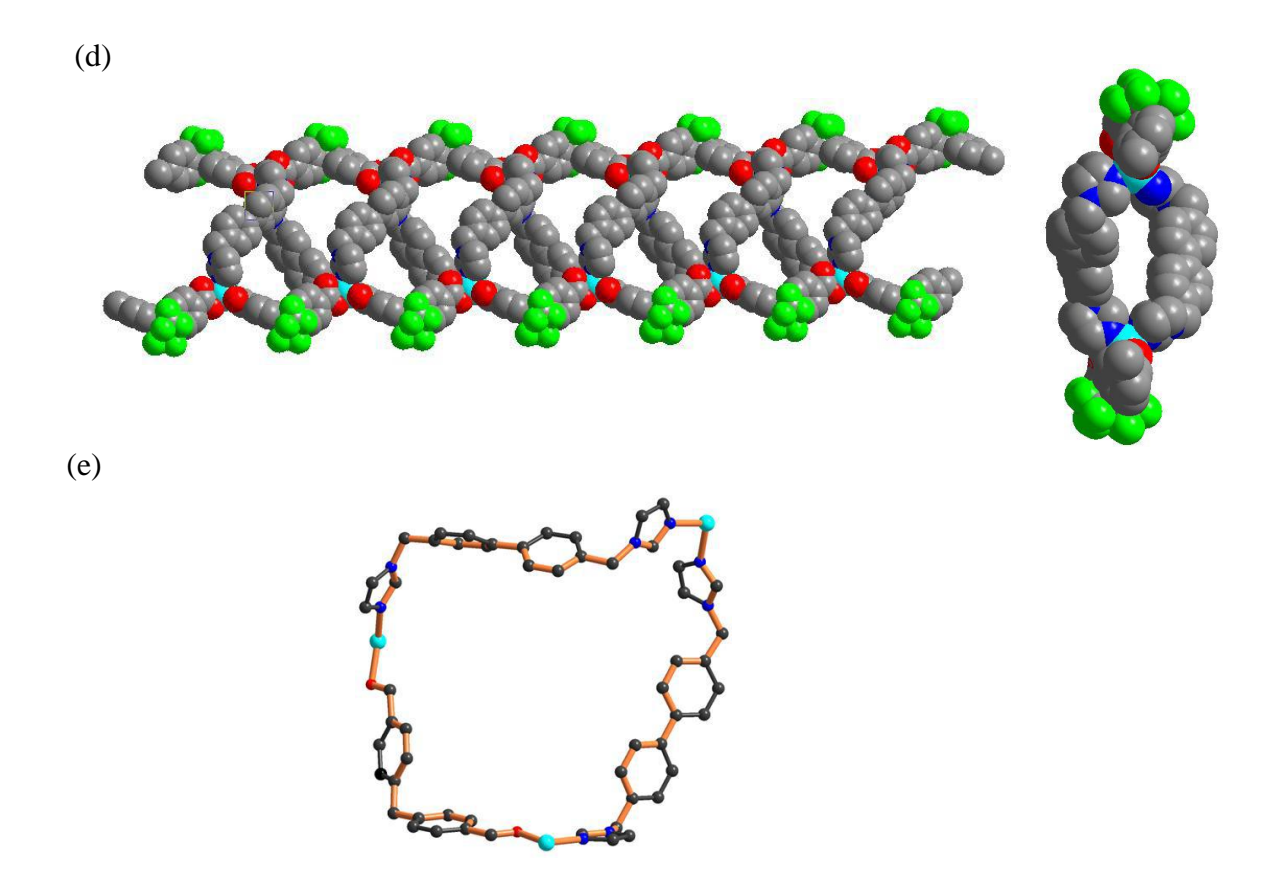
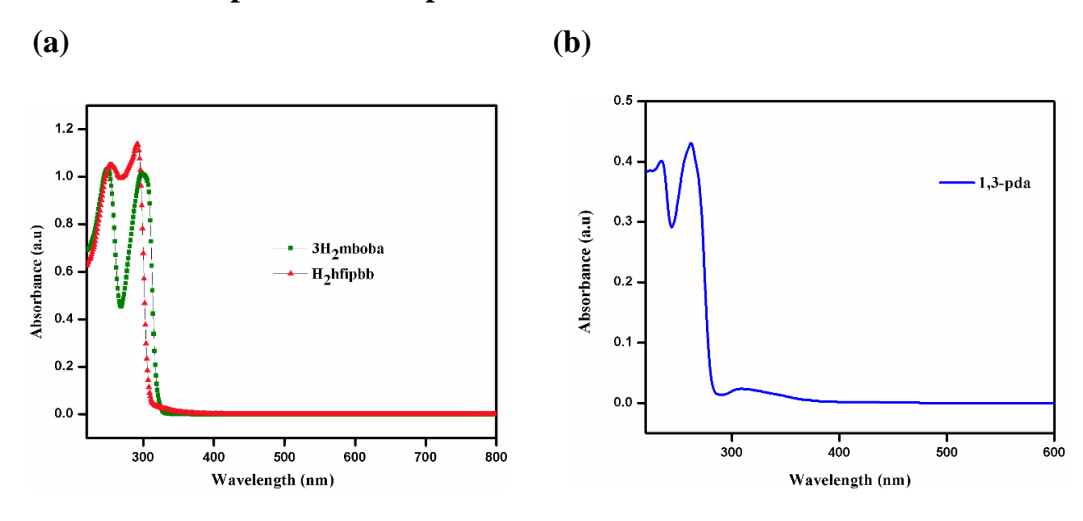


Figure 2. 3. Crystal structure of compound **3**: (a) asymmetric unit in the crystal structure, (b) 1D metal-acid chains, (c) the linking of the metal-acid chains by *bpbix* linker that can adopt two different conformations, Type I and Type II, (d) left: the space-filling plot of the supramolecular pipe and right: the front view of the pipe showing the internal hole of the pipe and (e) representation of the 47-membered metallo-macrocycle ring, the basic building unit of the pipe.

The metallo-macrocycle is separately shown in Figure 2.3e. In the pipe, the Co1-Co2 separation, created by the type I and type II bpbix ligands are 16.56\AA and 16.05\AA respectively.

2.3.2. Electronic Spectra of Compounds 1-3



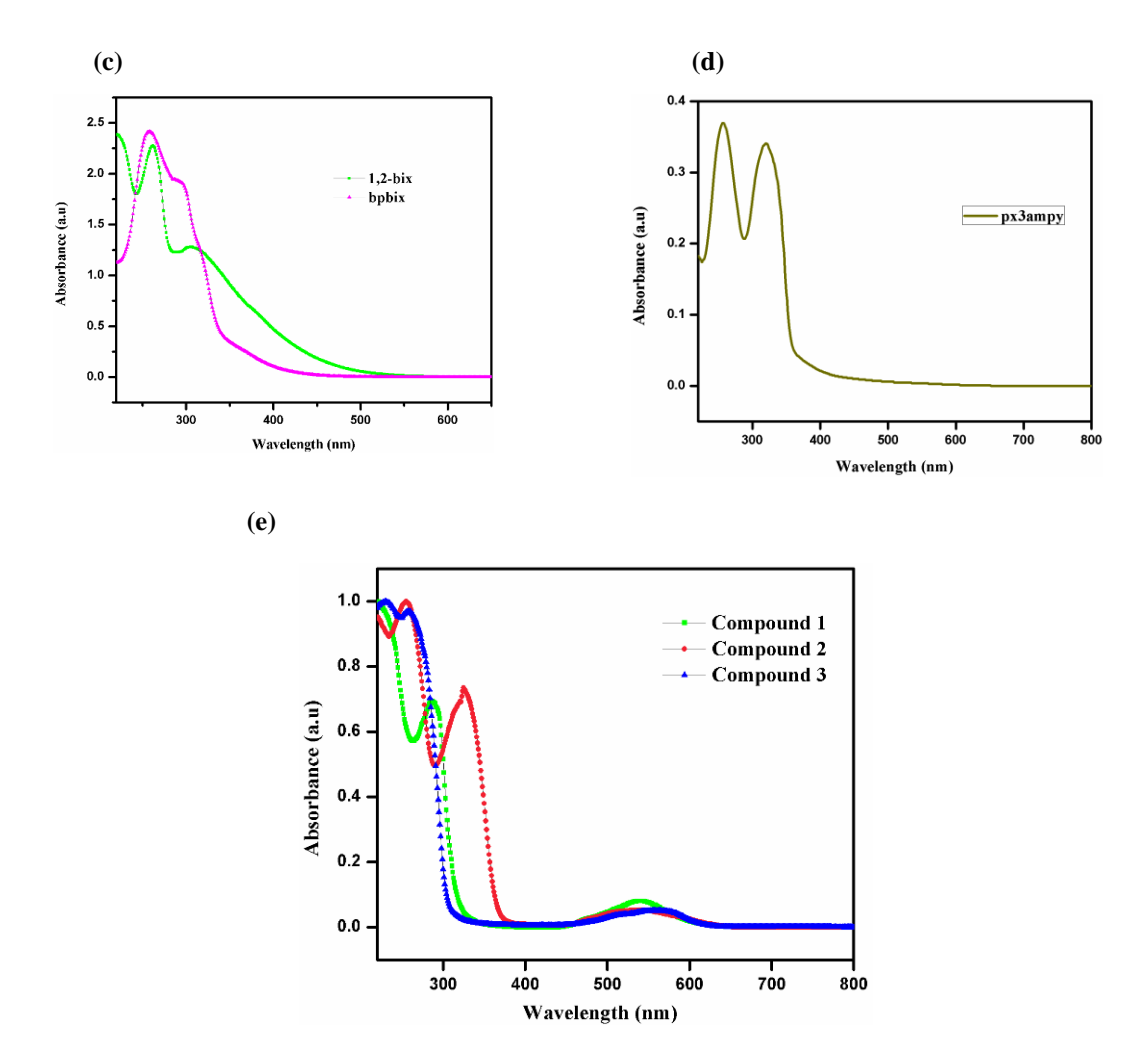


Figure 2.4. Solid state diffuse reflectance (electronic absorption) spectra of the ligands (a) 3mboba, hfipbb, (b)1,3-pda, (c)1,2-bix, (d) bpbix px3ampy and (e) compounds **1-3**.

The solid state electronic properties of the compounds 1-3 have been investigated and the relevant diffuse reflectance spectra are displayed in Figure 2.4. The adsorption peaks at 540, 286 (compound 1), 545, 325, 255 (compound 2) and 554, 258, 230 (compound 3) are observed in the respective spectra. All three compounds have almost identical d-d band at the lower energy range of 540 nm-560 nm. The higher energy bands are comparable with the electronic spectra of the ligands and can be assigned for the intraligand $\pi \cdots \pi^*$ transitions.

2.3.3. PXRD and Thermogravimetric Analysis (TGA)

Powder X-ray diffraction (PXRD) data for the compounds 1 - 3 have been recorded to ensure the phase purity of the products. The corresponding diffraction patterns for the simulated data (calculated from respective single crystal data) and observed data prove the bulk homogeneity of the crystalline solids (Figure 2.5).

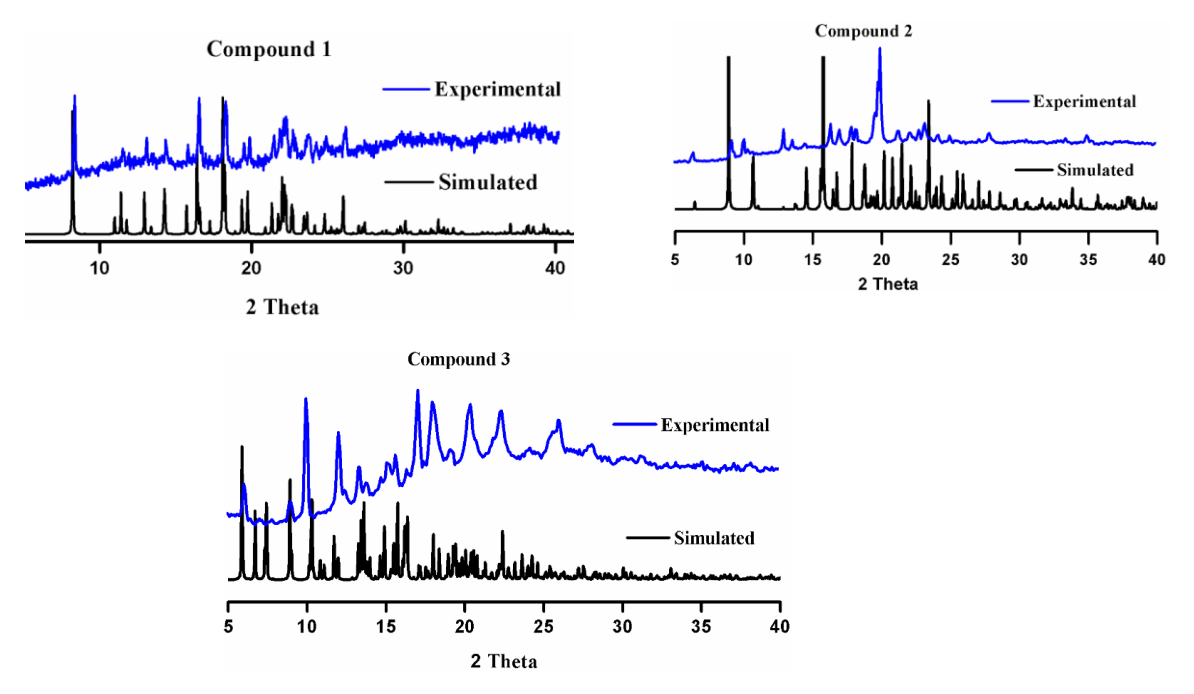


Figure 2. 5. Powder X-ray diffraction patterns of the compounds 1-3.

TGA curves have been recorded under the flow of N_2 for crystalline samples **1–3** in the temperature range 30–1000 °C (Figure 2.6). Compound **1** is stable up to 300° C and then it undergoes continuous weight loss in the temperature range of 300 – 800 °C indicating towards the decomposition of the organic part i.e. 3-mboba and 1,2-bix. The remaining weight is in accordance with the mass of CoO residue. The TGA curve of

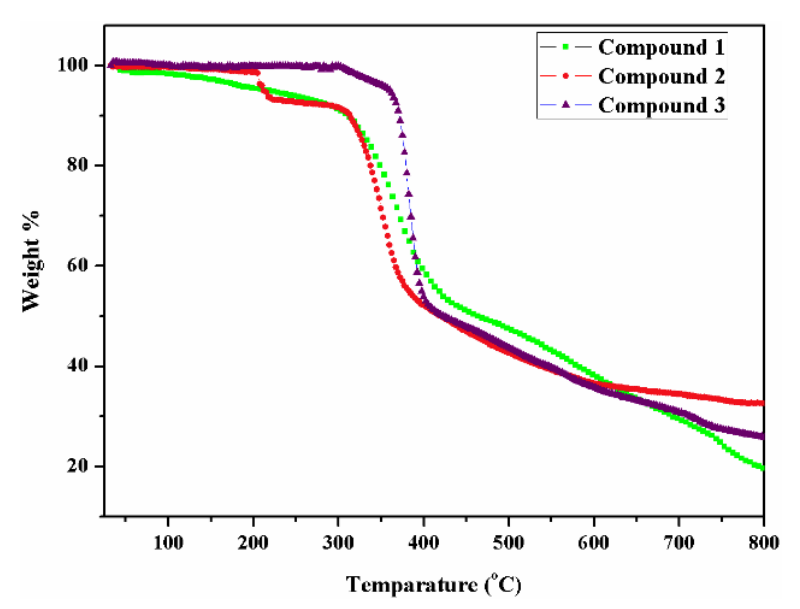


Fig.2. 6. Thermogravimetric plots of the compounds 1-3.

compound 2displays the weight loss 3.6% (calc.3.1%) in the temperature range of 205-217°C indicating loss of coordinated water molecules. It exhibits stability up to 300 °C

followed by continuous decomposition up to 800 °C. Finally, the remaining residue is presumed to be CoO. The TGA curve of compound 3 exhibits stability up to 360 °C, followed by a sharp weight loss due to decomposition of organic moieties present in the compound 3. The comparative thermogravimetric studies show that compound 3 is relatively stable. This is on a par with the formation of coordination polymer tube in the crystals of compound 3.

2.4. Conclusion

In this article, we have demonstrated that diverse metallo-macrocycles can be constructed from a library of three different dicarboxlylic acids (as ligands) and three different N,N linkers. For example, in compound $\{Co(3-mboba)(1,2-bix)_2\}_n$ (1), the formation of two different metallo-macrocycles, namely, 28-membered {Co₂(3-mboba)₂} ring and 24-membered $\{Co_2(1,2-bix)_2\}$ ring is observed; these two macrocycles link in an alternative fashion leading to the construction of one-dimensional coordination polymers the relevant crystals. In the crystal structure of compound $\{Co_2(1,3$ ligand pda)(px3ampy)(H_2O)₂ $\}_n$ **(2)**, a mixed metallo-macrocycle, $\{Co(1,3$ pda)(px3ampy)}, a 25-membered macrocycle ring, is formed. Because of unsaturation in the coordination sphere of cobalt(II) centres in this macrocycle, it undergoes further coordination with adjacent metallo-macrocycles to fulfil saturated coordination resulting in the formation of an 1D coordination of polymer. The metallo-macrocyle, observed in crystal $\{Co_3(hfipbb)(bpbix)_2\},\$ the structure of compound ${Co_2(hfipbb)_2(bpbix)_2}_n$ (3), is not only mixed-ligand macrocycle but also a relatively bigger 47-membered macrocycle with two bpbix linkers and one hfipbb dicarboxylic acid ligand. The relevant crystal structure shows the abundance of a supramolecular pipe, formation of which becomes possible by the adaptation of two different conformations of bpbix N,N linker.

Compounds **1**, **2** and **3** are not soluble in common solvents including water. Therefore, this system can be used as solid host to encapsulate the small molecules (as guests) in the cavities of the metallo-macrocycles in gas-solid / solid-liquid interface reactions. Interestingly, compound {Co₂(1,3-pda)(px3ampy)(H₂O)₂}_n (**2**) is characterized with two coordinated water molecules per merallo-macrocycle along the 1D coordination polymer. These two Co(II)-coordinated water molecules are lost from the system at around 210 °C, as indicated by thermogravimetric studies. Thus compound **2**, having Co^{II}–OH₂

moieties in the macrocycle, has potential to act as heterogeneous electrocatalyst for water oxidation. We are now working in these directions.

Table 1: Crystal data and structural refinement parameters for compounds 1–3.

-	1	2	3
Empirical formula	$C_{29}H_{24}CoN_4O_6\\$	$C_{56}H_{60}Co_2N_8O_{12}$	$C_{74}H_{52}Co_2F_{12}N_8O_8$
Formula weight	583.45	1154.98	1527.10
$T(K) / \lambda(\mathring{A})$	298(2)/0.71073	298(2) /0.71073	298(2) /0.71073
Crystal system	Triclinic	Triclinic	Monoclinic
Space group	P-1	P-1	P2 (1)/c
a (Å)	9.999(2)	9.495(11)	14.160(13)
b (Å)	12.493(3)	10.999(13)	30.094(3)
c (Å)	12.523(3)	14.303(16)	18.219(16)
α (°)	115.27(3)	82.666(2)	90.00
β (°)	98.85(3)	74.097(2)	111.424(10)
γ (°)	91.92(3)	64.650(2)	90.00
Volume (Å ³)	1337.0(5)	1298.4(3)	7227.8(11)
$Z, \rho_{calcd} (g \text{ cm}^{-3})$	2, 1.449	1, 2.086	4, 1.403
$\mu (\text{mm}^{-1}), F(000)$	0.693/602	5.021/784	0.550/3112
goodness- of-fit on F ²	1.122	1.050	1.038
$R1/wR2[I > 2\sigma(I)]$	0.0334/0.0914	0.0508/0.1109	0.0521/0.1395
R1/ wR2 (all data)	0.0427/0.1075	0.0663/0.1182	0.0676/0.1481
Largest diff peak/ hole (e Å-3)	0.253 /-0.295	0.507/-0.289	0.883/-0.403

2.5. References

- 1. (a) T. Kusukawa, M. Fujita, J. Am. Chem. Soc. 124 (2002) 13576;
 - (b)S. Tashiro, M. Tominaga, M. Kawano, B. Therrien, T. Ozki, M. Fujita, J. Am. Chem. Soc. 127 (2005) 4546;
 - (c)A.V. Davis, K.N. Raymond, J. Am. Chem. Soc. 127 (2005) 7912.
- 2. (a) J.R. Li, R.J. Kuppler, H.C. Zhou, Chem. Soc. Rev. 38 (2009) 1477;
 - (b) Z. Zhang, Y. Zhao, Q. Gong, Z. Li, J. Li, Chem. Commun. 49 (2013) 653;
 - (c) S.R. Venna, M.A. Carreon, J. Am. Chem. Soc. 132 (2010) 76;
 - (d) Y.S. Bae, K.L. Mulfort, H. Frost, P. Ryan, S. Punnathanam, L.J. Broadbelt, J.T. Hupp, R.Q. Snurr, Langmuir 24 (2008) 8592.
- 3. (a) L.J. Murray, M. Dinca, J.R. Long, Chem. Soc. Rev. 38 (2009) 1294;
 - (b) N.L. Rosi, J. Eckert, M. Eddaoudi, D.T. Vodak, J. Kim, M. O'Keeffe, O.M. Yaghi, Science 300 (2003) 1127;
 - (c) X. Zhao, B. Xiao, A.J. Fletcher, K.M. Thomas, D. Bradshaw, M.J. Rosseinsky, Science 306 (2004) 1012;
 - (d) K. Sumida, D.L. Rogow, J.A. Mason, T.M. McDonald, E.D. Bloch, Z.R. Herm, T.-H. Bae, J.R. Long, Chem. Rev. 112 (2011) 724.
- (a) P. Horcajada, C. Serre, G. Maurin, N.A. Ramsahye, F. Balas, M. Vallet-Regí,
 M. Sebban, F. Taulelle, G. Férey, J. Am. Chem. Soc. 130 (2008) 6774;
 - (b) P. Horcajada, C. Serre, M. Vallet-Regí, M. Sebban, F. Taulelle, G. Férey, Angew. Chem., Int. Ed. 45 (2006) 5974.
- 5. (a) Y.K. Hwang, D.-Y. Hong, J.-S. Chang, S.H. Jhung, Y.-K. Seo, J. Kim, A. Vimont, M. Daturi, C. Serre, G. Férey, Angew. Chem., Int. Ed. 47 (2008) 4144;
 - (b) J.S. Seo, D. Whang, H. Lee, S.I. Jun, J. Oh, Y.J. Jeon, K. Kim, Nature 404 (2000) 982;
 - (c) C.-D. Wu, A. Hu, W. Lin, J. Am. Chem. Soc. 127 (2005) 8940;
 - (d) C.-D. Wu, W. Lin, Angew. Chem., Int. Ed. 46 (2006) 1075;
 - (e) S.J. Lee, W. Lin, Acc. Chem. Res. 41 (2008) 521.
- 6. (a) N. Yanai, K. Kitayama, Y. Hijikata, H. Sato, R. Matsuda, Y. Kubota, M. Takata, M. Mizuno, T. Uemura, S. Kitagawa, Nat. Mater. 10 (2011) 787;
 - (b) L.E. Kreno, K. Leong, O.K. Farha, M. Allendorf, R.P. Van Duyne, J.T. Hupp, Chem. Rev. 112 (2011) 1105;

- (c) S. Achmann, G. Hagen, J. Kita, I. Malkowsky, C. Kiener, R. Moos, Sensors (2009) 1574.
- 7. (a) T. Yamada, K. Otsubo, R. Makiura, H. Kitagawa, Chem. Soc. Rev. 42 (2013) 6655;
 - (b) M. Sadakiyo, T. Yamada, H. Kitagawa, J. Am. Chem. Soc. 131 (2009) 9906;
 - (c) J.M. Taylor, R.K. Mah, I.L. Moudrakovski, C.I. Ratcliffe, R. Vaidhyanathan, G.K.H. Shimizu, J. Am. Chem. Soc. 132 (2010) 14055;
 - (d) M. Sadakiyo, H. Okawa, A. Shigematsu, M. Ohba, T. Yamada, H. Kitagawa, J. Am. Chem. Soc. 134 (2012) 5472;
 - (e) J.A. Hurd, R. Vaidhyanathan, V. Thangadurai, C.I. Ratcliffe, I.L. Moudrakovski, G.K. Shimizu, Nat. Chem. 1 (2009) 705;
 - (f) D. Umeyama, S. Horike, M. Inukai, Y. Hijikata, S. Kitagawa, Angew. Chem., Int. Ed. 50 (2011) 11706.
- 8. (a) J. Gu, Y. Cui, X. Liang, J. Wu, D. Lv, A.M. Kirillov, Cryst. Growth Des. 16 (2016) 4658;
 - (b) J. Gu, Y. Cui, J. Wu, A.M. Kirillov, RSC Adv. 5 (2015) 78889;
 - (c) J. Gu, A.M. Kirillov, J. Wu, D. Lv, Y. Tang, J. Wu, Cryst. Eng. Comm. 15 (2013) 10287;
 - (d) S.S.P. Dias, M.V. Kirillova, V. André, J. Kłak, A.M. Kirillov, Inorg. Chem. 54 (2015) 5204.
- 9. T.-H. Chen, I. Popov, Y.-C. Chuang, Y.-S. Chen, O.Š. Miljanic´, Chem. Commun. 51 (2015) 6340.
- 10. (a) L.F. Lindoy, K.-M. Parkb, S.S. Lee, Chem. Soc. Rev. 42 (2013) 1713;
 - (b) H. Zhang, R. Zou, Y. Zhao, Coord. Chem. Rev. 292 (2015) 74.
- (a) C.C. Wang, G.B. Sheu, S.Y. Ke, C.Y. Shin, Y.J. Cheng, Y.T. Chen, C.H. Cho,
 M.L. Ho, W.T. Chen, R.H. Liao, G.H. Lee, H.S. Sheu, Cryst. Eng. Comm. 17 (2015) 1264;
 - (b) J.H. Park, A.R. Jeong, J.W. Shin, M.J. Jeong, C.S. Cho, K.S. Min, Inorg. Chem. Commun. 57 (2015) 44;
 - (c) X.D. Zhu, Z.J. Lin, T.F. Liu, B. Xu, R. Cao, Cryst. Growth. Des. 12 (2012) 4708;
 - (d) X.R. Meng, D.C. Zhong, L. Jiang, H.Y. Li, T.B. Lu, Cryst. Growth. Des. 11 (2011) 2020.

- 12. M.J. Prakash, M.S. Lah, Chem. Commun. (2009) 3326.
- 13. (a) P. Manna, B.K. Tripuramallu, S. Bommakanti, S.K. Das, Dalton Trans. 44 (2015) 2852;
 - (b) M.-L. Zhang, Ji.-J. Wang, Z.-Z. Ma, L. Qiao, New J. Chem. 41 (2017) 12139;
 - (c) B.K. Tripuramallu, P. Manna, S.K. Das, Cryst. Eng. Comm. 16 (2014) 4816.
- 14. (a) Y.-Q. Lan, S.-L. Li, J.-S. Qin, D.-Y. Du, X.-L. Wang, Z.-M. Su, Q. Fu, Inorg. Chem. 47 (2008) 10600;
 - (b) A. Karmakar, I. Goldberg, Cryst. Eng. Comm. 13 (2011) 339;
 - (c) A. Karmakar, I. Goldberg, Cryst. Eng. Comm. 13 (2011) 350.
- 15. B.K. Tripuramallu, P. Manna, S.N. Reddy, S.K. Das, Cryst. Growth. Des. 12 (2012) 777.
- 16. P. Manna, S.K. Das, Cryst. Growth. Des. 15 (2015) 1407.
- 17. (a) L.N. Zhu, S. Gao, L.H. Huo, Acta. Crystallogr., Sect. E (2007), E63 o4459;
 - (b) R.Y. Zou, F.B. Xu, Q.S. Li, H.B. Song, H. Lv, Z.Z. Zhang, Acta Crystallogr., Sect. E (2003), E59 o1312.
- 18. (a) SAINT: Software for the CCD Detector System; Bruker Analytical X-ray Systems Inc: Madison, WI, 1998;
 - (b) SADABS: Program for Absorption Correction; Sheldrick, G.M. University of Gottingen: Gottingen, Germany. 1997;
 - (c) SHELXS-97: Program for Structure Solution; Sheldrick, G. M. University of Gottingen: Gottingen, Germany, 1997;
 - (d) SHELXL-97: Program for Crystal Structure Analysis; Sheldrick, G.M. University of Gottingen: Gottingen, Germany, 1997.

A 'two-in-one' crystal having two different dimensionality in the extended structures: A series of cadmium(II) coordination polymers from V-shaped organic linkers

Three Cd(II) containing coordination polymers, formulated as $\{Cd(oba)(biip)\}_n \cdot nH_2O$ (1), $\{Cd(sdba)(biip)\}_n \cdot n5H_2O$ (2) and $\{[Cd_{1.5}(hfipbb)_2(biip)_{1.5}(H_2O)][Cd(hfipbb)(biip)]\}_n \cdot n2H_2O$ (3), have been synthesized by using ditopic V-shaped ligands *i.e.*, H_2oba (4,4'-oxydibenzoic acid), H_2sdba (4,4'-thiodibenzoic acid), $H_2hfipbb$ {4,4'-(perfluoropropane-2,2-diyl)dibenzoic acid} and an auxiliary linker, biip {3,5-di(1H-imidazol-1-yl)pyridine} under solvothermal conditions. Compounds 1–3 are characterized by single crystal X-ray diffraction analysis, IR spectroscopy, thermogravimetric (TG) and elemental analyses. Compound 1 contains a 3D framework, formed by the connectivity of $\{CdO_4N_2\}$ secondary building unit (SBU) with the organic linkers, whereas compound 2 is a 2D coordination polymer. Interestingly, unlike to compounds 1 and 2, compound 3 possesses a distinctive structural feature having two crystallographically independent polymeric motifs (polymers, A and B) having two different dimensionality within the same crystal, *i.e.*, coordination polymer A (CP-A) that forms a one-dimensional motif and coordination polymer B (CP-B), which has a two-dimensional structure.

3.1. Introduction

The synthesis of new coordination polymers (CPs) or metal-organic framework (MOF) containing compounds by the rational combination of organic ligands and metals through the 'self-assembly' process is an interesting aspect of 'structural chemistry'. An infinite number of coordination polymers with different dimensionalities (one, two and three) have been synthesized from various metal ions in combination with linear and non-linear organic building units (OBUs) as spacer linkers. MOF containing compounds have been extensively explored in different interdisciplinary areas due to their wide range of potential applications, for example, in gas adsorption and separation, ¹ catalysis, ² sensing, ³ host—guest induced separation, ⁴ drug delivery ⁵ etc. The design and construction of these materials are not only significant for their functional applications, but also because of their ability to form aesthetically pleasing structures. The formation of interesting architectures is, somewhat, predicted by the crystal engineering which, in turn, is governed by the supramolecular interactions, such as hydrogen bonding, halogen interactions and other non-covalent interactions, present in the concerned material.

Recently, increasing number of publications are seen in the literature reporting either 'entangled polymeric systems' or 'polythreaded supramolecular architectures', in which two or more independent polymeric motifs are packed within the same crystal having same or different dimensionalities.⁶ In general, the entangled coordination networks or MOFs are formed either by simple interpenetration (parallel or inclined interpenetration of individual layers) or by inextricable interpenetration as seen in polycatenanes, polyrotaxanes, molecular knots, polythreaded networks and so on.⁷

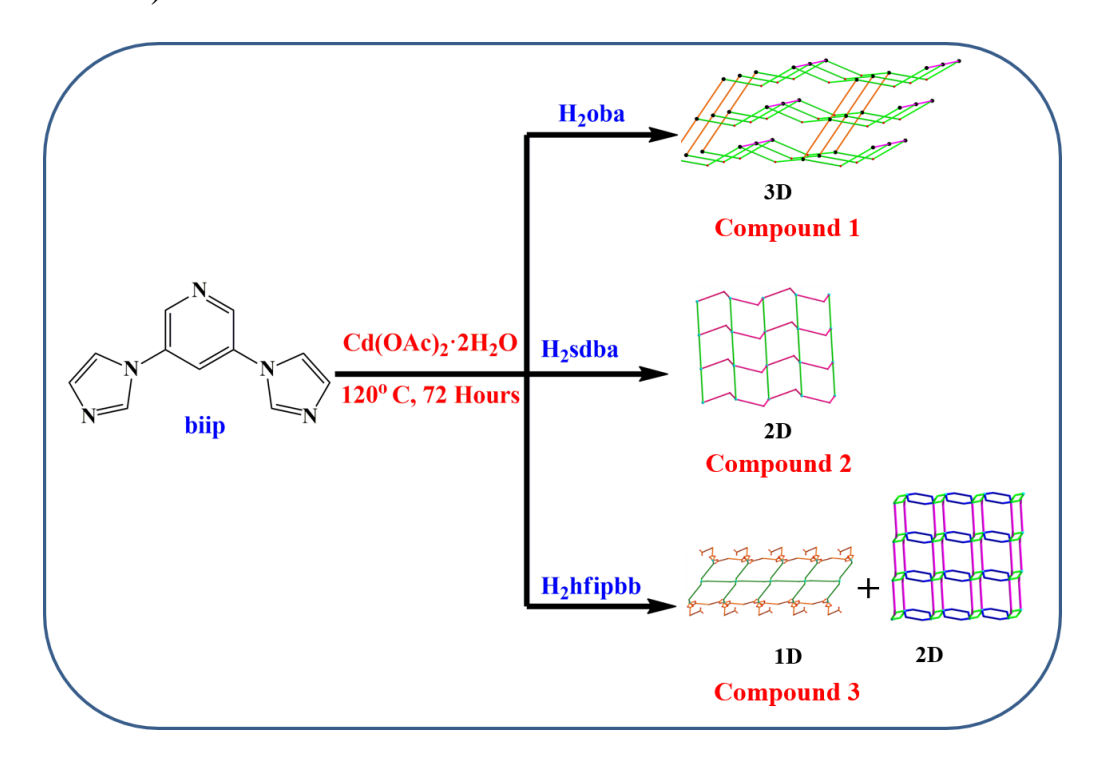
Many up-to-date investigations are focused on the design of new molecule-based functional materials. In this regard, Batten and Robson reported a variety of interpenetrating structures.⁸ However, distinctive coordination polymers co-existing within the same crystal structure, are fairly rare in the literature. Coordination polymers having diverse structural motifs with different dimensionality within the same crystal are found to result in the formation of **2D** and **3D** structures, for example: 2D layers + 1D double linear chain + 1D chains \Rightarrow 3D, 9,10,11 2D layers + 2D layers \Rightarrow 3D, 12,13,14 1D chains + 2D net \Rightarrow 2D, 15 1D chains \Rightarrow 3D, 16 2D sheets + 3D network \Rightarrow 3D, 17 2D sheets \Rightarrow 2D networks, 18 1D chain + 2D layers \Rightarrow 3D

net,¹⁹ 1D ladders + 1D chains \Rightarrow 3D,²⁰ 2D square grids + 1D linear chain \Rightarrow 3D,²¹ 1D double chain + 2D net \Rightarrow 2D polycatenation,²² 1D ribbons + 2D network \Rightarrow 3D,²³ two 1D chains + two 2D double layers \Rightarrow 3D,²⁴ three 1D chains + 2D layers \Rightarrow 3D,¹¹ 1D ribbons of rings + 2D network \Rightarrow 3D,²⁵ 3D network + 3D network \Rightarrow 3D²⁶ supramolecular structures.

Herein, we have synthesized three new coordination polymers starting from Cd(OAc)₂·2H₂O and three ditopic V-shaped ligands (as shown in Scheme 1) i.e., H2oba (4,4'-oxydibenzoic acid), H2sdba (4,4'-thiodibenzoic acid), H2hfipbb {4,4'-(perfluoropropane-2,2-diyl)dibenzoic acid} and a N,N linker, biip {3,5-di(1Himidazol-1-yl)pyridine} under solvothermal conditions. All these compounds $\{Cd(oba)(biip)\}_n \cdot nH_2O$ (1), $\{Cd(sdba)(biip)\}_n \cdot n5H_2O$ (2),and $\{[Cd_{1.5}(hfipbb)_2(biip)_{1.5}(H_2O)][Cd(hfipbb)(biip)]\}_n \cdot n2H_2O$ (3) are characterized by routine spectral techniques, such as, Infrared- and electronic absorptionspectroscopy, thermal analysis including CHN analysis and unambiguously by single crystal X-ray diffraction (SCXRD) studies. Compound 1 shows a threedimensional network, whereas compound 2 exhibits a two-dimensional structure. In contrast to compounds 1 and 2, compound 3 possesses a distinctive structural feature having two crystallographically independent polymeric motifs (coordination polymers -A and -B) within the same crystal with two different dimensionality; CP-

Scheme 3.1. The V-shaped ligands, used to synthesize the compounds 1–3 in the present study.

A forms a one-dimensional motif and **CP-B** is a two-dimensional structure (see Scheme 2).



Scheme 5.2. Representation of synthetic protocol of compounds 1–3.

The interpenetration of **1D** chains of **CP-A** into the **2D** layers of **CP-B** results in an overall three-dimensional supramolecular architecture in the crystal structure of compound **3**. All three compounds show good thermal stability as evidenced by the TGA analysis.

3.2. Experimental

3.2.1. Materials and physical Methods

All the chemicals and solvents were received as reagent grade and used without any further purification. The chemicals H_2 oba, H_2 sdba, H_2 hfipbb were purchased from Aldrich. The metal salt {Cd(OAc) $_2 \cdot 2H_2O$ } and DMF solvent were procured from SDFCL and Finar (India), respectively. The auxiliary ligand, biip-{3,5-di(1H-imidazol-1-yl)pyridine}, was prepared following the literature procedure.²⁷

3.2.2. Characterization

Elemental analyses were determined by FLASH EA series 1112 CHNS analyser. Thermogravimetric analyses were carried out on a STA 409 PC analyser under the flow of N_2 gas with a heating rate of 5 °C min⁻¹, in the temperature range of 30–750 °C. Infrared

spectra of solid samples obtained as KBr pellets on a JASCO-5300 FT-IR spectrophotometer. Powder X-ray diffraction patterns were recorded on a Bruker D8-Advance diffractometer using graphite monochromated CuKα1 (1.5406 Å) and Kα2 (1.54439 Å) radiations. All the compounds were synthesized in 23 mL Teflon-lined stainless-steel vessels (Thermocon, India) under solvothermal conditions. The electronic absorption spectra have been recorded in the solid state on a UV-2600 Shimadzu UV-visible spectrophotometer at room temperature. Gas adsorption isotherms of all the compounds were performed by using Autosorb iQ, Quantachrome gas adsorption analyzer.

3.2.3. Synthesis

Synthesis of compound $\{Cd(oba)(biip)\}_n \cdot nH_2O(1)$

A mixture of Cd(OAc)₂·2H₂O (0.1 mmol, 26.6 mg), H₂oba (0.1 mmol, 25.8 mg), and biip (0.1 mmol, 21.1 mg), taken in a mixed solvent — H₂O (6 mL) and DMF (2 mL) — was stirred for 30 minutes and then the pH of the reaction mixture was adjusted to 6.1 by adding few drops of aq. NaOH solution (0.5 M conc.). The resulting reaction mixture was then placed in a 23 mL Teflon-lined stainless-steel autoclave, which was sealed and heated at 120 °C for 72 hours. The autoclave was allowed to cool to room temperature over 48 hours to obtain colourless block shaped crystals of compound **1** in 67.5% yield (based on Cd). Anal. Calcd. for $C_{25}H_{19}N_5CdO_6$ (Mr = 597.86): C, 50.22%; H, 3.2%; N, 11.71%. Found: C, 50.29%; H, 2.83%; N, 11.65%. IR (KBr pellet, cm⁻¹): 1593(br), 1551(m), 1500(m), 1391(br), 1303(s), 1257(m), 1164(s), 1102(m), 1014(m), 952(m), 880(m), 849(m), 777(s), 658(s), 606(m), 523(m), 503(m).

Synthesis of compound $\{Cd(sdba)(biip)\}_n \cdot n5H_2O(2)$

Compound **2** was prepared by following the same procedure as that of compound **1** except that the ligand H_2 sdba (0.1 mmol, 30.6 mg) was used in place of H_2 oba ligand and the pH of the reaction mixture was adjusted to 7.5 in this case. After the completion of the reaction, colourless block shaped crystals were obtained by filtration in 62.4% yield (based on Cd). Anal. Calcd. for $C_{25}H_{27}CdN_5O_{11}S$ (Mr = 717.98): C, 41.82%; H, 3.79%; N, 9.75%. Found: C, 41.32%; H, 3.65%; N, 9.56%. IR (KBr pellet, cm⁻¹): 3256(br), 1589(s), 1547(m), 1507(m), 1395(m), 1316(m), 1297(m), 1270(m), 1250(m), 1163(m), 1134(s), 1100(m), 1070(s), 1011(m), 956(m), 936(m), 850(m), 783(s), 744(m), 727(m), 691(m), 648(m), 618(s), 580(m).

Synthesis of compound $\{[Cd_{1.5}(hfipbb)_2(biip)_{1.5}(H_2O)][Cd(hfipbb)(biip)]\}_n \cdot n2H_2O$ (3)

Compound **3** was also prepared by following the same procedure used for synthesizing compound **1** except that the ligand H_2 oba was replaced with H_2 hfipbb (0.1 mmol, 39.4 mg) and the pH of the reaction mixture was adjusted to 6.5. The resulting colorless needle shaped crystals were isolated by filtration in 60.5% yield (based on Cd). Anal. Calcd. for $C_{80.5}H_{52}Cd_{2.5}F_{18}N_{13}O_{15}$ (Mr = 2064.38): C, 46.84%; H, 2.54%; N, 8.82%. Found: C, 46.19%; H, 2.41%; N, 8.65%. IR (KBr pellet, cm⁻¹): 3114(br), 1672(m), 1600(m), 1512(m), 1394(s), 1316(m), 1249(s), 1209(m), 1166(s), 1135(m), 1070(m), 1010(m), 970(m), 943(m), 928(m), 897(m), 849(m), 800(m), 777(m), 747(m), 723(s), 700(s), 651(m).

3.2.4. Single Crystal X-ray Structure Determination of the Compounds 1–3

Data for single-crystals of all the compounds 1-3 were collected on a Bruker D8 Quest CCD diffractometer under a Mo-K α ($\lambda = 0.71073$ Å) graphite monochromatic X-ray beam with a crystal-to-detector distance of 40 mm. The data reduction was performed using Apex-II Software.²⁸ Empirical absorption corrections using equivalent reflections were performed with the SADABS program.²⁹ Structure solutions, and full-matrix leastsquares refinement were carried out using standard crystallographic software package for all the compounds. 30,31 All the non-hydrogen atoms were refined anisotropically. Hydrogen atoms on the C atoms were introduced at calculated positions on their respective parent atoms and were included in the refinement riding model. Attempts to locate hydrogen atoms for the solvent molecules (water- for all compounds) in the crystal structures through Fourier electron density map were not successful. Hence these atoms were made to fix on their parent atoms at calculated positions. The carboxylate oxygen atoms of oba²⁻ and sdba²⁻ i.e., O4 and O6 in the crystal structures of compounds 1 and 2, respectively, exhibit some disorder because of diffused electron densities which in turn leads to splitting of these atoms. The Alert 2 A (large solvent Accessible VOIDS) in compounds 2 and 3 is the result of removing residual electron density of the disordered solvent molecules using PLATON tool of WINGX software package. In compound 3, the pyridine ring of biip ligand along with half part of the imidazole ring in CP-A resides in highly disordered environment, due to which we could not model this part of the ligand, despite of several attempts. This resulted in Alert 2A and 2B pertaining to the ADP issues of C81, N12 and C76 of biip ligand. The corresponding unit cell and refinement parameters for the single crystals of all three compounds are given in Table 3.1.

3.3. Results and Discussion

3.3.1. Synthesis

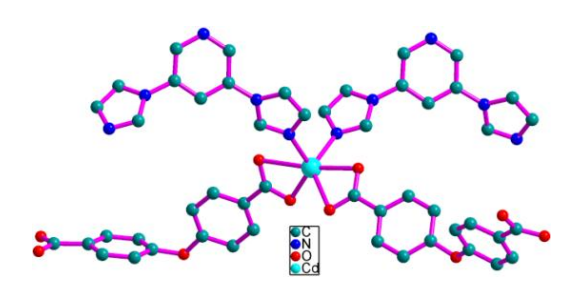
In this work, three different dicarboxylic acids (Schemes 1 and 2) and a common neutral 'N' donor ligand (biip) have been employed to synthesize three different compounds $\{Cd(oba)(biip)\}_n \cdot nH_2O$ (1), $\{Cd(sdba)(biip)\}_n \cdot n5H_2O$ (2) and $\{[Cd_{1.5}(hfipbb)_2(biip)_{1.5}(H_2O)][Cd(hfipbb)(biip)]\}_n \cdot n2H_2O$ (3). In all three concerned syntheses, NaOH has been utilized to deprotonate the carboxylic acids. The temperature and time duration of the solvothermal syntheses have been kept identical for all three syntheses. Even then, the title compounds show diversity in terms of their supramolecular structures. This is because the dicarboxylic acids, H_2 oba, H_2 sdba and H_2 hfipbb — the V-shaped ligands used to synthesize compounds 1, 2 and 3, respectively — are diverse in relation to their non-aromatic components excluding the dicarboxylic acids.

3.3.2. Description of Crystal Structures

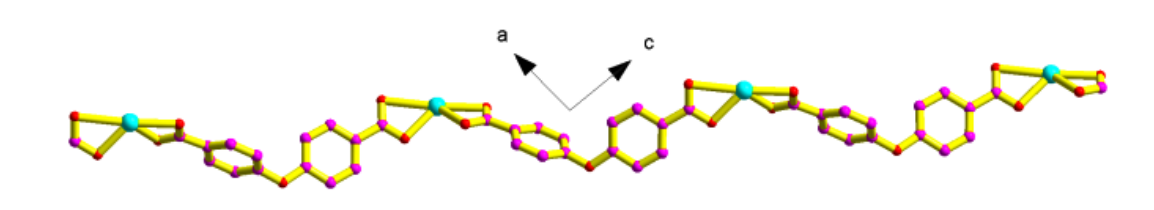
Compound $\{Cd(oba)(biip)\}_n \cdot nH_2O(1)$

Single crystal X-ray analysis reveals that the compound $\{Cd(oba)(biip)\}_n \cdot nH_2O$ (1) crystallizes in monoclinic space group C2/c. The concerned asymmetric unit consists of one Cd(II) center, one oba²-ligand, one bijp ligand and a lattice water molecule. As shown in Figure 3.1a, the Cd(II) centre is coordinated by the four oxygen atoms and two nitrogen atoms from two oba²- ligands and two biip ligands respectively, to form a distorted octahedral {CdO₄N₂} coordination sphere which act as a secondary building unit (SBU) in this compound. All the Cd-O bond distances are in the range of 2.213-2.663 Å and Cd-N bond distances are 2.239 and 2.359 Å. The bond angles between the Cd(II) centre and coordinated atoms are in the range of 54.4-135°. The dihedral angles between the two carboxylate groups and the two phenyl rings of oba²⁻ ligand are 81.77° and 74.04°, respectively. The dihedral angle between two imidazole rings of biip ligand is found to be 71.98°. The carboxylate groups of oba²⁻ ligand attain bidentate μ_1 - η^1 : η^1 coordination mode while connecting to the metal center. In this way, each oba²⁻ ligand connects to two Cd(II) metal centres from two sides resulting in the formation of 1D metal-acid chain along the crystallographic 'ac' plane as shown in Figure 3.1b. The two metal centre's within the onedimensional chain are separated through oba²⁻ at a distance of 15.32 Å.

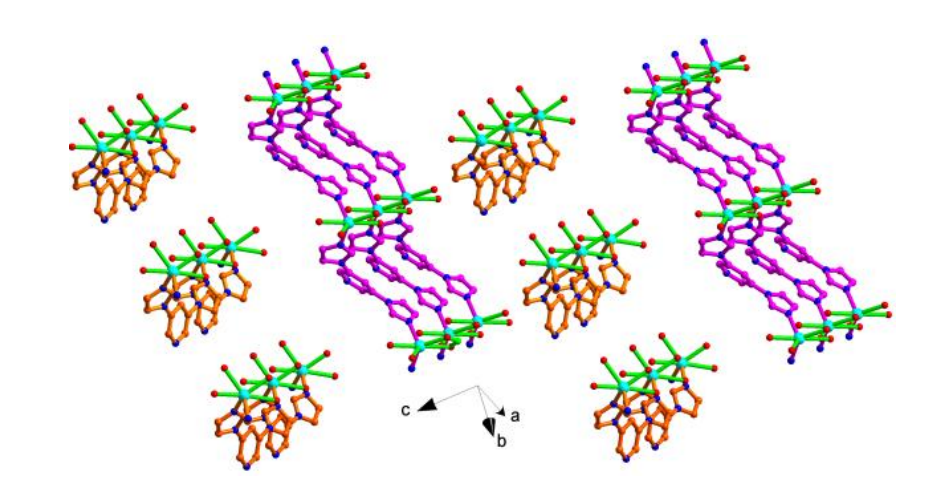




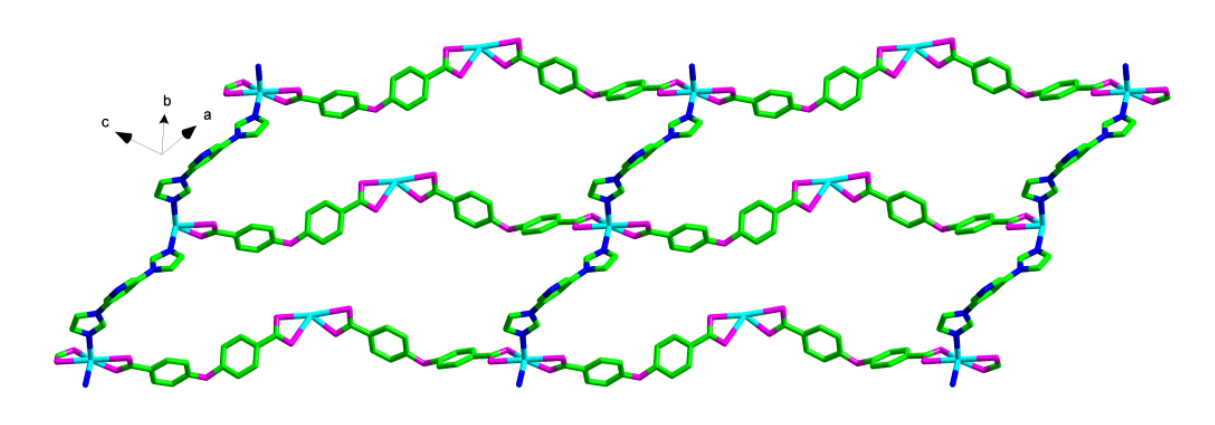
(b)



(c)



(d)



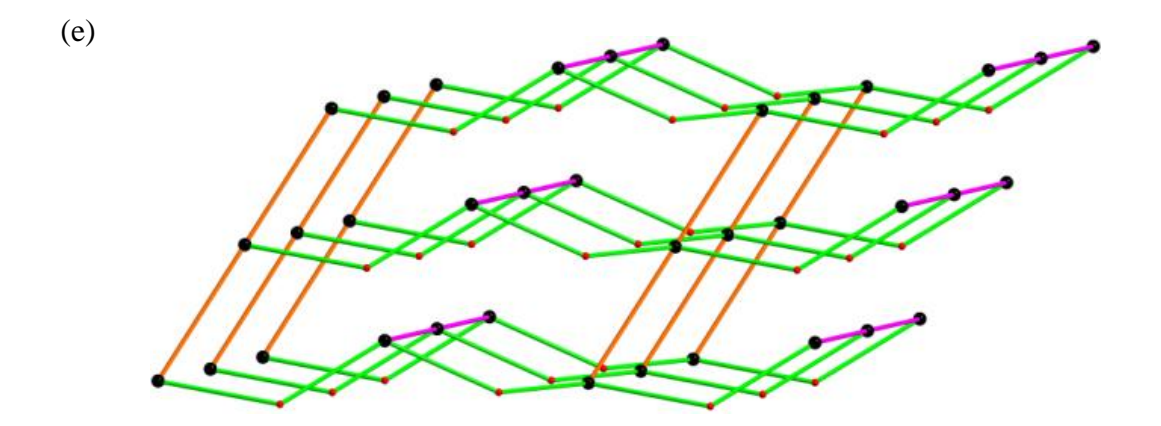


Figure 3.1 Crystal structure of compound $\{Cd(oba)(biip)\}_n \cdot nH_2O$ (1): (a) Molecular diagram representing the coordination environment around the Cd(II) metal ion; hydrogen atoms are omitted for clarity, (b) 1D chain, formed by the connectivity of oba^{2^-} ligands with the Cd(II) metal centers along the crystallographic 'ac' plane, (c)The biip linkers are coordinated to the metal centres to form two different 1D metal-linker chains in two different crystallographic axes *i.e.*, 'a' and 'b', (d) 2D layered structure, formed due to connectivity of 1D chains with the biip linkers and (e) 3D topological representation of 1.

On the other hand, the biip linkers are coordinated to the metal centres to form two different 1D metal-linker chains in two different crystallographic axes *i.e.*, 'a' and 'b' (Figure 3.1c). The Cd(II) centers in 1D metal-acid-chains, that are parallel to each other, are connected by biip ligands (through N donors) along the crystallographic 'a' axis resulting in the formation of 2D layered structure as shown in Figure 3.1d. These 2D layers are further are pillared by the biip linkers along the crystallographic 'b' axis to give an overall 3D structure for compound 1 (Figure 3.1e).

Compound $\{Cd(sdba)(biip)\}_{n} \cdot n5H_2O(2)$

Single crystal X-ray analysis of compound $\{Cd(sdba)(biip)\}_n\cdot 5nH_2O$ (2) shows that it is a 2D coordination polymer, which crystallizes in the monoclinic space group P2(1)/c. The relevant asymmetric unit contains one Cd(II) metal centre, one completely deprotonated $sdba^{2-}$, one biip ligand and lattice water molecules as shown in Figure 3.2a (four lattice water molecules are present in highly disordered environment affecting the overall data, hence the SQUEEZE option was employed). In the crystal structure, the Cd(II) ion is coordinated by four oxygen atoms from two $sdba^{2-}$ and two nitrogen atoms from two biip ligands resulting in a distorted octahedral $\{CdO_4N_2\}$ coordination moiety, which acts as a secondary building unit (SBU). The relevant Cd-O bond lengths are in the range of 2.229-2.673 Å and the Cd-N bond lengths are 2.222 and 2.236 Å. The bond angles around the Cd(II) metal centre are in the range of 54.67 to 136.17° . The dihedral angle between the two imidazole rings in the biip is found to be 63.62° , which is lesser than the

dihedral angle between the same found in the crystal structure of compound 1. The carboxylate groups of $sdba^{2-}$ ligand exhibit μ_1 - η^1 : η^1 coordination mode and connect to

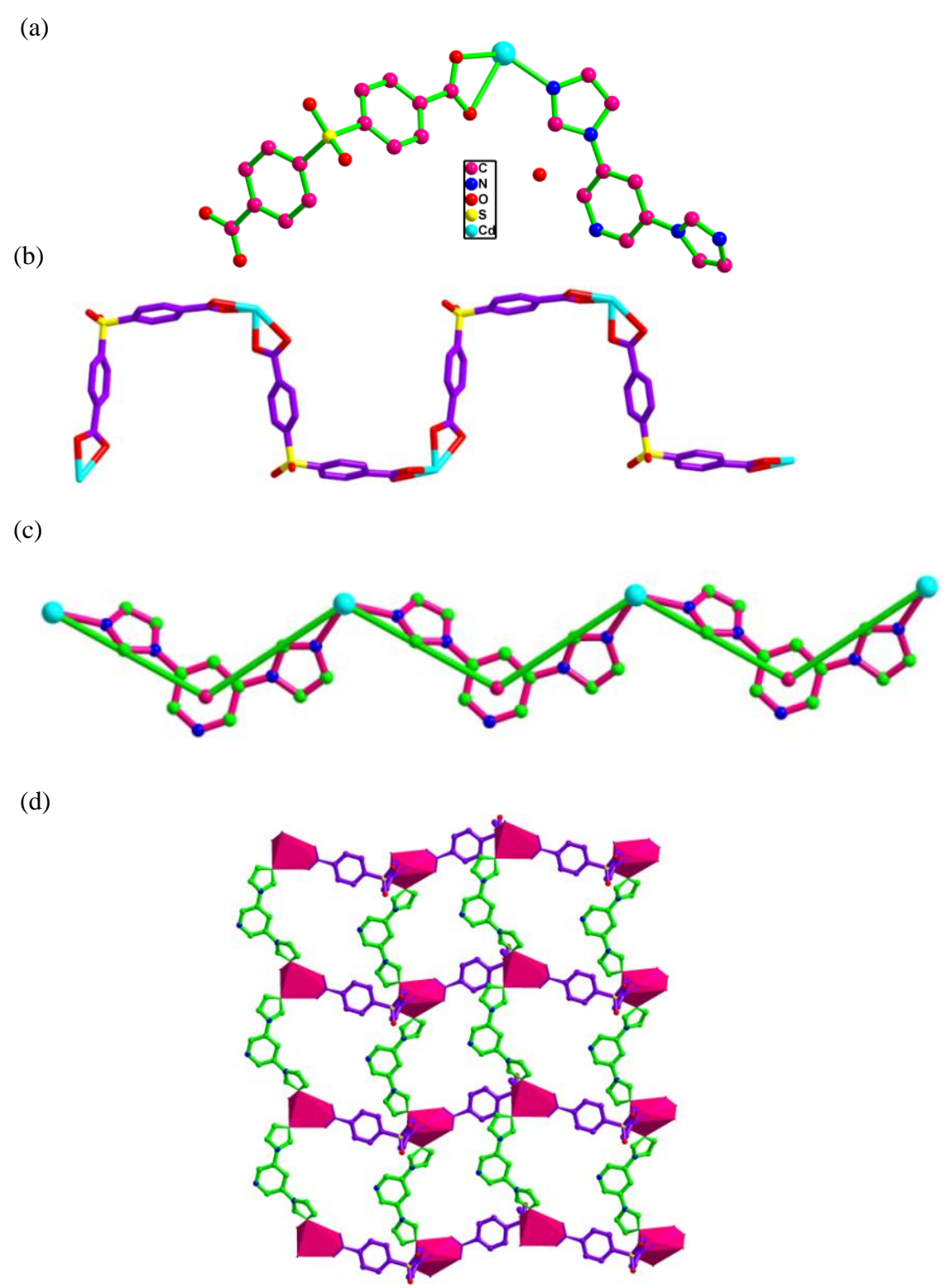


Figure 3.2 Crystal structure of compound $\{Cd(sdba)(biip)\}_n \cdot n5H_2O$ (2): (a) Asymmetric unit, (b) 1D square wave-like chain, formed by the connectivity of $sdba^{2-}$ ligands with Cd(II) metal centers, (c) 1D chain with the V-shaped geometry of the biip ligand and (d) 2D structure, formed by the connectivity of $sdba^{2-}$ and biip ligands with the SBUs.

Cd(II) centres resulting in the formation of 1D square wave-like chain (Figure 3.2b). Two Cd(II) centres along the chain are separated by the sdba²⁻ ligands through a distance of 13.59 Å. The biip ligands are coordinated to Cd(II) centres resulting the formation of 1D zig-zag chainlike arrangement (Figure 3.2c). The crossover of these two 1D chains through metal centers results in the formation of a 2D structure as represented in Figure 3.2d.

Compound $\{[Cd_{1.5}(hfipbb)_2(biip)_{1.5}(H_2O)][Cd(hfipbb)(biip)]\}_n \cdot n2H_2O$ (3)

Single crystal X-ray diffraction analysis reveals that, compound $\{[Cd_{1.5}(hfipbb)_2(biip)_{1.5}(H_2O)][Cd(hfipbb)(biip)]\}_n \cdot n2H_2O$ (3) crystallizes in triclinic space group P-1. As shown in Figure 3.3a, the asymmetric unit contains two coordination polymers i.e., $\{Cd_{1.5}(hfipbb)_2(biip)_{1.5}(H_2O)\}$ (**CP-A**) and $\{Cd(hfipbb)(biip)\}_n$ (**CP-B**), and lattice water molecules. The relevant structure contains highly disordered solvent molecules in the crystal sktructure; hence the SQUEEZE option was used. This squeezed electron density accounts for one water molecule per asymmetric unit (ASU), which is consistent with the CHN- and TGA- experimental analyses.

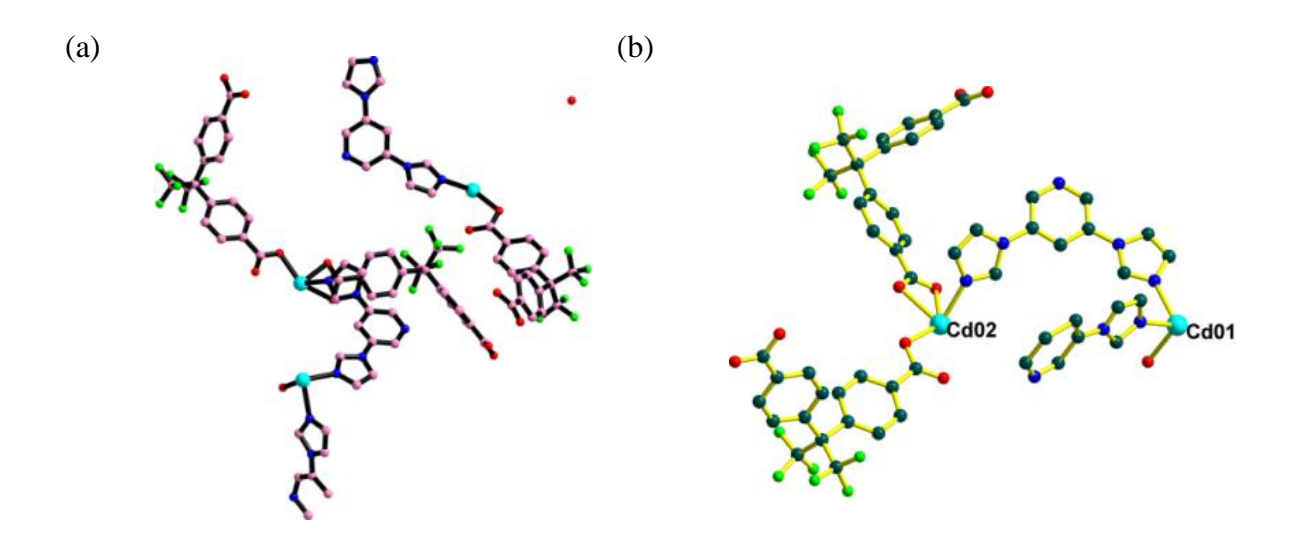
Structural depiction of {Cd_{1.5}(hfipbb)₂(biip)_{1.5}(H₂O)} (**CP-A**):

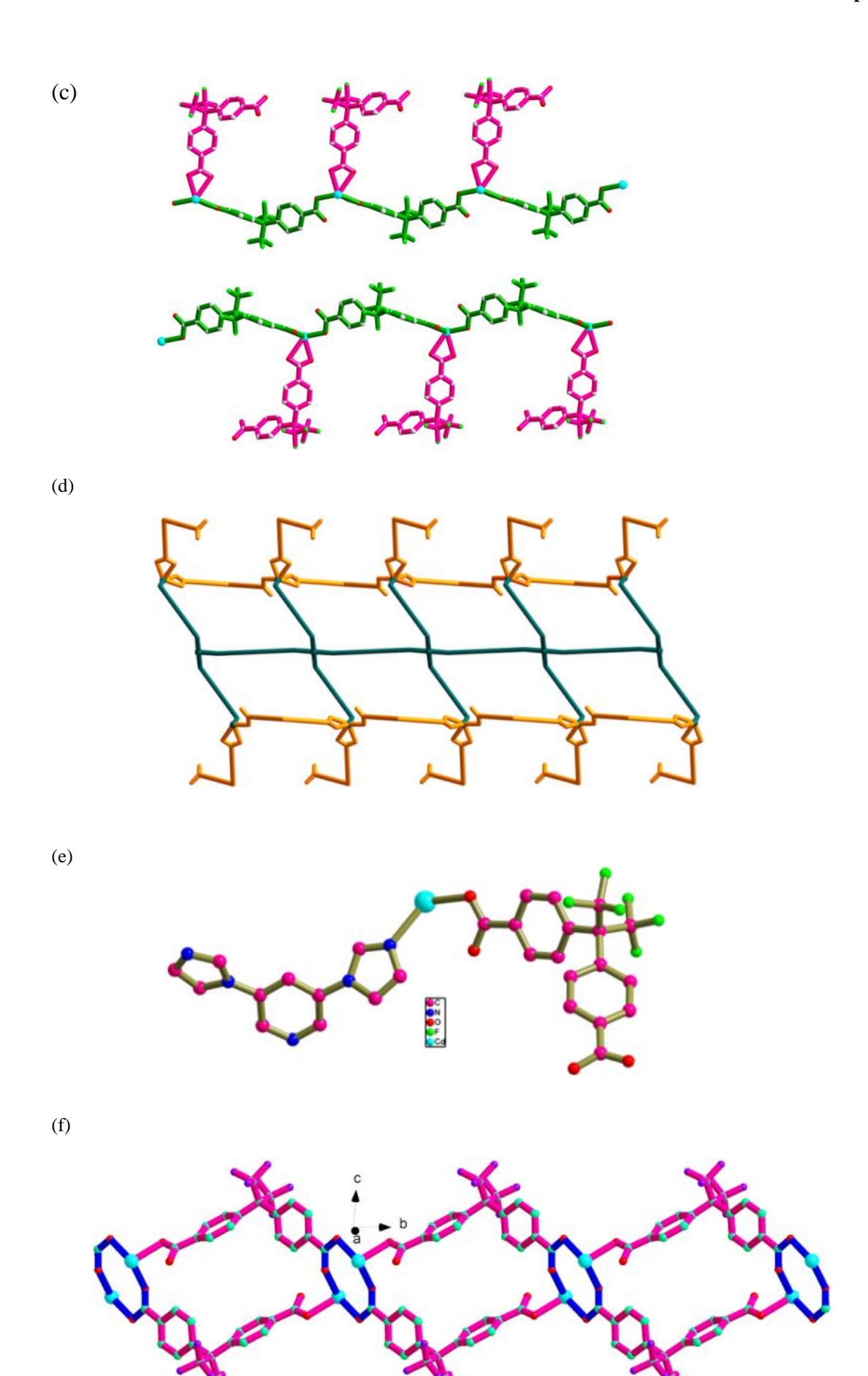
CP-A consists of two crystallographically independent Cd(II) ions (Cd01 and Cd02), two hfipbb²⁻, two biip linkers and one coordinated water molecule (Figure 3.3b). Overall, in the crystal structure, the Cd01 is in slightly distorted octahedral environment defined by two oxygen atoms and four nitrogen atoms from two coordinated water molecules and four biip linkers, respectively. The Cd02 also adopts distorted octahedral coordination geometry, which is completed by five oxygen atoms and one nitrogen atom from three hfipbb²⁻ ligands and one biip linker, respectively. In **CP-A**, the Cd–O bond distances are in range of 2.206–2.645 Å, which are similar to those of other reported cadmium complexes³² and Cd–N bond distances are in the range of 2.242–2.333 Å. The hfipbb ligands adopt different coordination modes towards Cd02 in **CP-A**: one hfipbb²⁻ exhibits μ_1 - η^1 : η^1 and μ_1 - η^1 : η^0 , while the other hfipbb²⁻ shows μ_1 - η^1 : η^1 coordination mode—leading to the formation of metal acid chains as shown in Figure 3.3c. These metal acid chains are further connected by Cd01 metal ions through the biip linkers, resulting in the formation of 1D ribbon-like structure (Figure 3.3d).

Structural depiction of {Cd(hfipbb)(biip)}_n (**CP-B**):

CP-B includes one Cd(II) ion, one hfipbb²⁻ and one bijp ligand as shown in Figure 3.3e. In this, each cadmium ion (named as Cd03) is six coordinated by four oxygen atoms and two nitrogen atoms from two hfipbb²⁻ ligands and two biip linkers, respectively, affording distorted octahedral geometry around cadmium(II) ion. The {Cd₂(COO)₂} dimeric unit is formed by the connectivity of two carboxylate groups in bridging bidentate mode with a Cd---Cd separation of 4.286 Å, acting as secondary building unit (SBU) in the crystal structure. The Cd-O bond distances are in range of 2.229-2.733 Å. The Cd-N bond distances are 2.290 and 2.373 Å. The bond angles within the Cd(II) coordination geometry are in the range of $81-164.7^{\circ}$. One carboxylate group of hfipbb²⁻ shows monodentate μ_1 - $\eta^1:\eta^0$ coordination fashion and the other carboxylate group shows bidentate $\mu_2-\eta^1:\eta^1$ coordination fashion towards cadmium(II). The connectivity of SBUs with the hfipbb²⁻ ligands leads to the formation of 1D metal acid chain along the crystallographic 'bc' plane, having a separation of 13.083 Å between two dimers (Figure 3.3f). The biip linkers are connected to the two different {Cd₂(COO)₂} dimeric units of adjacent chains resulting in a Cd₂(biip)₂ macrocycle along the crystallographic 'ac' plane, finally leading to the formation of a 1D chainlike structure (Figure 3.3g) and the separation created by biip linkers between the two dimers in this chain is 10.958 Å. The cross over connectivity of Cd-hfipbb²⁻ chain and Cd(II)-biip chain through the {Cd₂(COO)₂} dimer results in the formation of 2D structure as shown in Figure 3.3h.

The crystal packing of 1D chains of **CP-A** (shown in Figure 3.3d) and 2D layers of **CP-B** (shown in Figure 3.3h), finally results in an overall three-dimensional supramolecular architecture of compound **3** (Figure 3.3i).





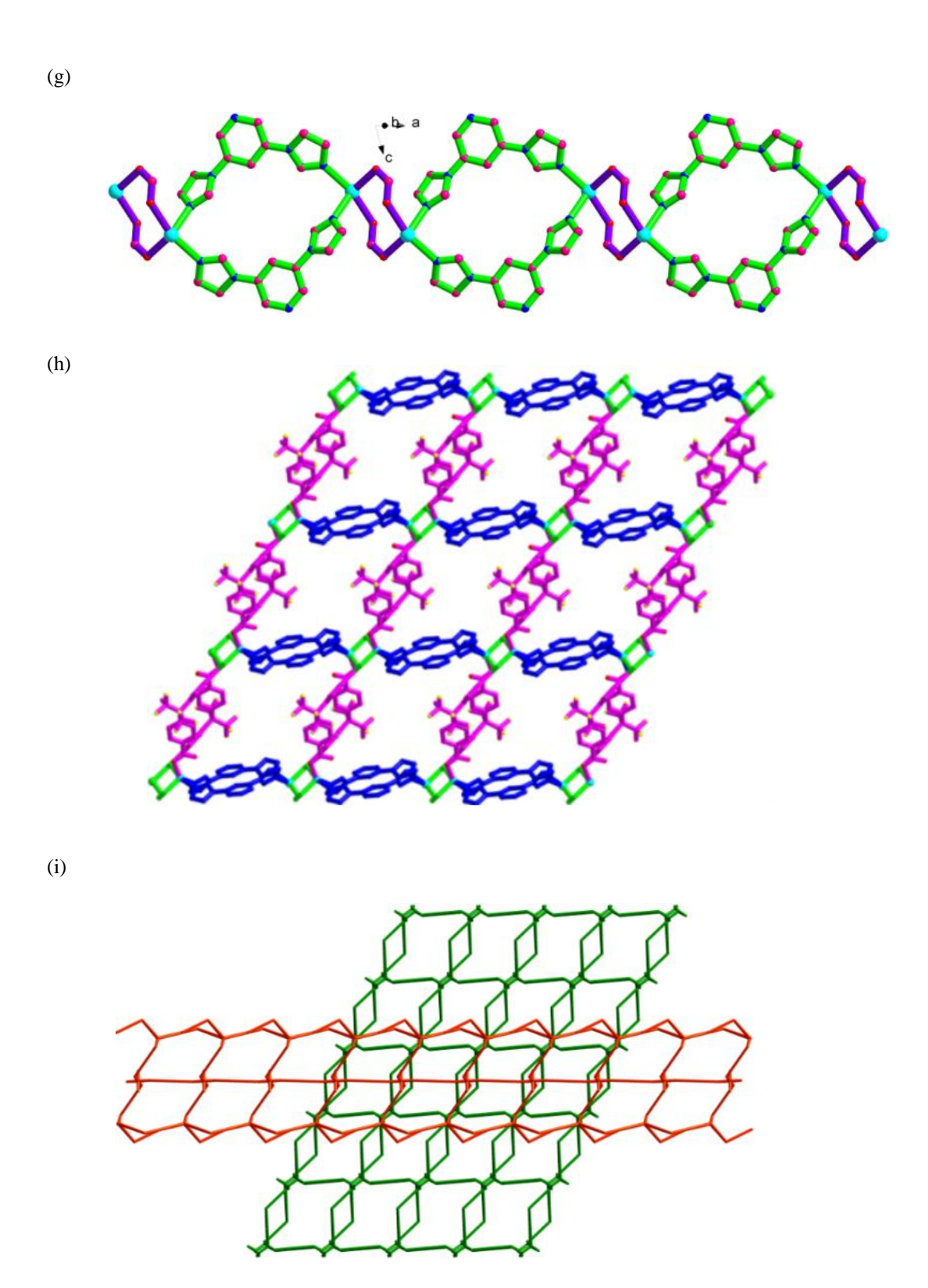


Figure 3.3 Crystal structure of compound $\{[Cd_{1.5}(hfipbb)_2(biip)_{1.5}(H_2O)][Cd(hfipbb)(biip)]\}_n \cdot n2H_2O$ (3): (a) asymmetric unit of 3, (b) the basic unit in CP-A, (c) metal-acid chains of CP-A coordinated by the hfipbb²-ligands with Cd02 metal ions, (d) topological representation of 1D structure of CP-A, (e) the basic unit in CP-B, (f) 1D metal acid chain of CP-B, formed due to the connectivity of hfipbb²-ligands and SBUs along the crystallographic 'bc' plane, (g) 1D chainlike structure of CP-B, connected by the $[Cd_2(biip)_2]$ macrocycle and $[Cd_2(COO)_2]$ dimeric units along the crystallographic 'ac' plane, (h) 2D structure of CP-B and (i) a simplified representation of compound 3 formed via interpenetration of CP-A (red) into the 2D layer of CP-B (green).

In all three compounds, the common auxiliary linker is biip {3,5-di (1H-imidazol-1-yl)pyridine}. It is known that first-row transition metal compounds containing imidazole type ligands have potential to act as the agents of anticancer and antitumor activity. ³³ So, compounds **1–3**, described in the present work, have some biological relevance.

3.3.3. Powder X-ray Diffraction (PXRD) Patterns of the Compounds 1-3

Powder X-ray diffraction (PXRD) data for compounds **1–3** have been recorded to confirm the phase purity of all synthesized compounds. The matching of patterns of simulated data (calculated from respective single crystal data) with the corresponding observed diffraction data proves the bulk homogeneity of the crystalline solids (Figure 3.4).

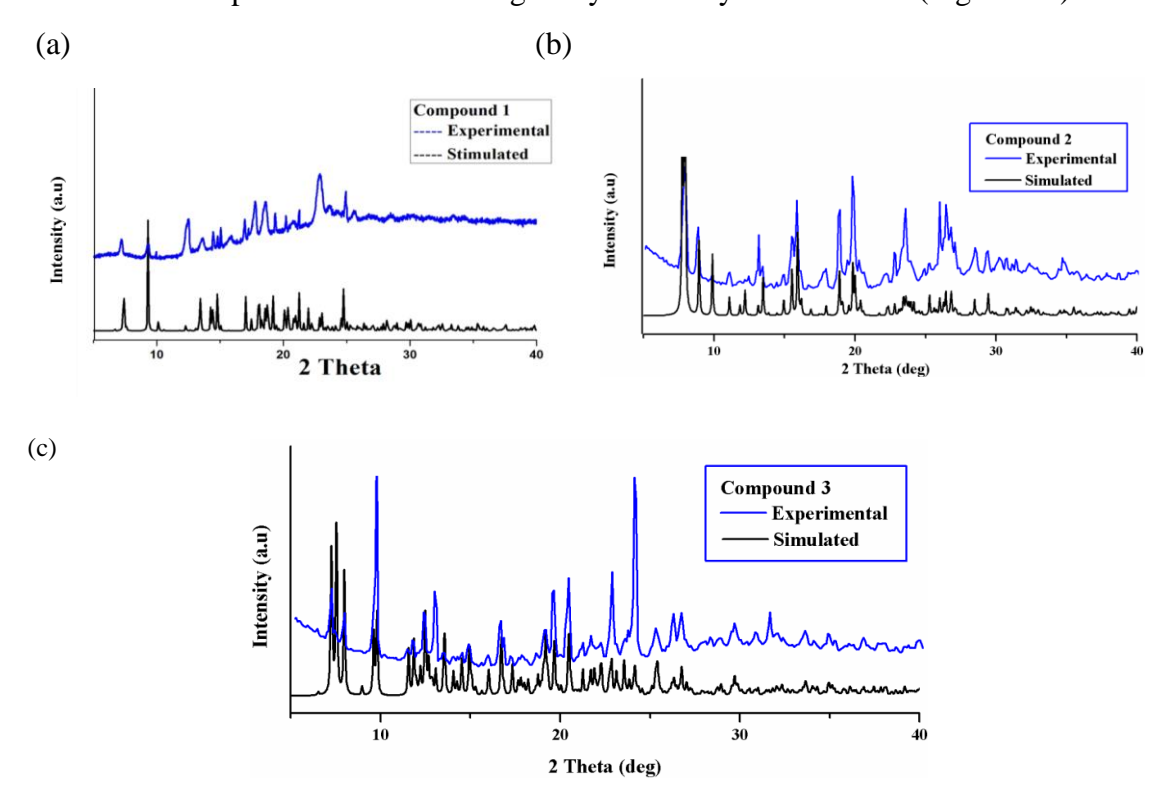


Figure 3.4 Observed powder X-ray diffraction patterns of the compounds 1–3 (blue curves), including simulated patterns obtained from respective single crystal data (black curves).

3.3.4. Thermogravimetric Analysis (TGA) Curves of the Compounds 1–3

Thermogravimetric (TG) plots have been recorded under flow of N_2 gas for the crystalline compounds **1–3** in the temperature of 30–750 °C (Figure 3.4). The compound **1** is found to be stable up to 400 °C and the weight loss of 2.8% (calcd. 3%) in the range of 30–120 °C corresponds to the loss of lattice water molecule. Beyond 400 °C, it shows continuous weight loss indicating the decomposition of organic ligands *i.e.*, oba²⁻ and biip, present in

compound 1. TGA curve of compound 2 shows weight loss of 11.8% (calcd. 12.5%) in the temperature of 30–90 °C corresponding to the loss of lattice water molecules, and then it undergoes continuous weight loss after 320 °C leading to decomposition of the framework material. The TGA profile of compound 3, exhibits stability up to 250 °C. The weight loss of 3 % (calcd. 3.17%) beyond this temperature (250 °C to 400 °C) corresponds to removal of coordinated and lattice water molecules. After 400 °C, it displays significant weight loss indicating the collapse of framework integrity.

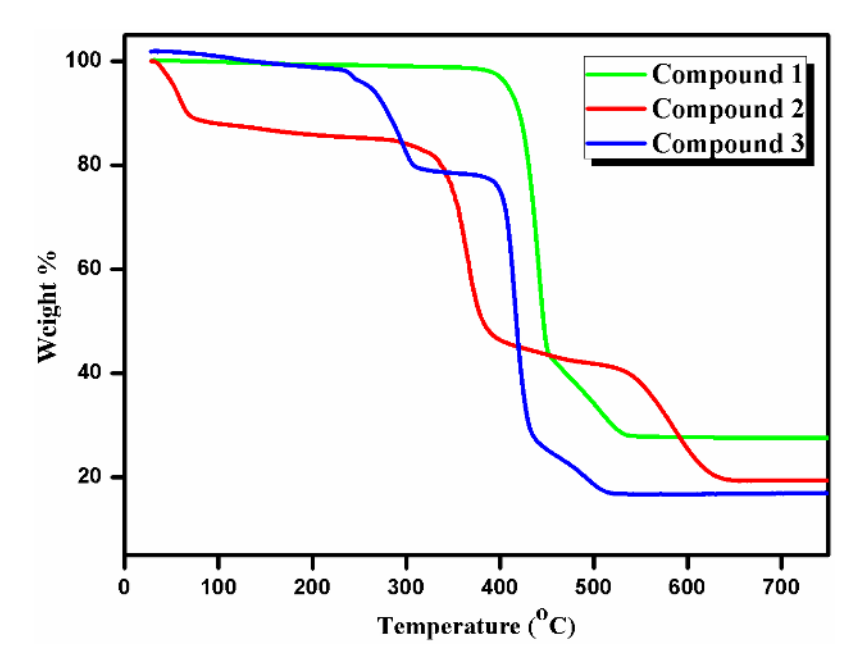
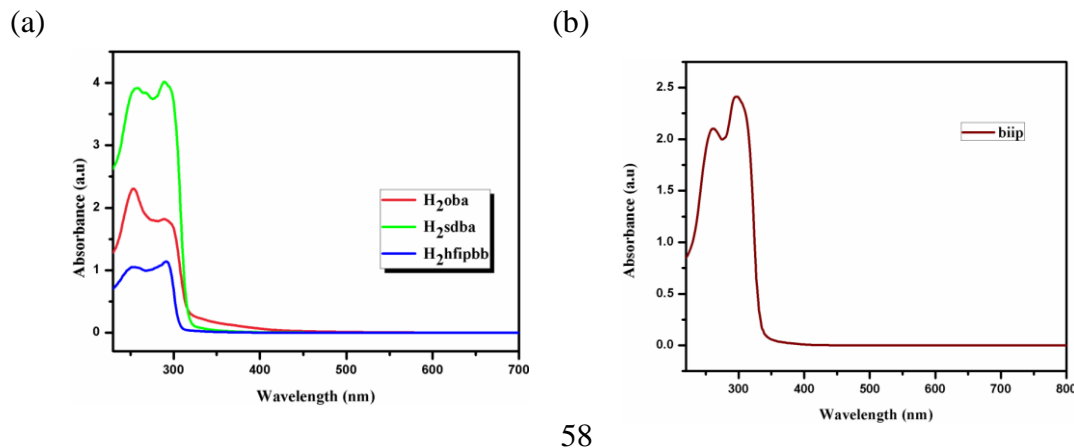


Figure 3.4 Thermogravimetric plots of the compounds 1–3.

3.3.5. Electronic Spectra (DRS) of Compounds 1–3

The solid-state diffuse reflectance spectra (DRS) of compounds 1-3 are recorded along with the free ligands i.e., H₂oba, H₂sdba, H₂hfipbb and biip at room temperature (see Figures 3.5a and 3.5b). The absorption maxima are observed at 259, 289 nm for compound 1 and 248, 286 nm for compound 2, whereas compound 3 exhibits absorption maxima at 240, 280 nm (Figure 3.5c).



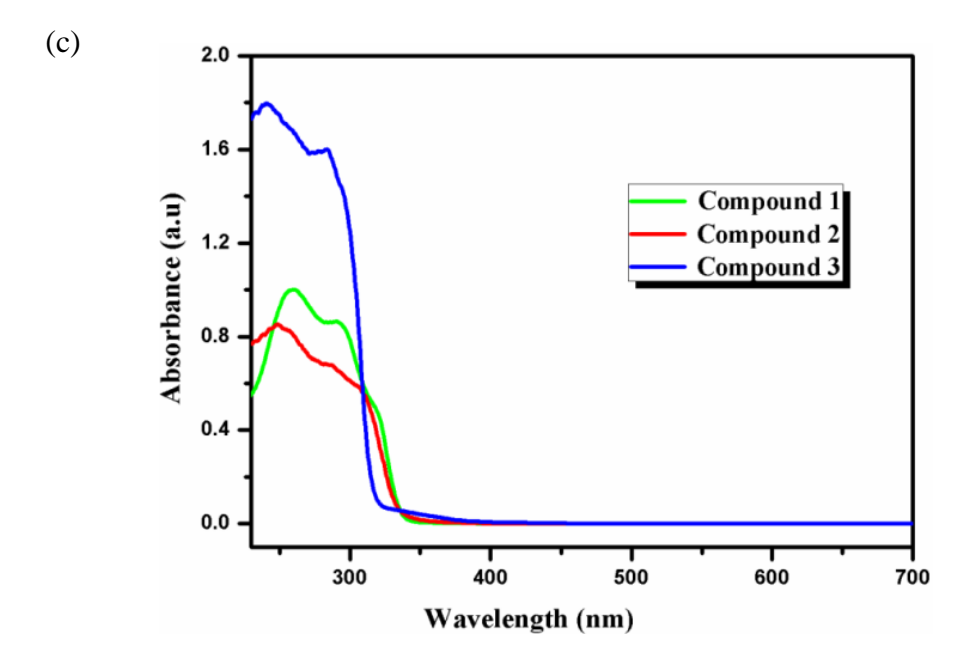
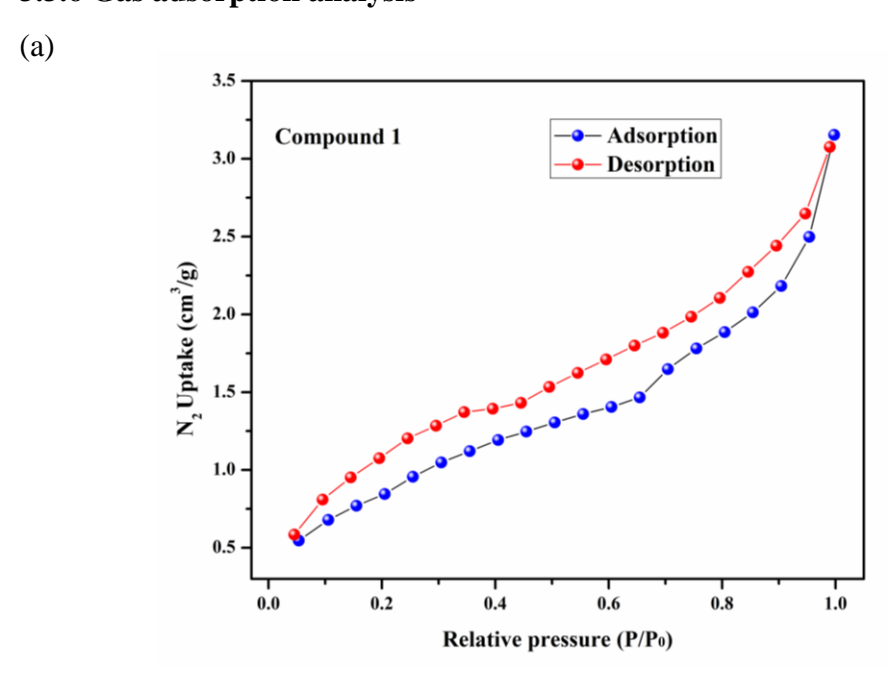


Figure 3.5 Solid state diffuse reflectance (electronic absorption) spectra of the ligands (a) H_2 oba, H_2 sdba, H_2 hfipbb, (b)biip, and (c) compounds 1–3.

The corresponding free ligands show absorption bands at 253, 289 nm (for H_2 oba); 257,267, 289 nm (for H_2 sdba); 253, 291 nm (for H_2 hfipbb) and 261, 296 nm (for biip) in their respective electronic absorption spectra (Figures 3.5a and 3.5b). Hence, the absorption bands of compounds **1–3** can be attributed to the intra-ligand charge transfer transitions by comparing with their corresponding free ligand spectra.

3.3.6 Gas adsorption analysis



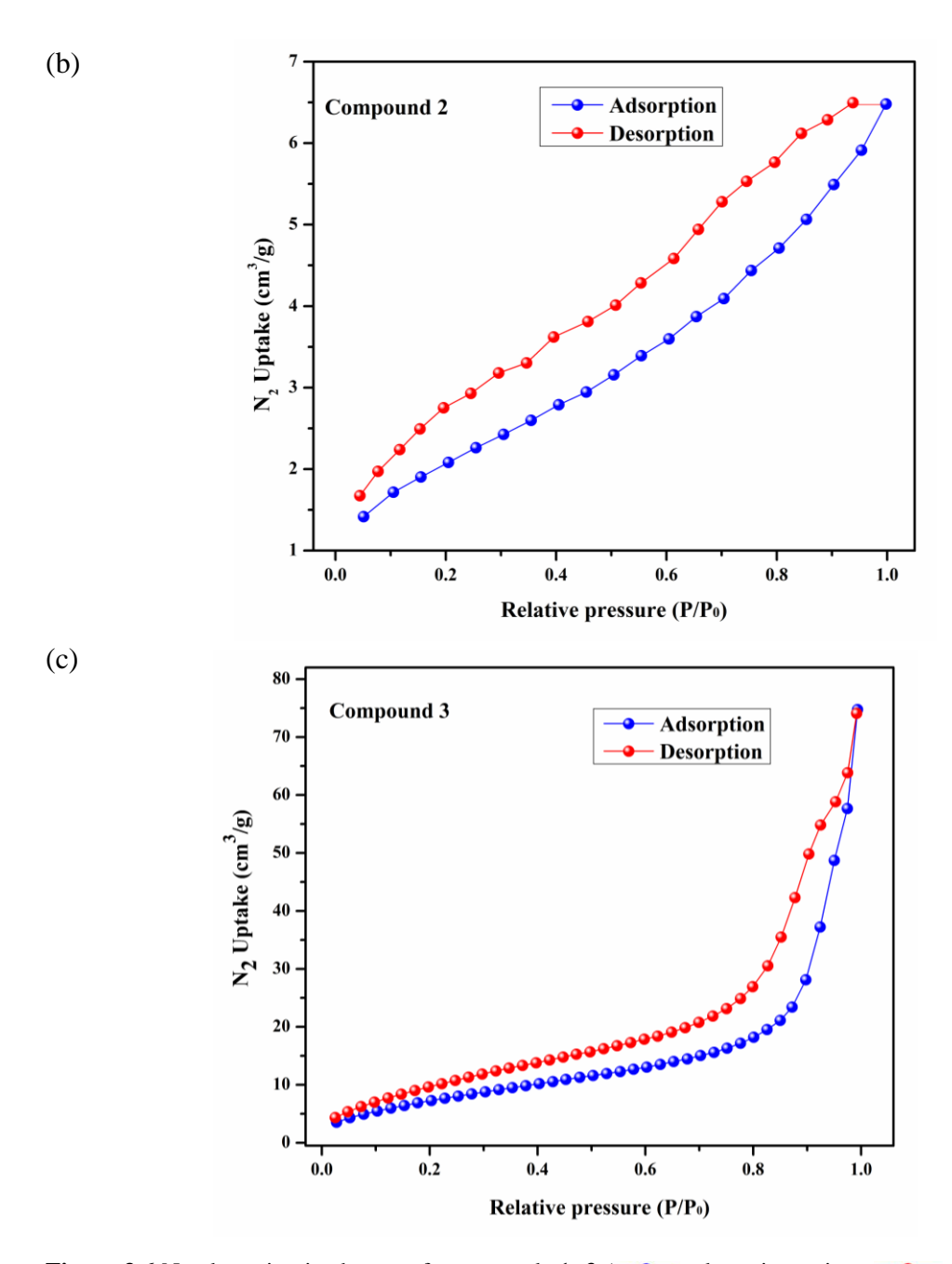


Figure 3.6 N_2 adsorption isotherms of compounds 1–3 (\longrightarrow adsorption points; \longrightarrow desorption points) at 77K: (a) compound 1, (b) compound 2 and (c) compound 3.

The gas-adsorption measurements of compounds 1-3 were performed at 77 K. The compounds were preheated at 473K and evacuated under dynamic vacuum for 6 h to generate activated samples prior to the analysis. Figure 3.6 describes the N_2 sorption properties of compounds 1-3, with a maximum N_2 uptake of 3.15, 6.48 and 74.45 cm³ g-1 (STP) at P/Po =0.99 relative pressure, respectively. The N_2 adsorption isotherms of 1-3 display a characteristic type III adsorption isotherm curves, and the calculated Brunauer—

Emmett-Teller (BET) surface area were found to be 3.37, 7.65 and 29.10 m² g⁻¹, respectively.

3.4. Conclusions and future scope

In summary, we have employed angular ligands i.e., H₂oba (4,4'-oxydibenzoic acid), H₂sdba (4,4'-thiodibenzoic acid), H₂hfipbb {4,4'-(perfluoropropane-2,2-diyl)dibenzoic acid} and an auxiliary linker, biip (3,5-di(1H-imidazol-1-yl)pyridine) along with $Cd(OAc)_2 \cdot 2H_2O$ to synthesize three coordination polymers $\{Cd(oba)(biip)\}_n \cdot nH_2O$ (1), $\{Cd(sdba)(biip)\}_n \cdot n5H_2O$ **(2)** and $\{[Cd_{1.5}(hfipbb)_2(biip)_{1.5}(H_2O)]$ $[Cd(hfipbb)(biip)]_n \cdot n2H_2O$ (3) under solvothermal conditions by heating the corresponding reaction mixtures at 120 °C for three days. All the compounds have been analysed by routine characterization techniques, such as, Infrared spectroscopy (IR), UV-DRS, CHNS and thermal analysis (TGA). The structures of all the compounds are unambiguously determined by single crystal X-ray diffraction (SCXRD) studies. The structural analysis reveals that the compound 1 forms a three-dimensional network by means of pillaring of 2D layers by secondary linkers, whereas the compound 2 is a twodimensional structure. Interestingly, the compound 3 consists of two distinct and crystallographically independent polymeric motifs (CP-A and CP-B) that are packed together within the same crystal. CP-A forms a one-dimensional coordination polymer, whereas **CP-B** is a two-dimensional structure. The interpenetration of 1D chains of **CP-A** into the 2D layers of **CP-B** gives an overall three-dimensional supramolecular architecture to compound 3. The bulk purity of all the compounds have been ensured by powder X-ray diffraction (PXRD) studies. Thermal stabilities are determined by TGA measurement, which shows that these compounds exhibit good stability, except that they lose solvent molecules in the lower temperature region.

All the three compounds possess the d¹⁰ metal ion *i.e.*, cadmium (II) ion in their crystal structures, coordinated to different organic ligands and a common secondary linker. Interestingly, the compound **3** exhibits two-in-one kind of system, where two polymers coexist in one crystal structure having different dimensionalities. This encourages us to develop a synthetic route to generate such compounds with multiple dimensionalities which could have potential applications. We are currently working in this direction.

Table 3.1: Crystal data and structural refinement parameters for compounds 1–3

	1	2	3
Empirical formula	$C_{25}H_{19}N_5CdO_6$	$C_{25}H_{27}N_5CdO_{11}S$	$C_{80.5}H_{52}Cd_{2.5}F_{18}N_{13}O_{15}$
Formula weight	597.86	717.98	2064.38
$T(K) / \lambda(A)$	297(2)/ 0.71073	297(2)/ 0.71073	297(2)/ 0.71073
Crystal system	Monoclinic	Monoclinic	Triclinic
Space group	C2/c	P2(1)/c	P-1
a (Å)	17.4954(7)	11.7676(5)	13.8241(19)
b (Å)	12.6153(5)	19.7794(8)	15.109(2)
c (Å)	22.1892(10)	13.9176(5)	23.106(4)
α (°)	90.00	90.00	78.213(6)
β (°)	95.2010(10)	104.5080(10)	74.280(6)
γ (°)	90.00	90.00	64.202(5)
Volume (ų)	4877.2(4)	3136.1(2)	4161.8(11)
Z , ρ_{calcd} (g cm ⁻³)	8, 1.628	4, 1.368	1, 1.633
$\mu \text{ (mm}^{-1}), F(000)$	0.947/ 2400	0.808/1296	0.747 /2036
Goodness- of-fit on F ²	1.033	0.970	1.052
$R1/wR2[I > 2\sigma(I)]$	0.0246/0.0706	0.0371/0.1062	0.0738/0.1450
R1/wR2 (all data)	0.0264/0.0730	0.0436/0.1106	0.1292/0.1647
Largest diff peak/ hole (e Å-3)	0.444 /-0.654	0.882/-0.883	0.614 /-1.016

3.5. References

- 1. (a) M. Kurmoo, Chem. Soc. Rev. 38 (2009) 1353;
 - (b) M. D. Allendorf, C. A. Bauer, R. K. Bhakta and R. J. T. Houk, Chem. Soc. Rev. 38 (2009) 1330;
 - (c) J.-R. Li, J. Sculley and H.-C. Zhou, Chem. Rev. 112 (2012) 869;
 - (d) J. Liu, P. K. Thallapally, B. P. McGrail, D. R. Brown and J. Liu, Chem. Soc. Rev. 41 (2012) 2308;
 - (e) K. Sumida, D. L. Rogow, J. A. Mason, T. M. McDonald, E. D. Bloch, Z. R. Herm, T.-H. Bae and J. R. Long, Chem. Rev. 112 (2012) 724;
 - (f) S. Chaemchuen, N. A. Kabir, K. Zhou and F. Verpoort, Chem. Soc. Rev. 42 (2013) 9304.
- 2. (a) C. Beghidja, G. Rogez, J. Kortus, M. Wesolek and R. Welter, J. Am. Chem. Soc. 128 (2006) 3140;
 - (b) M. Du, Z.-H. Zhang, C.-P. Li, J. Ribas-Ariño, N. Aliaga-Alcalde and J. Ribas, Inorg. Chem. 50 (2011) 6850;
 - (c) B.-W. Hu, J.-P. Zhao, E. C. Sañudo, F.-C. Liu, Y.-F. Zeng and X.-H. Bu, Dalton Trans. (2008) 5556;
 - (d) Z. Duan, Y. Zhang, B. Zhang and D. Zhu, J. Am. Chem. Soc. 131 (2009) 6934;
 - (e) T. K. Prasad, M. V. Rajasekharan and J.-P. Costes, Angew. Chem., Int. Ed. 46 (2007) 2851.
- 3. L. E. Kreno, K. Leong, O. K. Farha, M. Allendorf, R. P. Van Duyne and J. T. Hupp, Chem. Rev. 112 (2012) 1105.
- 4. (a) A. J. Fletcher, E. J. Cussen, D. Bradshaw, M. J. Rosseinsky and K. M. Thomas, J. Am. Chem. Soc. 126 (2004) 9750;
 - (b) L. Alaerts, C. E. A. Kirschhock, M. Maes, M. A. van der Veen, V. Finsy, A. Depla, J. A. Martens, G. V. Baron, P. A. Jacobs, J. F. M. Denayer and D. E. De Vos, Angew. Chem., Int. Ed. 46 (2007) 4293.
- (a) P. Horcajada, C. Serre, G. Maurin, N. A. Ramsahye, F. Balas, M. Vallet-Regí,
 M. Sebban, F. Taulelle and G. Férey, J. Am. Chem. Soc. 130 (2008) 6774;
 - (b) P. Horcajada, C. Serre, M. Vallet-Regí, M. Sebban, F. Taulelle and G. Férey, Angew. Chem., Int. Ed. 45 (2006) 5974.

- 6. (a) X.-L. Wang, C. Qin, E.-B. Wang, Y.-G. Li, Z.-M. Su, L. Xu and L. Carlucci, Angew. Chem., Int. Ed. 44 (2005) 5824;
 - (b) L. Carlucci, G. Ciani and D. M. Proserpio, CrystEngComm, 5 (2003) 269.
- 7. (a) H. Wu, H.-Y. Liu, Y.-Y. Liu, J. Yang, B. Liu and J. -F. Ma, Chem. Commun. 47 (2011) 1818;
 - (b) S.J. Loeb, Chem. Soc. Rev. 36 (2007) 226;
 - (c) G.-P. Yang, L. Hou, X.-J. Luan, B. Wu and Y.-Y. Wang, Chem. Soc. Rev. 41 (2012) 6992.
- (a) S. R. Batten and R. Robson, Angew. Chem., Int. Ed. 37 (1998) 1460;
 (b) S. R. Batten, CrystEngComm 3 (2001) 67.
- 9. K. Biradha and M. Fujita, Chem. Commun. (2002) 1866.
- 10. M. A. Nadeem, M. Bhadbhade, R. Bircher and J. A. Stride, CrystEngComm 12 (2010) 1391.
- 11. B. Li, S.-Q. Zang, C. Ji, R. Liang, H.-W. Hou, Y.-J. Wu and T. C. W. Mak, Dalton Trans. 40 (2011) 10071.
- 12. L. Carlucci, G. Ciani and D. M. Proserpio, New J. Chem. 22 (1998) 1319.
- 13. B. Zheng and J. Bai, CrystEngComm 11 (2009) 271.
- 14. C.-C. Wang, W.-C. Chung, H.-W. Lin, S.-C. Dai, J.-S. Shiu, G.-H. Lee, H.-S. Sheu and W. Lee, CrystEngComm 13(2011) 2130.
- 15. J. Wang, X. Zhu, Y.-F. Cui, B.-L. Li and H.-Y. Li, CrystEngComm 13 (2011) 3342.
- 16. Y.-C. Chuang, W.-L. Ho, C.-F. Sheu, G.-H. Lee and Y. Wang, Chem. Commun. 48 (2012) 10769.
- 17. D. M. Shin, I. S. Lee, Y. K. Chung and M. S. Lah, Chem. Commun. (2003) 1036.
- 18. M. Roy, A. A. Lonardo, D. N. K. Pham, A. Kreider-Mueller, J. A. Golen and D. R. Manke, CrystEngComm 21 (2019) 4255.
- 19. M. Du, X.-J. Jiang and X.-J. Zhao, Chem. Commun. (2005) 5521.
- 20. M. B. Zaman, M. D. Smith and H.-C. zur Loye, Chem. Commun. (2001) 2256.
- 21. D. Hagrman, R. P. Hammond, R. Haushalter and J. Zubieta, Chem. Mater. 10 (1998) 2091.
- 22. G. Mahmoudi and A. Morsali, CrystEngComm 11 (2009) 50.
- 23. X. Zhu, X.-G. Liu, B.-L. Li and Y. Zhang, CrystEngComm 11 (2009) 997.

- 24. S.-Y. Ke, Y.-F. Chang, H.-Y. Wang, C.-C. Yang, C.-W. Ni, G.-Y. Lin, T.-T. Chen, M.-L. Ho, G.-H. Lee, Y.-C. Chuang and C.-C. Wang, Cryst. Growth Des. 14 (2014) 4011.
- 25. B. Li, Y. Peng, B. Li and Y. Zhang, Chem. Commun. (2005) 2333.
- 26. J.-J. Shen, M.-X. Li, Z.-X. Wang, C.-Y. Duan, S.-R. Zhu and X. He, Cryst. Growth Des. 14 (2014) 2818.
- 27. L. Luo, Y. Zhao, Y. Lu, T.-a. Okamura and W.-Y. Sun, Polyhedron 38 (2012) 88.
- 28. APEX II, Version 2 User Manual, M86-E01078; Bruker Analytical X-ray Systems: Madison, WI, USA, (2006).
- 29. SADABS: Program for Absorption Correction; G.M. Sheldrick, University of Gottingen: Gottingen, Germany. (1997).
- 30. G. M. Sheldrick, SHELXT Integrated space-group and crystal-structure determination. Acta Cryst. A71 (2015) 3.
- 31. G. M. Sheldrick, Crystal structure refinement with SHELXL. Acta Cryst. C71 (2015) 3.
- 32. (a) Q.-G. Zhai, C.-C. Zhang, S.-N. Li, Y.-C. Jiang and M.-C. Hu, Inorg. Chem. Commun. 14 (2011) 1982;
 - (b) X.-L. Wang, S. Yang, G.-C. Liu, J.-X. Zhang, H.-Y. Lin and A.-X. Tian, Inorg. Chim. Acta 375 (2011) 70.
- 33. D. Hernández-Romero, S. Rosete-Luna, A. López-Monteon, A. Chávez-Piña, N. Pérez-Hernández, J. Marroquín-Flores, A. Cruz-Navarro, G. Pesado-Gómez, D. Morales-Morales and R. Colorado-Peralta, Coord. Chem. Rev. 439 (2021) 213930.

Diverse coordination architectures based on a flexible multidentate carboxylate ligand and N-donor linkers: synthesis, structure, supramolecular chemistry and related properties

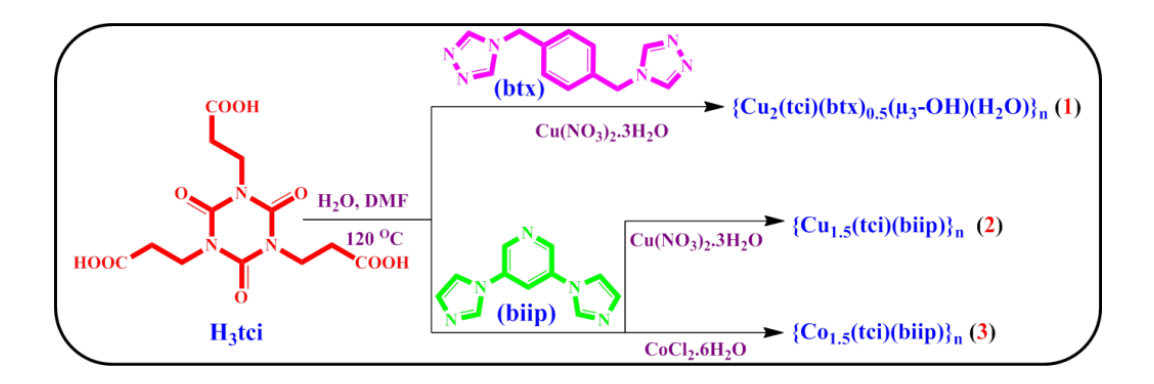
Three new metal-organic framework (MOF) containing compounds, namely $\{Cu_2(tci)(btx)_{0.5}(\mu_3OH)(H_2O)\}_n$ (1), $\{Cu_{1.5}(tci)(biip)\}_n$ (2), $\{Co_{1.5}(tci)(biip)\}_n$ (3) $[H_3tci=tris(2-carboxyethyl)]$ isocyanurate, btx=1,4-bis(triazol-1-yl-methyl)benzene, biip = 3,5-bis(imidazole-1-yl)pyridine] have been successfully synthesized through the assembly of metal ions [Cu(II)] ion for compounds 1 and 2, Co(II) for compound 3] with H_3tci and two different N-donor ligands under solvothermal conditions. All compounds were characterized by IR spectroscopy, elemental and thermogravimetric (TG) analyses, powder X-ray diffraction (PXRD) studies and finally, the structures of all compounds were unambiguously determined by single-crystal X-ray diffraction (SCXRD) technique. Compound 1 is a 1D coordination polymer, constructed by the connectivity of copper tetramer as a secondary building unit (SBU) with the H_3 tci and btx ligands. Whereas the crystal structure of compound 2 possesses two different SBUs *i.e.*, paddlewheel and square involving Cu(II). The connectivity of these two SBUs results in the formation of 2D layers which are further pillared by biip ligand to result in a 3D structure. In the case of compound 3, both Co1 and Co2 exhibit distorted octahedral geometry in their SBUs. Further, the connectivity of these SBUs with tci³⁻ and biip ligands results in the formation of a 3D framework.

4.1. Introduction

The design and construction of metal-organic frameworks (MOFs) have fascinated great consideration not only because of their intriguing architectures and topologies but also due to their huge potential applications in gas storage, ¹ sensing, ² drug delivery, ³ catalysis, ⁴ ion exchange, magnetism, etc. A great deal of research has been done in optimizing the synthetic procedures to obtain new materials including, the utilization of single ligand (either carboxylate or N-linker) or mixed ligand strategies (two different carboxylate or Nlinkers, or a combination of carboxylate ligand and N-linker). Most of the reported structures were constructed by using the rigid organic linkers, whereas the flexible organic linkers are less preferred owing to the possibility of attaining n-number of conformations within the given reaction conditions, which in turn, complicates the predictability of the resulting structures. In contrast, the flexible ligands offer the unique properties in resulting materials.^{7,8} Generally, the dicarboxylate ligands are chosen as bridging ligands to obtain extended structures which further pillared by the secondary ligands in resulting materials of diverse dimensions; on the other hand, polydentate carboxylate ligands are found to be good candidates, essentially due to their multiple coordination sites and diverse coordination modes for achieving metal-carboxylate poly clusters, such as di-, tri- and higher-nuclearity clusters, which are useful in exploring certain functional properties such as magnetism, sensing and so on. 9-11

By choosing appropriately well-designed and multi-functional organic ligands, interesting functional coordination networks with useful properties could be obtained. In this regard, we have chosen the flexible organic carboxylate ligand *i.e.*, H₃tci {tris(2-carboxyethyl) isocyanurate} due to the following reasons: (i) multidenticity (three –COOH groups), (ii) conformational liberty imposed by three (–CH₂-CH₂–) arms, which generally assumes *cis,cis,cis* and *cis,cis,trans* conformations, (iii) secondary (–c=o–) functional moiety, and (iv) the diverse coordination modes of the carboxyl group. The versatile nature of this ligand has been utilized to construct various coordination polymers with different metal ions such as Mg(II), ¹² Mn(II), ^{13,14} Co(II), ¹⁵⁻¹⁷ Cu(II), ¹⁸⁻²⁴ Zn(II), ²⁵⁻³² Cd(II), ^{33,34}, and some lanthanide ions. ³⁵⁻⁴⁰ Auxiliary ligands also play an important role in the construction of coordination polymers/MOFs. They increase the stability of the structure by pillaring or connecting the individual layers, thereby modulating the resulting framework structure. In this line, we reported diverse coordination polymers having diverse physical properties using such flexible and auxiliary ligands. ⁴¹⁻⁴⁷

Herein, we describe syntheses, structures and properties of three coordination polymers based on H₃tci ligand, {Cu₂(tci)(btx)_{0.5}(µ₃-OH)(H₂O)}_n (1), {Cu_{1.5}(tci)(biip)}_n (2), {Co_{1.5}(tci)(biip)}_n (3) (see Scheme 1). Compound 1 is a one-dimensional coordination polymer, in which copper tetramer acts as a secondary building unit (SBU) which coordinates to H₃tci and btx ligands. In the case of compound 2, paddle wheel and square planar Cu(II) act as SBUs, connected by tci³⁻ ligand to result in two-dimensional layered networks, which are further pillared by biip linker affording 3D structure. Compound 3 has also three-dimensional structure, in which the distorted Co1 and Co2 octahedral SBUs are coordinated to tci³⁻ ligand resulting in three-dimensional metal-acid networks, where the biip ligand acts as a pillar. All these compounds were well characterized by routine spectral techniques including single-crystal X-ray diffraction studies.



Scheme 4.1. Representation of synthetic protocol of compounds 1–3.

4.2. Experimental

4.2.1. Materials and physical methods

The chemicals $CoCl_2 \cdot 6H_2O$ and DMF (N,N-Dimethyl formamide) were purchased from Finar, India; whereas $Cu(NO_3)_2 \cdot 3H_2O$ and H_3 tci [tris(2-carboxyethyl)isocyanurate] chemicals were procured from SRL and TCI Chemicals, India, respectively. All the chemicals were received as reagent grade and used without any further purification. The ligands, biip [1,4-bis(triazol-1-yl-methyl)benzene] and btx [3,5-bis(imidazole-1-yl)pyridine] were prepared according to the literature procedures.

4.2.2. Characterization

Elemental analyses were determined by the FLASH EA series 1112 CHNS analyzer. Infrared spectra of solid samples were obtained as KBr pellets on a JASCO-5300 FT-IR spectrophotometer. Thermogravimetric analyses were carried out on an STA 409 PC

analyzer and corresponding masses were analyzed by QMS 403 C mass analyzer, under the flow of N_2 gas with a heating rate of 5 °C min⁻¹, in the temperature range of 30–800 °C. Powder X-ray diffraction patterns were recorded on a Bruker D8-Advance diffractometer using graphite monochromated CuK α 1 (1.5406 Å) and K α 2 (1.54439 Å) radiations. All the compounds were synthesized in 23 mL Teflon-lined stainless-steel vessels (Thermocon, India) under solvothermal conditions. The electronic absorption spectra have been recorded in the solid-state on a UV-2600 Shimadzu UV-visible spectrophotometer at room temperature.

4.2.3. Synthesis

Synthesis of compound $\{Cu_2(tci)(btx)_{0.5}(\mu_3-OH)(H_2O)\}_n$ (1):

A mixture of $\text{Cu}(\text{NO}_3)_2\cdot 3\text{H}_2\text{O}$ (24 mg, 0.1 mmol), H₃tci (34.5 mg, 0.1 mmol), and btx (23.8 mg, 0.1 mmol) was dissolved in 4 ml of distilled water and 2 ml DMF, which was then stirred for 30 minutes. The pH of the reaction mixture was adjusted to 7.4 by adding 0.5M NaOH solution and the resulting reaction mixture was placed in a 23 ml Teflon-lined stainless-steel autoclave, which was sealed and heated at 120 °C for 60 hours. The autoclave was allowed to cool to room temperature over 48 hours to obtain green needleshaped crystals of compound **1** (61% yield, based on Cu). Anal. Calcd, for $\text{C}_{18}\text{H}_{21}\text{N}_6\text{Cu}_2\text{O}_{11}$ (M_r =624.48): C, 34.62 %; H, 3.39 %; N, 13.46 %. Found: C, 34.71 %; H, 3.32 %; N, 13.36 %. IR (KBr pellet, cm⁻¹): 3128, 2969, 1961, 1687, 1599, 1473, 1435, 1391, 1364, 1282, 1205, 1145, 1079, 1052, 1013, 887, 854, 799, 761, 635.

Synthesis of compound $\{Cu_{1.5}(tci)(biip)\}_n(2)$:

A mixture of Cu(NO₃)₂·3H₂O (24 mg, 0.1 mmol), H₃tci (34.5 mg, 0.1 mmol), and biip (21.1 mg, 0.1 mmol) was dissolved in the mixed solvent of 4 ml of distilled water and the reaction mixture was 2 ml DMF, stirred for 30 minutes. The pH of the reaction mixture was adjusted to 7.5 by adding 0.5M NaOH solution and the resulting reaction mixture was placed and sealed in a 23 ml Teflon-lined stainless-steel autoclave. This was then heated at 120 °C for 3 days. The autoclave was allowed to cool to room temperature over 48 hours resulting in needle-shaped green crystals of compound **2**, in 68% yield (based on Cu). Anal. Calcd. for $C_{23}H_{21}N_8Cu_{1.5}O_9$ (M_r =648.78): C, 42.58 %; H, 3.26 %; N, 17.27 %. Found: C, 42.65 %; H, 3.29 %; N, 17.19 %. IR (KBr pellet, cm⁻¹): 3137, 3059, 1696, 1670, 1629, 1558, 1458, 1427, 1381, 1288, 1267, 1123, 1066, 1009, 957, 926, 901, 828, 771, 720, 653, 518.

Synthesis of compound $\{Co_{1.5}(tci)(biip)\}_n(3)$:

A mixture of $CoCl_2\cdot 6H_2O$ (24 mg, 0.1 mmol), H_3 tci (34.5 mg, 0.1 mmol), and biip (21.1 mg, 0.1 mmol) was dissolved in a mixed solvent of 4 ml of distilled water and 2 ml DMF, which was then stirred for 30 minutes. The pH of the reaction mixture was adjusted to 7.8 by adding 0.5M NaOH solution and the resulting reaction mixture was placed in a 23 ml Teflon-lined stainless-steel autoclave, which was sealed and heated at 120 °C for 72 hours. The autoclave was allowed to cool to room temperature over 48 hours to obtain red block crystals of compound **3** (63% yield, based on Co). Anal. Calcd. for $C_{23}H_{21}N_8Co_{1.5}O_9$ (M_r =641.86): C, 43.04 %; H, 3.30 %; N, 17.46 %. Found: C, 43.12 %; H, 3.38 %; N, 17.36 %. IR (KBr pellet, cm⁻¹): 3147, 3127, 3059, 1691, 1608, 1577, 1484, 1433, 1340, 1288, 1262, 1117, 1071, 1004, 947, 926, 844, 761, 658, 523, 467.

4.2.4. Single crystal X-ray structure determination of the compounds 1–3

Data for single-crystals suitable for structural determination of all the compounds 1-3 were collected on a Bruker D8 Quest CCD diffractometer under a Mo–K α (λ = 0.71073 Å) graphite monochromatic X-ray beam with a crystal-to-detector distance of 40 mm. The data reduction was performed using Apex- II Software. Empirical absorption corrections using equivalent reflections were performed with the program SADABS. Structure solutions and full-matrix least-squares refinement were carried out using standard crystallographic software for all the compounds. All the non-hydrogen atoms were refined anisotropically. Hydrogen atoms on the C atoms were introduced on calculated positions and were included in the refinement riding on their respective parent atoms. Crystal data and structure refinement parameters for compounds 1-3, are summarized in Table 4.1.

4.3. Results and Discussion

4.3.1. Synthesis

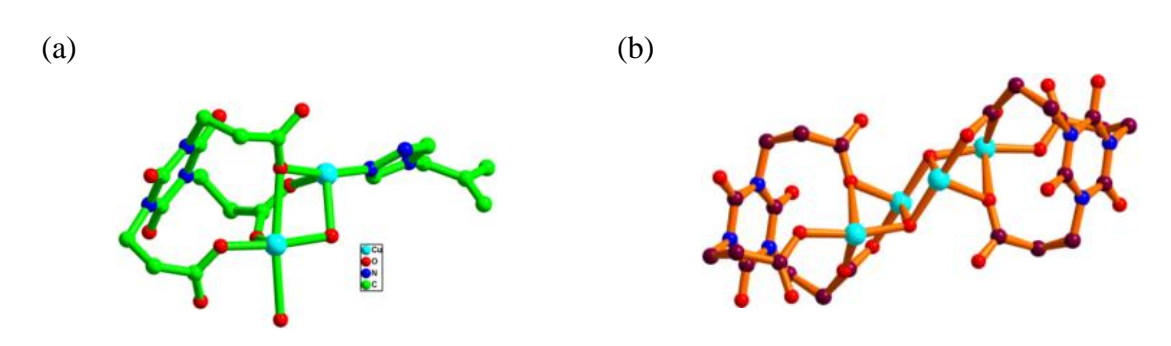
In this work, a common flexible tripodal carboxylate ligand *i.e.*, tris(2-carboxyethyl)isocyanurate (H₃tci) and two different neutral 'N' donor ligands (btx and biip) have been employed to obtain three different compounds $\{Cu_2(tci)(btx)_{0.5}(\mu_3-OH)(H_2O)\}_n$ (1), $\{Cu_{1.5}(tci)(biip)\}_n$ (2), $\{Co_{1.5}(tci)(biip)\}_n$ (3) as shown in Scheme 1. The deprotonation of the carboxylic acid groups was ensure by adding NaOH (0.5M) for all three concerned reactions. The temperature and time duration of the solvothermal syntheses have been kept identical for all three syntheses. All the three compounds show

diverse supramolecular architectures in spite of having a common primary ligand. This is due to the different chemical nature of secondary ligands, btx and biip — the V-shaped ligands and the two metal ions which were employed are different *i.e.*, Cu(II) and Co(II).

4.3.2. Description of crystal structures

${Cu_2(tci)(btx)_{0.5}(\mu_3\text{-OH})(H_2O)}_n$ (1)

Single-crystal X-ray diffraction (SCXRD) analysis reveals that the compound $\{Cu_2(tci)(btx)_{0.5}(\mu_3-OH)(H_2O)\}_n$ (1) is crystallized in triclinic space group 'P-1'. The asymmetric unit of compound 1 consists of two crystallographically independent Cu(II) centers, one tci3- ligand, half of the btx linker, one coordinated water molecule, and one μ₃-OH species (Figure 4.1a). One Cu(II) metal ion is in octahedral geometry where in three positions are occupied by the three oxygen atoms from one tci³⁻ acid ligand, one position is occupied by the µ₃-OH, one position is occupied by oxygen atom from coordinated water, and another position is occupied by N atom of btx ligand. Another Cu(II) metal center is in square pyramidal geometry where two positions are occupied by two oxygen atoms from one tci³- acid ligand, two positions are occupied by two oxygen atoms from the µ₃-OH, and the fifth position is occupied by N atom of the one btx ligand. All the Cu-O bond distances are in the range of 1.917-2.561 Å and the Cu-N bond distances are 2.021 and 2.031 Å. Three carboxylate groups of the tci³⁻ ligand adopt three different coordination modes in this compound. Among them one carboxylate group of the tci^{3-} connects to the copper metal ion in monodentate μ_1 - η^1 : η^0 coordination mode, other two carboxylate groups of the tci³⁻ connect to the metal ion in two different bidentate modes, *i.e.*, $\mu_1 - \eta^1 : \eta^1$ and $\mu_2 - \eta^2 : \eta^0$ coordination mode to results the formation of metal-acid structure (Figure 4.1b). The connectivity of the linkers with Cu(II) centers gives a unique cupper tetramer as the SBU unit (Figure 4.1c). Further, the btx connectivity with the SBUs results $\{Cu_2(btx)\}_n$ 1D linear single chain (Figure 4.1d). The final connectivity of the tci^{3-} and btx with the SBUs results in the formation of a 1D network (Figure 4.1e).



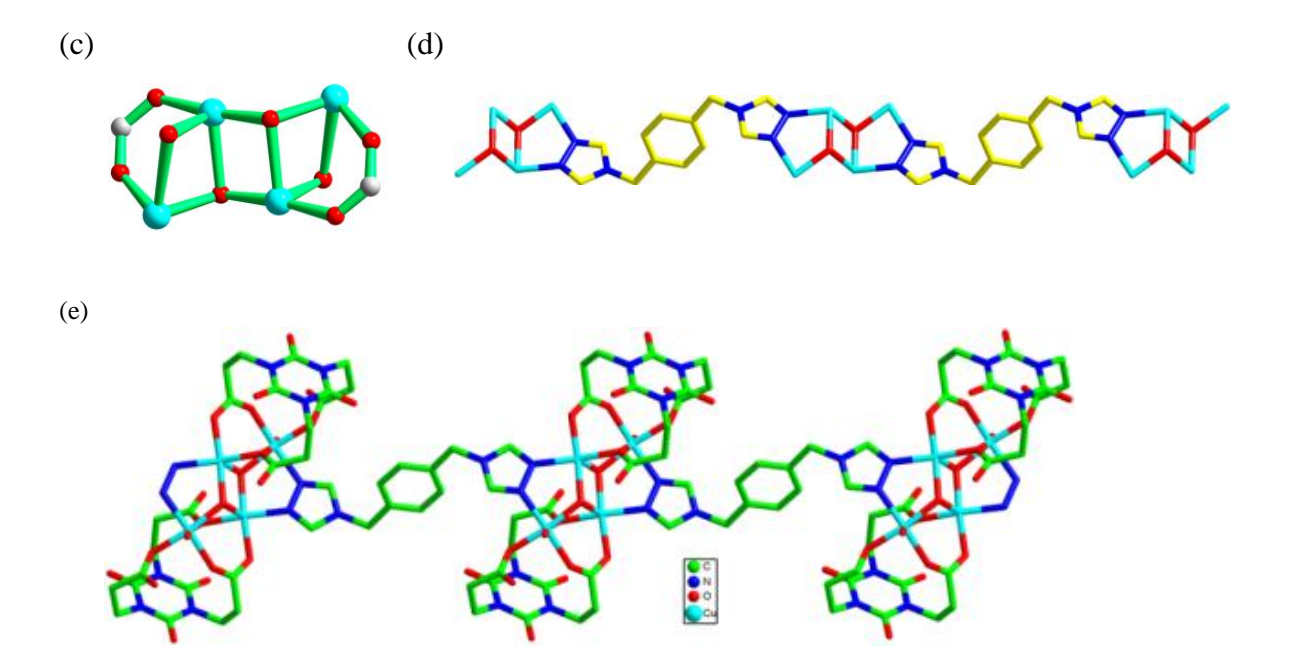


Figure 4.1. Single-crystal structural analysis of compound $\{Cu_2(tci)(btx)_{0.5}(\mu_3\text{-OH})(H_2O)\}_n$ (1): (a) asymmetric unit of compound 1; (b) metal-acid structure, connectivity of the acid linker tci^{3-} with Cu(II) metal ions; (c) Cu(II) tetramer as the SBU unit; (d) 1D chainlike arrangement in the crystal structure formed by the connectivity of btx ligand and Cu(II) metal ions; (e) 1D chain of compound 1 formed by the connectivity of the tci^{3-} and btx ligand with the SBU

$\{Cu_{1.5}(tci)(biip)\}_n(2)$

Single crystal structural studies reveal that compound $\{Cu_{1.5}(tci)(biip)\}_n(2)$ crystallizes in the triclinic space group '*P*-1'. As shown in Figure 4.2a the molecular diagram consists of a $\{Cu_2(COO)_4\}$ paddle-wheel in which the apical sites are coordinated to the imidazole nitrogen atoms of two biip ligands. Each Cu(II) ion in the paddle-wheel is in distorted octahedral geometry constituted by the four oxygen atoms from the four tci^{3-} ligands in the basal plane and one nitrogen atom from the biip ligand in the apical position, and the other apical positions of both metal centers are connected to form a long bond between them. The Cu1-Cu1A bond distance in the paddle-wheel is 2.677 Å, which is considered to be a long bond. Cu2 is in square planar geometry surrounded by two oxygen atoms from two tci^{3-} ligands and two nitrogen atoms from two biip ligands. The Cu-O bond distances are in the range of 1.963–1.98 Å and the Cu-N bond distances are in the range of 2.004–2.137 Å. The Cu1 and Cu2 are bridged by tci^{3-} ligands. The carboxylate groups of tci^{3-} ligand adopts two different coordination modes; two of them are coordinated to the Cu1 metal ion in a bidentate chelating $(\mu_2-\eta^1:\eta^1)$ coordination fashion, and the other carboxylate group is coordinated to Cu2 metal ion in a monodentate $(\mu_1-\eta^1:\eta^0)$

coordination fashion. Each tci³⁻ ligand connects to two Cu1 metal ions and one Cu2 metal ion in its trans-trans-trans conformations to form 2D metal-acid layer structure (Figure 4.2b). The Cu1 and Cu2 metal ions are arranged alternatively. These adjacent 2D metal-acid layers are further connected by secondary linker biip by creating a separation of 10.373 Å to form a layered pillared 3D framework. The biip linker connects Cu1 and Cu2 between the adjacent layers, in which the imidazole nitrogen atom of one end of the linker coordinates to the Cu1 center, which has distorted octahedral geometry (paddlewheel), and the other end imidazole nitrogen of the linker is attached to the Cu2 center, which has square planar coordination sphere as shown in the Figure 4.2c. The overall connectivity of the 2D metal acid sheets with the biip linkers results in the formation of a 3D framework (Figure 4.2d).

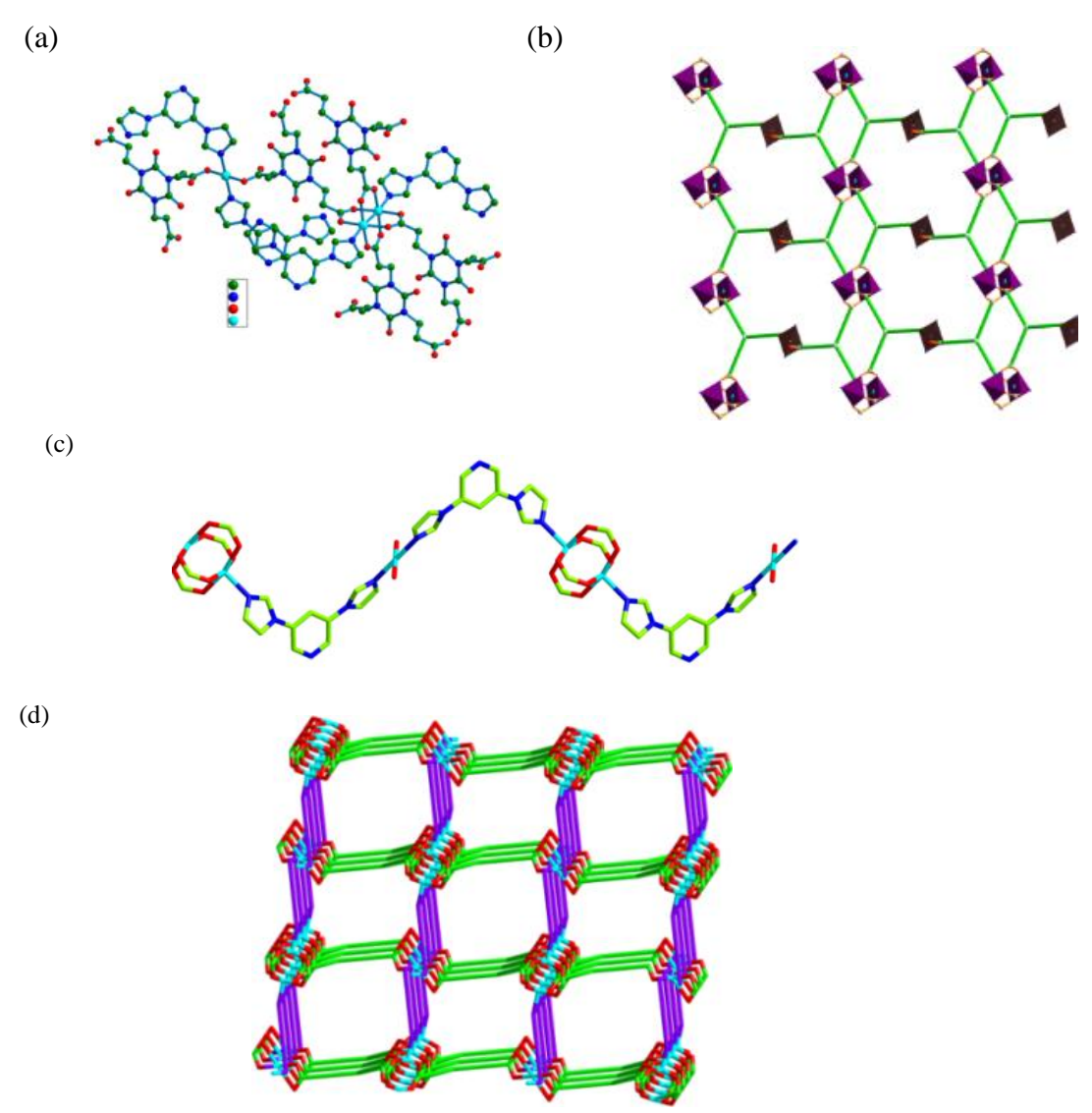
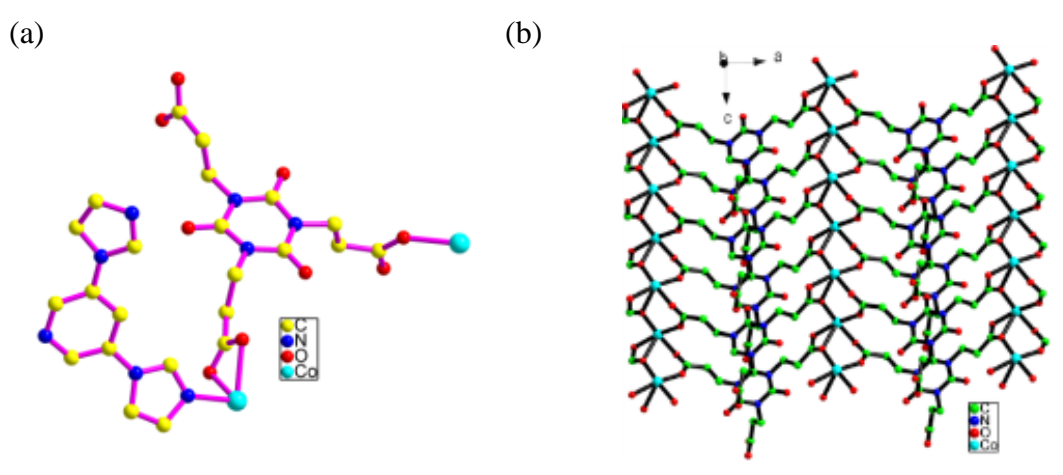


Figure 4.2. Crystal structure depiction of compound $\{Cu_{1.5}(tci)(biip)\}_n$ (2): (a) Molecular diagram of the compound 2, hydrogen atoms are omitted for clarity. (b) 2D metal-acid layer, connectivity of the acid linker

tci³⁻ with Cu(II) metal ions. (c) The Cu1 and Cu2 metal ions are arranged alternatively by the connectivity with biip linkers. (d) 3D topological representation in the crystal structure of of the compound 2.

Compound $\{Co_{1.5}(tci)(biip)\}_n$ (3)

SCXRD analysis of compound $\{Co_{1.5}(tci)(biip)\}_n$ (3) reveals a three-dimensional (3D) framework that crystallizes in the monoclinic space group 'P2(1)/c'. The asymmetric unit contains two Co(II) ions, one tci³⁻ ligand and one bijp ligand as shown in Figure 4.3a. Co1 metal is in distorted octahedral geometry where four positions are occupied by four oxygen atoms from two different tci³⁻ ligands in the basal plane and the epical positions are occupied by two nitrogen atoms from two different bijp ligands. Co2 metal is also in distorted octahedral geometry where five positions are occupied by oxygen atoms from four different tci³⁻ ligands and the other position is occupied by nitrogen atom from bijp ligand. The Co-O bond distances are in the range of 2.052 to 2.330 Å and the Co-N bond distances are in the range of 2.102–2.113 Å. The bond angles around the Co1 Centre are in the range of 60.44-180° and the bond angles around the Co2 are in the range of 82.74-174.4°. Three carboxylate groups of tci³- ligand adopt three different coordination modes: among these, two carboxylate groups adopt bidentate coordination modes in different ways, i.e., $\mu_2 - \eta^1 : \eta^1$; $\mu_1 - \eta^1 : \eta^1$ (chelate) and the other one is in tridentate $\mu_2 - \eta^2 : \eta^1$ coordination mode. The tci3- ligand coordinates to two Co2 centers: from one side it coordinates to one Co2 center in a tridentate mode and on the other side, it coordinates to another Co2 center in a bidentate bridging mode to result in a two-dimensional Co2-acid layer in the crystallographic 'ac' plane as shown in Figure 4.3b, whereas the third carboxylate group of the tci³- ligand coordinates to the Co1 center in a bidentate chelating mode to form three-dimensional (3D) metal-acid network (Figure 4.3c). Further, the biip ligand connects both the Co1 and Co2 centers within the metal-acid 3D structure, giving rise to an overall 3D network (Figure 4.3d).



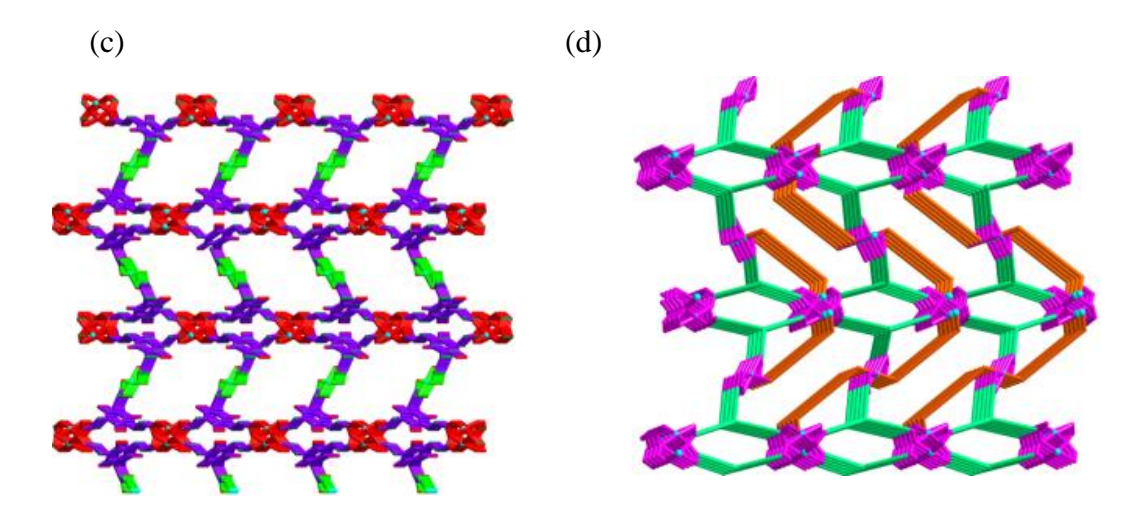


Figure 4.3. Interpretation of crystal structure of compound $\{Co_{1.5}(tci)(biip)\}_n$ (3): (a) The basic unit of compound 3. (b) Two-dimensional Co2-acid layers formed by the connectivity of tci^{3-} ligands and Co2 centers in the crystallographic 'ac' plane. (c) Three-dimensional (3D) metal-acid network, formed due to coordination of Co(II) centers with tci^{3-} ligands. (d) Overall 3D structure formed by the connectivity of the tci^{3-} and biip ligands with the Co(II) centers.

4.3.3. PXRD and Thermogravimetric Analysis (TGA)

Powder X-ray diffraction (PXRD) data for compounds **1–3** have been recorded to ensure the phase purity of these products. The well-matching between the experimentally observed diffraction peaks and the corresponding patterns from simulated data (calculated from respective single crystal data) prove the bulk homogeneity of these crystalline solids (Figure 4.4).

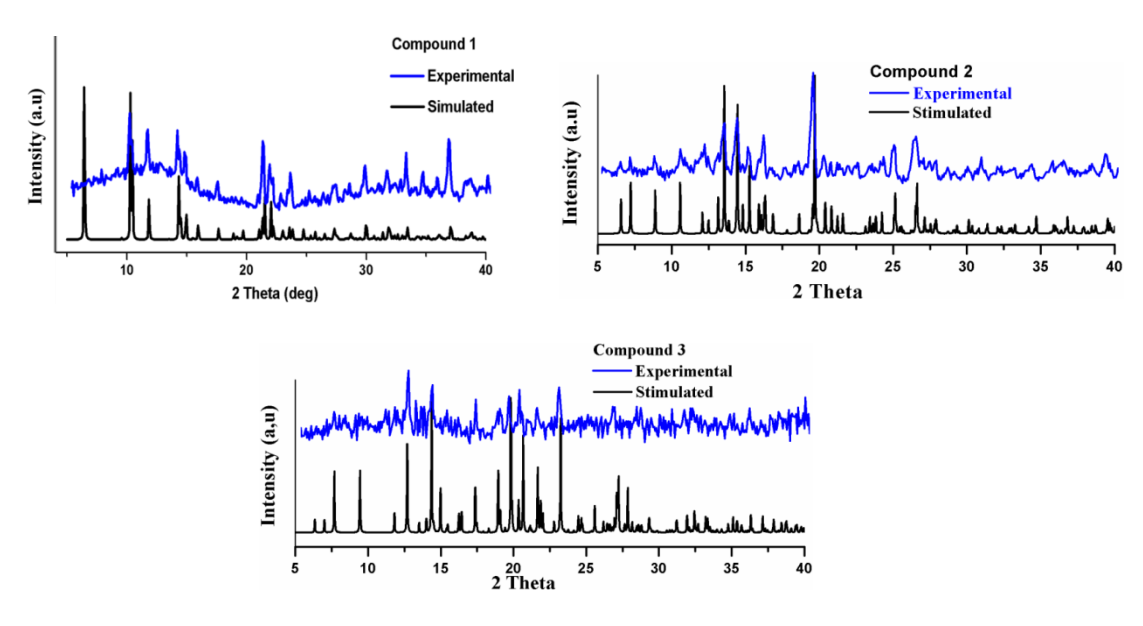


Figure 4.4. Powder X-ray diffraction patterns of the compounds 1-3 (blue curves), including simulated patterns obtained from respective single crystal data (black curves). Thermogravimetric analysis (TGA) has been performed under the flow of N_2 gas in the

temperature range of 30-800 °C in the powdered phase. The TGA plots of compounds

1–3 are shown in Figure 4.5. Compound **1** is stable up to 250 °C and then it undergoes continuous weight loss in the temperature range of 250–800 °C indicating the decomposition of the organic parts, *i.e.* H₃tci and btx ligands. The TGA curve of compound **2** exhibits stability up to 280 °C and undergoes continued weight loss attributed to the decomposition of btx and tci^{3–} ligands. Compared to compounds **1** and **2**, compound **3** shows high thermal stability up to 360 °C, followed by decomposition with a weight loss up to 800 °C attributed to the consecutive losses of the tci^{3–} ligand and the biip linker molecule.

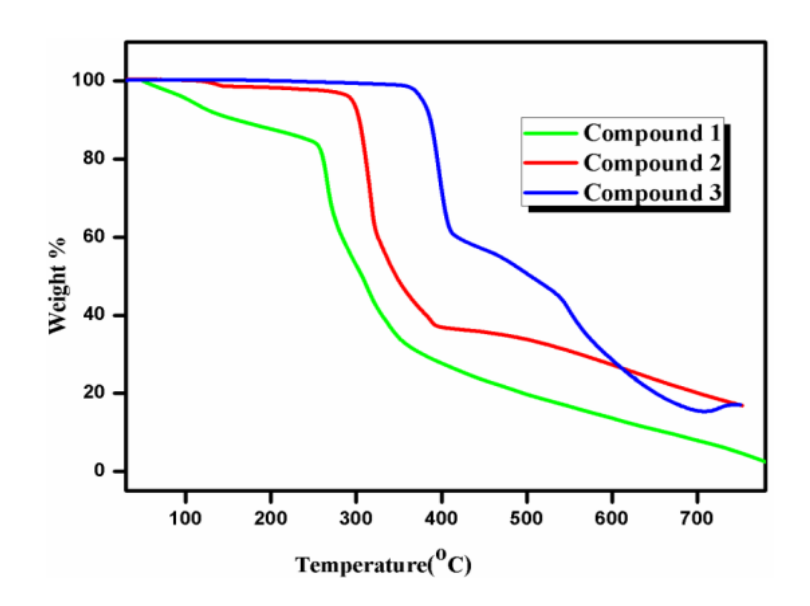


Figure 4.5. Thermogravimetric curves of the compounds 1–3.

4.3.4. Electronic Spectra of Compounds 1, 2 and 3

The electronic absorption spectra of compounds **1–3** are recorded in solid-state diffuse reflectance (DRS) mode at room temperature. The absorption peaks for compound **1** are observed at 650, 460, 250 nm in its electronic spectrum (Fig. 5). Likewise, the electronic absorptions at 490, 355, 247 nm (compound **2**) and 550, 500, 474, 280 nm (compound **3**) are observed in the respective diffuse reflectance spectra as shown in Fig. 5. The lower energy bands, in all the compounds, are assigned due to the d-d transitions of metal ions present in these materials, *i.e.*, Cu(II) ion in compounds **1** and **2** and Co(II) ion in compound **3**. Apart from these metal-based transitions, all compounds exhibit higher energy bands in the wavelength range of 247–355 nm, that are ascribed to the ligand-centered transitions by comparing with the electronic spectra of the free ligands, used to prepare the title compounds (Fig. S3, Supporting Information).

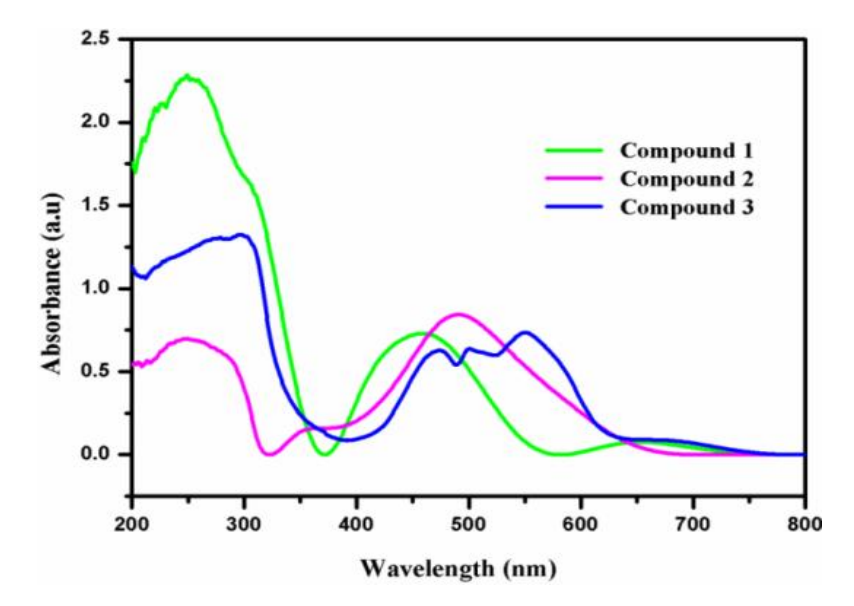
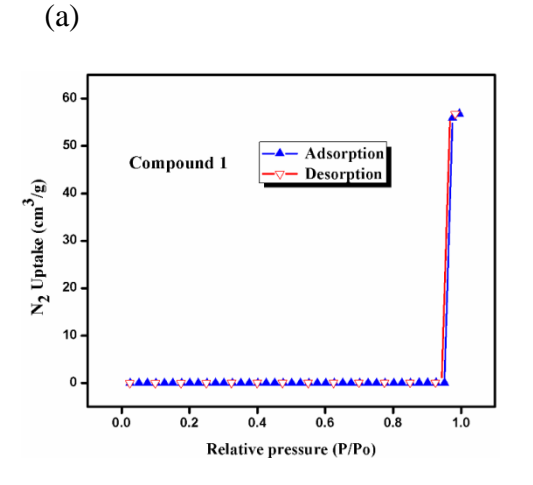
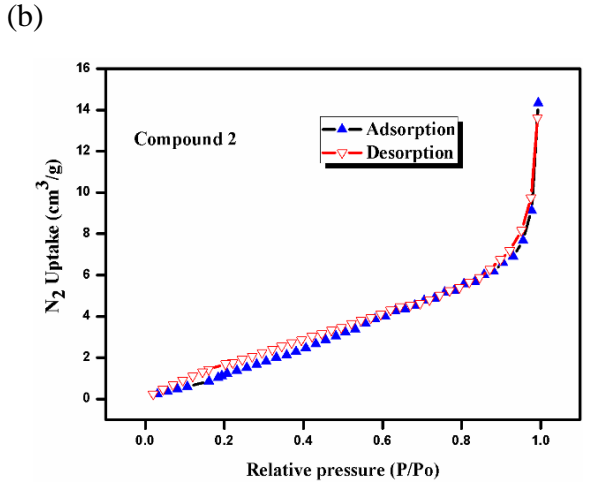


Figure 4.6. Solid state-diffuse reflectance spectra (DRS) of (a) compounds 1, 2 and 3

4.3.5. Gas adsorption analysis

The nitrogen sorption measurements of compounds **1–3** were executed with liquid nitrogen Dewar at 77 K. Before going to analysis, the compounds were heated at 373 K for degassing under dynamic vacuum to activate the samples for 10 hours. As shown in Fig. 6, the nitrogen adsorption-desorption properties of compounds **1–3** were measured at P/Po = 0.99 relative pressure with a maximum N₂ uptake of 56.7450, 14.3255, 11.7686 cm³/g (STP), respectively. The isotherms of compounds **1–3** appear to be characteristic of type III adsorption isotherm curves, indicating macroporous structures for compounds **1–3**. The BET (Brunauer– Emmett–Teller) surface areas of **1–3** are found to be 3.615, 10.672 and 14.356 m²/g correspondingly. The CO₂ adsorption isotherms of compounds **1–3** have been obtained at 273 K with temperature-controlled circulating water bath. The samples were degassed for 10 hours at 393 K for activation. The CO₂ adsorption isotherms (Fig. 7)





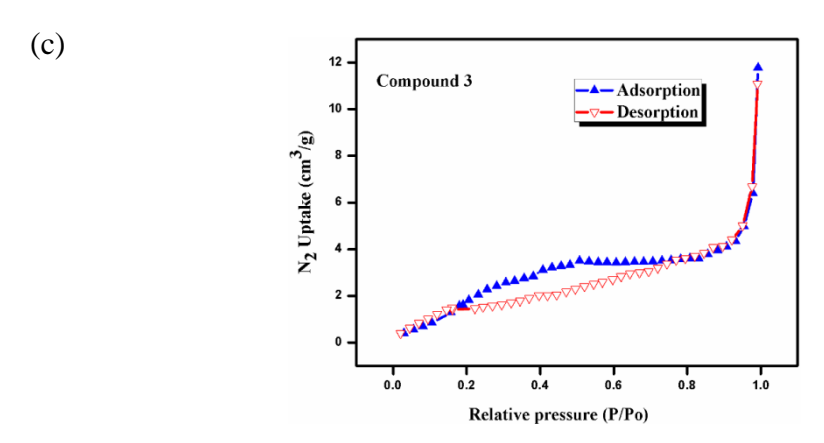


Figure 4.7. N₂ adsorption-desorption isotherms for compounds **1–3** at 77 K: (a) compound 1, (b) compound 2, (c) compound 3.

for compounds **1–3** show CO₂ uptake of 13.0984, 1.5111 and 1.1317 cm³/g (STP) at P/Po relative pressure, respectively. The CO₂ adsorption isotherms of compounds **1–3** were obtained at 273 K with temperature-controlled circulating water bath and degassed the samples for 10 hours at 393 K for activation. The CO₂ adsorption isotherms for compounds **1–3**, illuminating the uptake of 13.0984, 1.5111 and 1.1317 cm³/g (STP) at P/Po relative pressure in that order (Figure 4.8).

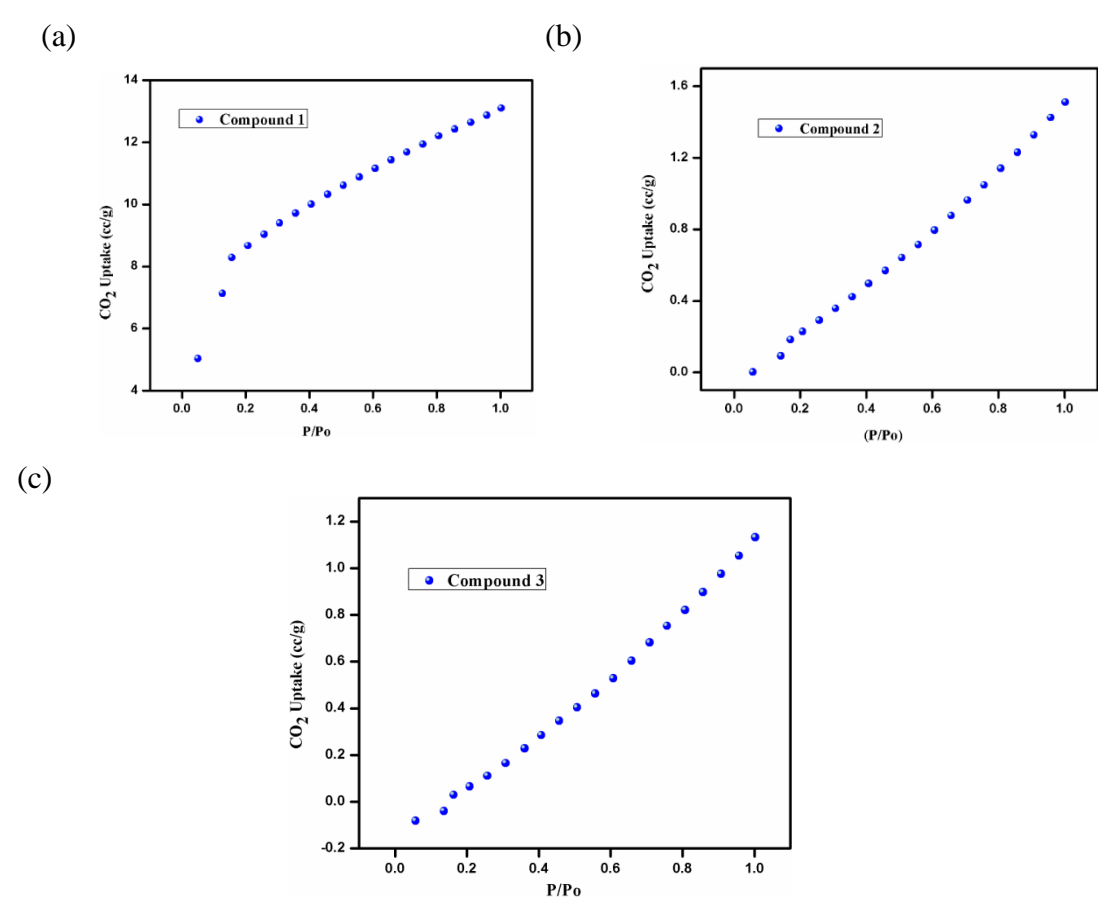


Figure 4.8. CO_2 adsorption isotherms for compounds **1–3** at 373 K: (a) compound 1, (b) compound 2, (c) compound 3.

4.4. Conclusions and future scope

In summary, in this work, three new coordination polymers have been synthesized by using tripodal flexible carboxylic ligand {tris(2-carboxyethyl) isocyanurate} and two Ndonor secondary ligands, btx, and bijp. All three compounds are structurally characterized, besides their routine spectral analyses. In compound 1, ligand tci³⁻ is coordinated to the copper tetramer (SBU) with mono- and bi-dentate coordination modes and the resulting metal-acid chain is further bridged by btx ligand to results one-dimensional coordination polymer. In compound 2, the tci³⁻ ligand is connected to two different SBUs i.e., paddlewheel and square planar Cu(II) in bidentate chelating and monodentate coordination modes respectively, resulting in the creation of 2D metal-acid layers. These metal-acid layers are pillared by the bijp ligand leading to the formation of a 3D framework. On the other hand, in compound 3, the tci³- ligand coordinates to Co1 and Co2 with tridentate and chelate bidentate modes to result in a metal-acid network structure. The overall connectivity of tci3- and biip with cobalt(II) metal ions result in the formation of a 3D network in the crystal structure of compound 3. Thus, all the three compounds exhibit a unique behaviour in the construction of secondary building units (SBUs) in their respective crystal structures in relation to the geometry of the metal ions involved. We have observed that compound 3 exhibits good thermal stability compared to those of compounds 1 and 2. Compounds 1-3 have been characterized by obtaining gas adsorption BET isotherms including CO₂ adsorption studies.

Interestingly, the compound 1 exhibits a metal-water coordination along with the μ_3 -OH linkage within the tetrameric motif. This kind of structural arrangement is crucial in electrochemical catalysis involving electrocatalytic water splitting. We are currently working in this direction.

Table 4.1: Crystal data and structure refinement parameters for compounds 1–3

	1	2	3
Empirical formula	C ₁₈ H ₂₁ Cu ₂ N ₆ O ₁₁	$C_{23} H_{21} Cu_{1.5} N_8 O_9$	$C_{23}H_{21}Co_{1.5}N_8O_9$
Formula weight	624.48	648.78	641.86
$T(K)/\lambda(Å)$	100(2) /0.71073	100(2) /0.71073	100(2) /0.71073
Crystal system	Triclinic	Triclinic	Monoclinic
Space group	P-1	P-1	P2 (1)/c
a (Å)	8.4907(6)	7.510(2)	12.6430(7)
b (Å)	9.4850(7)	12.476(3)	27.8804(15)
c (Å)	14.0489(10)	14.006(4)	6.7417(3)
α (°)	102.240(3)	79.241(10)	90
β (°)	93.681(3)	77.270(11)	92.350(2)
γ (°)	94.337(3)	85.150(12)	90
Volume (Å ³)	1098.79(14)	1256.2(6)	2374.4(2)
$Z, \rho_{calcd} (Mg/m^3)$	2, 1.888	1, 1.715	2, 1.796
$\mu (\text{mm}^{-1}), F(000)$	2.012/634	1.353 /661	1.136 /1310
Goodness- of-fit on F ²	1.039	1.023	1.072
$R1/wR2[I > 2\sigma(I)]$	0.0325/0.0791	0.0384/0.0789	0.0354/0.0836
R1/ wR2 (all data)	0.0416/0.0858	0.0608/0.0856	0.0367/0.0843
Largest diff peak/ hole (e Å-3)	0.490 /-0.646	0.600 /-0.345	1.327 /-0.47

4.5. References

- 1. K. Kobalz, M. Kobalz, J. Mollmer, U. Junghans, M. Lange, J. Bergmann, S. Dietrich, M. Wecks, R. Glaser, H. Krautscheid, Inorg. Chem. 55 (2016) 6938.
- 2. P. Li, H. Zhan, S. Tian, J. Wang, X. Wang, Z. Zhu, J. Dai, Y. Dai, Z. Wang, C. Zhang, X. Huang and W. Huang, Acs Appl. Mater. Interfaces. 11 (2019) 13624.
- 3. I.A. Lázaro, R.S. Forgan, Coord. Chem. Rev. 380 (2019) 230.
- 4. D. Yang and B.C. Gates, ACS Catal. 9 (2019) 1779.
- 5. Y. Noori and K. Akhbari, RSC Adv. 7 (2017) 1782.
- 6. G. M. Espallargas, E. Coronado, Chem. Soc. Rev. 47 (2018) 533.
- 7. Z.-J. Lin, J. Lü, M. Hong, R. Cao, Chem. Soc. Rev. 43 (2014) 5867.
- 8. J.J.M. Tellado, D.D. Díaz, CrystEngComm 17 (2015) 7978.
- 9. J.-S. Li, M.-Y. Zhang, Z.-b. Han, Synthesis and Reactivity in Inorganic, Metal-Organic, and Nano-Metal Chemistry 43 (2013) 805.
- S. K. Ghosh, W. Kaneko, D. Kiriya, M. Ohba, S. Kitagawa, Angew. Chem. Int. Ed. 47 (2008) 8843.
- 11. M.-Y. Zhang, W.-J. Shan, Z.-B. Han, CrystEngComm 14 (2012) 1568.
- 12. R.-Y. Chen, D. Tian, T.-L. Hu, Z. Chang, Inorg. Chem. Commun. 49 (2014) 131.
- 13. H. Li, Z. Xu, B. Zhao, Y. Jia, R. Ding, H. Hou, Y. Fan, CrystEngComm 16 (2014) 2470.
- 14. M.-Y. Zhang, W.-J. Shan, Z.-B. Han, CrystEngComm 14 (2012) 1568.
- 15. D. Tian, S. Liu, D. Zhang, Z. Chang, T. Hu, X. Bu, Sci China Chem 56 (2013) 1693.
- Y.-L. Bai, X. Bao, S. Zhu, J. Fang, M. Shao, H. Shi, Eur. J. Inorg. Chem. 2014 (2014) 1275.
- 17. M.-Y. Zhang, R. Xu, Z.-B. Han, Z. Anorg. Allg. Chem. 638 (2012) 675.
- 18. M. Y. Zhang, G. X. Zhang, J. Q. Gao, Z. B. Han, Russian Journal of Coordination Chemistry 38 (2012) 279.
- 19. C. Hou, Y.-L. Bai, X. Bao, L. Xu, R.-G. Lin, S. Zhu, J. Fang, J. Xu, Dalton Trans. 44 (2015) 7770.

- 20. Q. Zhu, C. Shen, C. Tan, T. Sheng, S. Hu, X. Wu, Dalton Trans. 41 (2012) 9604.
- 21. H. Li, H. Yao, E. Zhang, Y. Jia, H. Hou, Y. Fan, Dalton Trans. 40 (2011) 9388.
- 22. D. Tian, X.-J. Liu, R.-Y. Chen, Y.-H. Zhang, Chinese Chemical Letters 26 (2015) 499.
- 23. Z.-B. Han, M.-Y. Zhang, D.-Q. Yuan, S. Fu, G.-X. Zhang, X.-F. Wang, CrystEngComm 13 (2011) 6945.
- 24. Z.-B. Han, G.-X. Zhang, M.-H. Zeng, D.-Q. Yuan, Q.-R. Fang, J.-R. Li, J. Ribas, H.-C. Zhou, Inorg. Chem., 49 (2010) 769.
- 25. S. Sun, G.X. Zhang, J.Q. Gao, Z.B. Han, Russian Journal of Coordination Chemistry 38 (2012) 315.
- 26. L. Cui, P. C. Zhao, Russian Journal of Coordination Chemistry 39 (2013) 316.
- 27. Z.-B. Han, G.-X. Zhang, CrystEngComm 12 (2010) 348.
- 28. H. Li, B. Zhao, R. Ding, Y. Jia, H. Hou, Y. Fan, Cryst. Growth Des. 12 (2012) 4170.
- 29. A.-R. Li, Q.-Q. Guo, L. Li, H.-W. Hou, Y.-T. Fan, Polyhedron 71 (2014) 17.
- 30. S. Fu, G.-X. Zhang and Z.-B. Han, Z. Anorg. Allg. Chem. 637 (2011) 2153.
- 31. H. Gao, X.-h. Lou, Q.-T. Li, W.-J. Du, C. Xu, Inorg. Chim. Acta. 412 (2014) 46.
- 32. P. Cui, J. Wu, X. Zhao, D. Sun, L. Zhang, J. Guo, D. Sun, Cryst. Growth Des. 11 (2011) 5182.
- 33. C.-W. Lv, J. Li, Y.-W. Liu, X. Li, Z. Yuan, Journal of Molecular Structure 1100 (2015) 1.
- 34. S. K. Ghosh, S. Kitagawa, CrystEngComm 10 (2008) 1739.
- 35. S. K. Ghosh, S. Bureekaew, S. Kitagawa, Angew. Chem. Int. Ed. 47 (2008) 3403.
- 36. Y.-X. Chen, B.-Y. Chen, J.-H. Yang, G.-Q. Qin, Z. Anorg. Allg. Chem. 640 (2014) 390.
- 37. L. Liang, Y. Cai, N.S. Weng, R. Zhang, J. Zhao, J. Wang, H. Wu, Inorg. Chem. Commun. 12 (2009) 86.
- 38. S. K. Ghosh, J.-P. Zhang, S. Kitagawa, Angew. Chem. Int. Ed. 46 (2007) 7965.
- 39. G.-X. Zhang, W. Zhang, Z.-B. Han, J Chem Crystallogr 41 (2011) 727.
- 40. Z.-B. Han, G.-X. Zhang, M.-H. Zeng, C.-H. Ge, X.-H. Zou, G.-X. Han, CrystEngComm 11 (2009) 2629.
- 41. B.K. Tripuramallu, S. Mukherjee and S.K. Das, Cryst. Growth Des. 12 (2012) 5579.

- 42. P. Manna and S. K. Das, Cryst. Growth Des. 15 (2015) 1407.
- 43. B.K. Tripuramallu and S.K. Das, Cryst. Growth Des. 13 (2013) 2426.
- 44. P. Manna, B.K. Tripuramallu and S.K. Das, Cryst. Growth Des. 14 (2014) 278.
- 45. P. Manna, B.K. Tripuramallu and S.K. Das, Cryst. Growth Des. 12 (2012) 4607.
- 46. B.K. Tripuramallu, P. Manna, S.N. Reddy, S K. Das, Cryst. Growth Des. 12 (2012) 777.
- 47. P. Manna, B.K. Tripuramallu, S. Bommakanti and S.K. Das, Dalton Trans. 44 (2015) 2852.
- 48. L. Luo, Y. Zhao, Y. Lu, T.-a. Okamura, W.-Y. Sun, Polyhedron 38 (2012) 88.
- 49. C.R. Murdock, D.M. Jenkins, J. Am. Chem. Soc. 136 (2014) 10983.
- 50. Bruker SMART, Version 5.625, SHELXTL, Version 6.12; Bruker AXS Inc.: Madison, Wisconsin, USA, (2000).
- 51. G. M. Sheldrick, Program for Refinement of Crystal Structures; University of Göttingen, Germany, (1997).
- 52. G. M. Sheldrick, Acta Crystallogr., Sect. A: Found. Crystallogr. 64 (2008) 112.
- 53. G. M. Sheldrick, Acta Crystallogr., Sect. C: Struct. Chem. 71 (2015) 3.

A series of coordination polymers- / metal-organic frameworks-containing four compounds, formulated $\{Cu_2(ADA)_2(biip)\}_n.4nH_2O$ **(1)**, $\{[(Co)(sdba)(biip)]_2\}_n.4nH_2O$ (2), ${Co(ADC)(biip)(H_2O)}_n$ (3) and ${(Co)(ADAH)_2(biip)}_n$ (4), have been synthesized by using flexible as well as rigid ligands, where H₂ADA = 1,3-adamantanediacetic acid; H₂ADC = 1,3adamantanedicarboxylic acid; H₂sdba (4,4'-thiodibenzoic acid) and an secondary linker, biip {3,5di(1H-imidazol-1- yl)pyridine} under solvothermal conditions. Compounds 1-4 have been well characterised by IR spectroscopy, single crystal X-ray diffraction analysis, thermogravimetric (TG) and elemental analyses. Compound 1 is 3D structure, formed by the connectivity of two different 2D- and 1D-metal-acid chains through the biip linkers. In the crystal structure of compound 2, one dimensional square wave-like chains are formed by the coordination of Co(II) with sdba²⁻ ligands and these chains are further connected by the biip ligand, leading to the formation of a 2D structure. The crystal structure of compound 3 consists of 2D sheets, constructed by the connectivity of Co(II) with N,N-linker and dicarboxylate ligand. In the crystal structure of compound 4, two altered metallo-macrocyles, 20-membered metal-acid {Co₂(ADA)₂} ring and another 20-membered metal-N-linker {Co₂(biip)₂}ring, are formed, and these macrocylic-rings are arranged alternatively, leading to the formation of a new 1D extended coordination polymer. The related supramolecular chemistry has been discussed for all four compounds.

5.1. Introduction

Metal-organic frameworks (MOFs)/coordination polymers (CPs) are generally porous crystalline solid materials that are formed by multidentate organic ligands with metal ions through the coordinate covalent bonds resulting in diverse supramolecular architectures of the concerned MOFs and CPs. The metal-ligand coordination bonds inorganizing molecular building blocks can lead to diverse supramolecular architectures of 1D, 2D and 3D networks. Yaghi and co-workers have coined the term MOF (metal organic framework) and now it is a popular field in chemstry. MOFs are explored in interdisciplinary areas and MOFs have pleasing structures / topologies. In general, MOFs have drawn considerable attention because of their potential applications in diverse areas, such as, gas storage, 2,3 separation, 4 heterogeneous catalysis, ^{5,6} drug delivery, ⁷ energy storage, ⁸ bio-medicine, ⁹ electrode materials for supercapacitance, 10 ultrasonics, 11 water treatment, 12 toxic material removal, 13 luminescence, ¹⁴⁻¹⁷ and sensing application. ¹⁸ More than 20000 MOFs have been reported, that are different from each other in terms of their designs, synthetic methods, pore sizes and topologies. Design and synthesis of MOFs/CPs having desired architectures and tailor-made properties can be one of the most important challenges in the field of framework materials. Toward achieving expected architectures, selection of a ligand or a linker is a vital factor as far as "flexibility versus rigidity" issue is concerned. 19,20 The flexibility and rigidity of the organic ligands/linkers, concerned in the assembly of coordination networks, has a great impact in transforming the functional properties of the networks to the concerned resulting compounds.²¹ In particular, flexibility plays in important role in controlling inherent properties including mechanical features of the framework materials.²² Many crystalline frameworks containing compounds have been discovered with dynamic behaviours in the last few decades. One predominantly essential mode of MOF flexibility is classified as breathing of the concerned crystals that refers to structural transitions induced by guest adsorption or desorption, involving noteworthy changes in the crystallographic unit cell volume and in the resultant pore size of the relevant MOF.²³

In contrast to the flexible ligands, rigid linkers have potential to predict the coordination patterns of the resulting MOF compounds. Rigid linkers having relatively high stability with certain topologies are in line with the prediction of final structures.²⁴ It is important to mention that, MOF synthesis always begins with the selection of two main interacting components: organic building units (OBUs, including various bridging polycarboxylic groups containing ligands) and secondary building units (SBUs, associated with metallic centres).

In this work, we have chosen the flexible as well as rigid linkers for the construction of four new coordination polymer containing compounds. The dicarboxylic acids are, rigid 1,3adamantanedicarboxylic acid (H₂ADC), flexible 1,3-adamantanediaceticacid (H₂ADA) and flexible 4,4'- thiodibenzoic acid(H₂sdba) as shown in Scheme 5.1. In this work, the common N,N linker is 3,5-di(1H-imidazol-1-yl)pyridine (biip) (see Scheme 5.1) and metal sources are Cu(NO₃)₂·3H₂O and CoCl₂·6H₂O. Herein we describe synthesis of four coordination $\{Cu_2(ADA)_2(biip)\}_n.4nH_2O$ **(1)**, $\{[(Co)(sdba)(biip)]_2\}_n.4nH_2O$ polymers (2), ${Co(ADC)(biip)(H_2O)}_n$ (3) and ${(Co)(ADAH)_2(biip)}_n$ (4), that have been characterization by the single crystal X-ray diffraction analysis. The ligand- and synthesis-schemes are shown in Schemes 5.1 and 5.2, respectively. Compound 1 exhibits the three-dimensional structure, whereas compounds 2 and 3 are two-dimensional architectures; compound 4 shows onedimensional extended coordination polymer.

COOH
H₂ADA
COOH

$$H_2$$
SDBA

COOH

 H_2 ADC

 H_2 ADC

Scheme 5. 1. The ligands used in this chapter.

$$\{(Co)(ADA)_{2}(biip)\}_{n} \ \ (4) \ \ \frac{Co(II)}{H_{2}ADA} \ \ \frac{Cu(II)}{H_{2}ADA} \ \ \{Cu_{2}(ADA)_{2}(biip)\}_{n}.4nH_{2}O \ \ (1)$$

$$\{Co(ADC)(biip)(H_{2}O)\}_{n} \ \ (3) \ \ \frac{Co(II)}{H_{2}ADC} \ \ \frac{Co(II)}{H_{2}SDBA} \ \ \{[(Co)(sdba)(biip)]_{2}\}_{n}.6nH_{2}O \ \ (2)$$

Scheme 5.2. Diagram of the synthetic protocol for the compounds 1-4, described in this chapter.

5.2. Experimental

5.2.1. Materials and physical methods

The chemicals $CoCl_2 \cdot 6H_2O$ and DMF (N,N-Dimethyl formamide) were purchased from Finar, India; whereas $Cu(NO_3)_2 \cdot 3H_2O$ chemical was acquired from SRL Chemicals, India. The chemicals H_2ADA , H_2ADC , H_2sdba were purchased from Sigma-Aldrich. All the chemicals were received as reagent grade and used without any further purification. The V-shaped ligand, biip [1,4-bis(triazol-1-yl-methyl)benzene], was prepared according to the literature procedures. ²⁵

5.2.2. Characterization

Elemental analyses were determined by the FLASH EA series 1112 CHNS analyzer. Infrared spectra of solid samples were obtained as KBr pellets on a JASCO-5300 FT-IR spectrophotometer. Thermogravimetric analyses were carried out on an STA 409 PC analyzer and corresponding masses were analyzed by QMS 403 C mass analyzer, under the flow of N_2 gas with a heating rate of 5 °C min⁻¹, in the temperature range of 30–800 °C. Powder X-ray diffraction patterns were recorded on a Bruker D8-Advance diffractometer using graphite monochromatedCuK α 1 (1.5406 Å) and K α 2 (1.54439 Å) radiations. All the compounds were produced in 23 mL Teflon-lined stainless-steel vessels (Thermocon, India) under solvothermal conditions. The electronic absorption spectra have been recorded in the solid-state on a UV-2600 Shimadzu UV-visible spectrophotometer at room temperature.

5.2.3. Synthesis

Synthesis of compound $\{Cu_2(ADA)_2(biip)\}_n.4n H_2O(1)$

A mixture of $\text{Cu(NO}_3)_2 \cdot 3\text{H}_2\text{O}$ (24 mg, 0.1 mmol), H_2ADA (25.2 mg, 0.1 mmol), and biip (21.1mg, 0.1 mmol) was suspended in 10 ml of distilled water and then stirred for 30 minutes. The pH of the reaction mixture was adjusted to 6.45 by adding 0.5M NaOH solution and the resulting reaction mixture was placed in a 23 ml Teflon-lined stainless-steel autoclave, which was sealed and heated at 120 °C for 72 hours. The autoclave was allowed to cool to room temperature over 48 hours to obtain green needle-shaped crystals of compound 1 (61% yield, based on Cu). IR (KBr pellet, cm⁻¹): 3448, 3127, 2897, 2843,2463, 2283, 2248, 2172, 2158, 2135, 2096, 2073, 2049, 2010, 1980, 1957, 1605, 1562, 1508, 1449, 1392, 1356, 1317, 1297, 1273, 1255, 1187, 1152, 1126, 1071, 1008, 959, 943, 885, 842, 826, 798, 773, 746, 692, 650, 625, 599, 567, 526.

Synthesis of Compound $\{[(Co)(sdba)(biip)]_2\}_n.4nH_2O(2)$

A mixture of $CoCl_2 \cdot 6H_2O$ (0.1 mmol, 23.7 mg), H_2sdba (0.1 mmol, 30.6 mg), and biip (0.1 mmol, 21.1 mg), taken in a mixed solvent — H_2O (6 ml) and DMF (2 ml) — was stirred for 30 minutes and then the pH of the reaction mixture was adjusted to 6.1 by adding 0.5 M aq. NaOH solution. The resulting reaction mixture was then placed in a 23 ml Teflon-lined stainless-steel autoclave, which was sealed and heated at 120 °C for 72 hours. The autoclave was allowed to cool to room temperature over 48 hours to obtain purple colour block crystals of compound **2** in 67.5% yield (based on Co). Anal.Calcd.for $C_{50}H_{46}Co_2N_{10}O_{18}S_2$ (Mr = 1256.95): C, 47.78%; H, 3.69%; N, 11.14%. Found: C, 50.29%; H, 2.83%; N, 11.65%. IR (KBr pellet, cm⁻¹): 3391, 3131, 2465, 2359, 2175, 2157, 2140, 2074, 2050, 2026, 2009, 1978, 1657,1599, 1557, 1508, 1448, 1385, 1318, 1296, 1239, 1163, 1131, 1099, 1069,1012, 947, 849, 781, 743, 725, 693, 650, 622, 577.

Synthesis of Compound $\{Co(ADC)(biip)(H_2O)\}_n(3)$

Compound **3** was prepared by following the same procedure as that of compound **2** except that the ligand H_2ADC (0.1 mmol, 22.4 mg) was used in place of H_2 sdba ligand and the pH of the reaction mixture was adjusted to 6.4 in this case. After the completion of the reaction, red colour block shaped crystals were obtained by filtration in 62.4% yield (based on Co). IR (KBr pellet, cm⁻¹): 3366, 3129, 2894, 2846, 2182, 2156, 2096, 2047, 2010, 1979, 1967,1940, 1600, 1544, 1527,1500, 1448,1421, 1388, 1306, 1260, 1238, 1180, 1122, 1107, 1073, 1059,1010, 952, 932, 908, 889, 834, 818, 796, 761, 730, 705, 672, 650, 614, 571.

Synthesis of Compound $\{(Co)(ADA)_2(biip)\}_n$ (4)

Compound **4** was prepared by following the same procedure as that of compound **1** except that CoCl₂·6H₂O (0.1 mmol, 23.7 mg) was used in place of Cu(NO₃)₂·3H₂O and the pH of the reaction mixture was adjusted to 7.3 in this case. After the completion of the reaction, purple colour block shaped crystals were obtained by filtration in 61% yield (based on Co). IR (KBr pellet, cm⁻¹): 3119, 2901, 2864, 2842, 2464, 2210, 2182, 2074, 2048, 2024, 2010, 1992, 1979, 1966, 1941, 1660, 1598, 1550, 1508, 1446, 14061342, 1319, 1287, 1265, 1220, 1174, 1144, 1117, 1102, 1073, 1062, 1004, 951, 933, 899, 863, 849, 808, 771, 745, 718, 695, 656, 638, 621, 600, 567, 526.

5.2.4. Single crystal X-ray structure determination of the compounds 1–4

Data for single-crystals suitable for structural determination of all the compounds 1-4 were collected on a Bruker D8 Quest CCD diffractometer under a Mo–K α (λ = 0.71073 Å) graphite monochromatic X-ray beam with a crystal-to-detector distance of 40 mm. The data reduction was performed using Apex- II Software. Empirical absorption corrections using equivalent reflections were performed with the program SADABS. Structure solutions and full-matrix least-squares refinement were carried out using standard crystallographic software for all the compounds. All the non-hydrogen atoms were refined anisotropically. Hydrogen atoms on the C atoms were introduced on calculated positions and were included in the refinement riding on their respective parent atoms. Crystal data and structure refinement parameters for compounds 1-4, are summarized in Table 5.1.

5.3. Results and Discussion

5.3.1. Synthesis

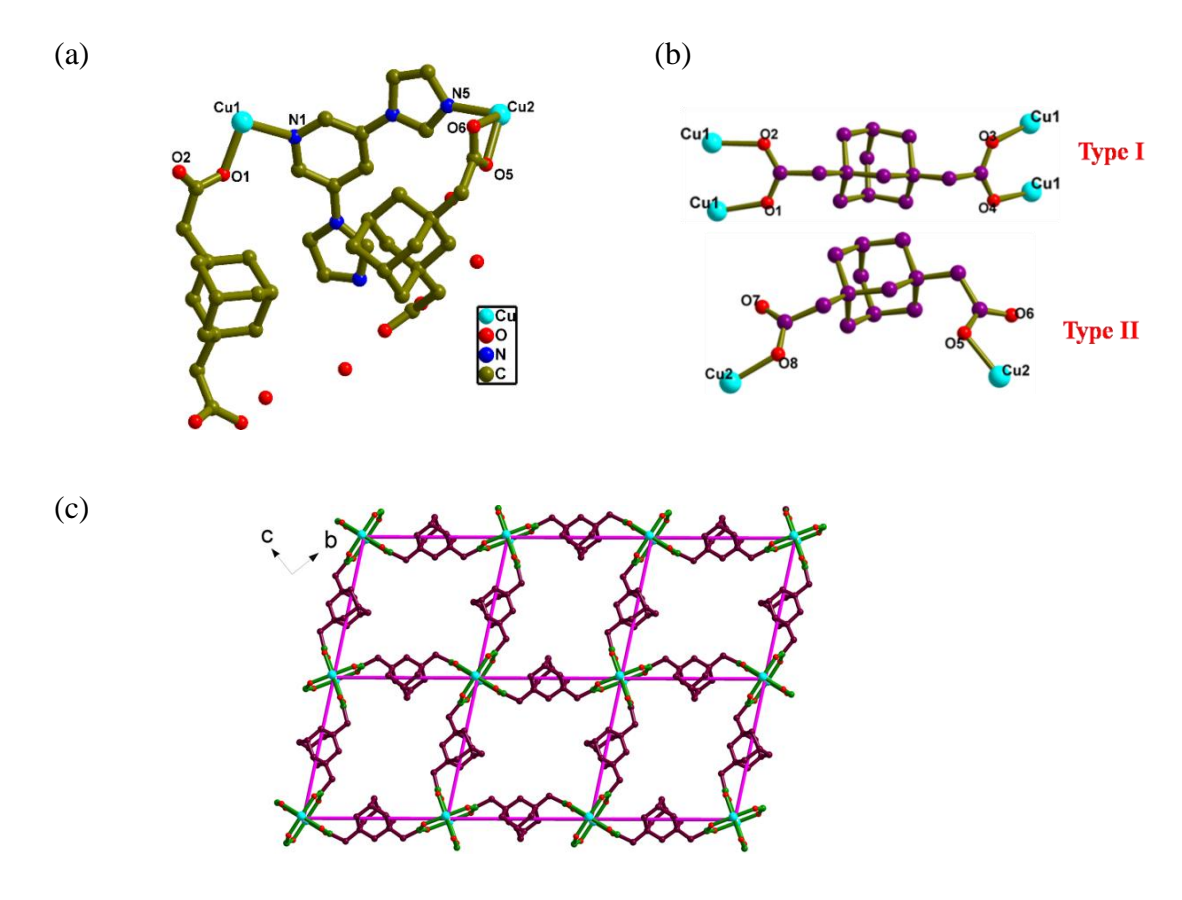
In this article, four different coordination polymers $\{Cu_2(ADA)_2(biip)\}_n.4nH_2O$ (1), $\{[(Co)(sdba)(biip)]_2\}_n.4nH_2O$ (2), $\{Co(ADC)(biip)(H_2O)\}_n$ (3) and $\{(Co)(ADAH)_2(biip)\}_n$ (4) have been synthesized solvothermally by using a common neutral 'N' ligand (biip). 0.5M NaOH was used to deprotonate the carboxylic acids in all concerned syntheses. The synthesis of all four compounds was performed at 120 °C for 5 days including cooling. All the compounds were insoluble in water and stable in air. The composition metal/acid/N-donor linker with a 1:1:1 ratio of the reaction mixtures for compounds 1–4 were executed, in the aqueous medium for compound 1 and 4; and mixed solvent— H_2O (6 ml) and DMF (2 ml) — used for compounds 2 and 3.

5.3.2. Description of Crystal structures

Compound $\{Cu_2(ADA)_2(biip)\}_n.4nH_2O(1)$

The result of crystallographic analysis reveals that compound $\{Cu_2(ADA)_2(biip)\}_n.4nH_2O(1)$ crystallizes in monoclinic space symmetry P2(1)/c. In the relevant crystal structure, the asymmetric unit contains the two crystallographically independent Cu(II) metal ions, two different ADA^{2-} , one biip and four lattice water molecules (Figure 5.1a). As shown in Figure 5.1b, each carboxylate groups of one ADA^{2-} ligand (type I) adopts the bidentate $\mu_2-\eta^1:\eta^0$ coordination mode and other ADA^{2-} (type II) exhibits monodentate $\mu_1-\eta^1:\eta^0$ fashion. In the

crystal structure, Cu1 adopts the formation of {Cu2(COO)4} paddle wheel as a SBU (secondary building unit), in which four oxygen atoms of carboxylate group of type I ADA²⁻ are connected to Cu1 metal ions with Cu-O bond distance in the range of 1.959 to 1.998Å along equatorial positions, nitrogen atom of pyridyl group of biip ligand with a distance of 2.200 Å at one of the apical position and other apical position of paddle wheel is occupied by copper metal atom with a distance of 2.602 Å. In the paddle wheel {Cu₂(COO)₄}, both the cupper atoms are present in the distorted octahedral geometry. In the crystal structure, torsion angle of type I ADA²⁻ is 24.32° viewed through the C1-C2-C13-C14, connected to the paddle wheels with alternating left and right turns of strand along the crystallographically 'a' and 'b' axes to result in the formation of 2D sheets (figure 5.1c). The bond angles around the Cu1 centre are in between 84.84 to 169.06°. In the relevant crystal structure, paddle wheels are separated by the ADA²⁻ with distance of 12.201Å. In this compound, Cu2 is in square planar geometry, which is comprised of two oxygen atoms from two type II acid ligands with the torsion angle of -87.71° (viewed through C15-C16-C27-C28) and two nitrogen atoms of imidazole ring from two different bijp linkers. The connectivity of copper centres with the type II ADA²⁻ leads to the formation of infinite 1D chain (Figure 5.1d). The bond angles around Cu2 centre exists in between 88.38° to 176.23° and these cupper atoms are separated



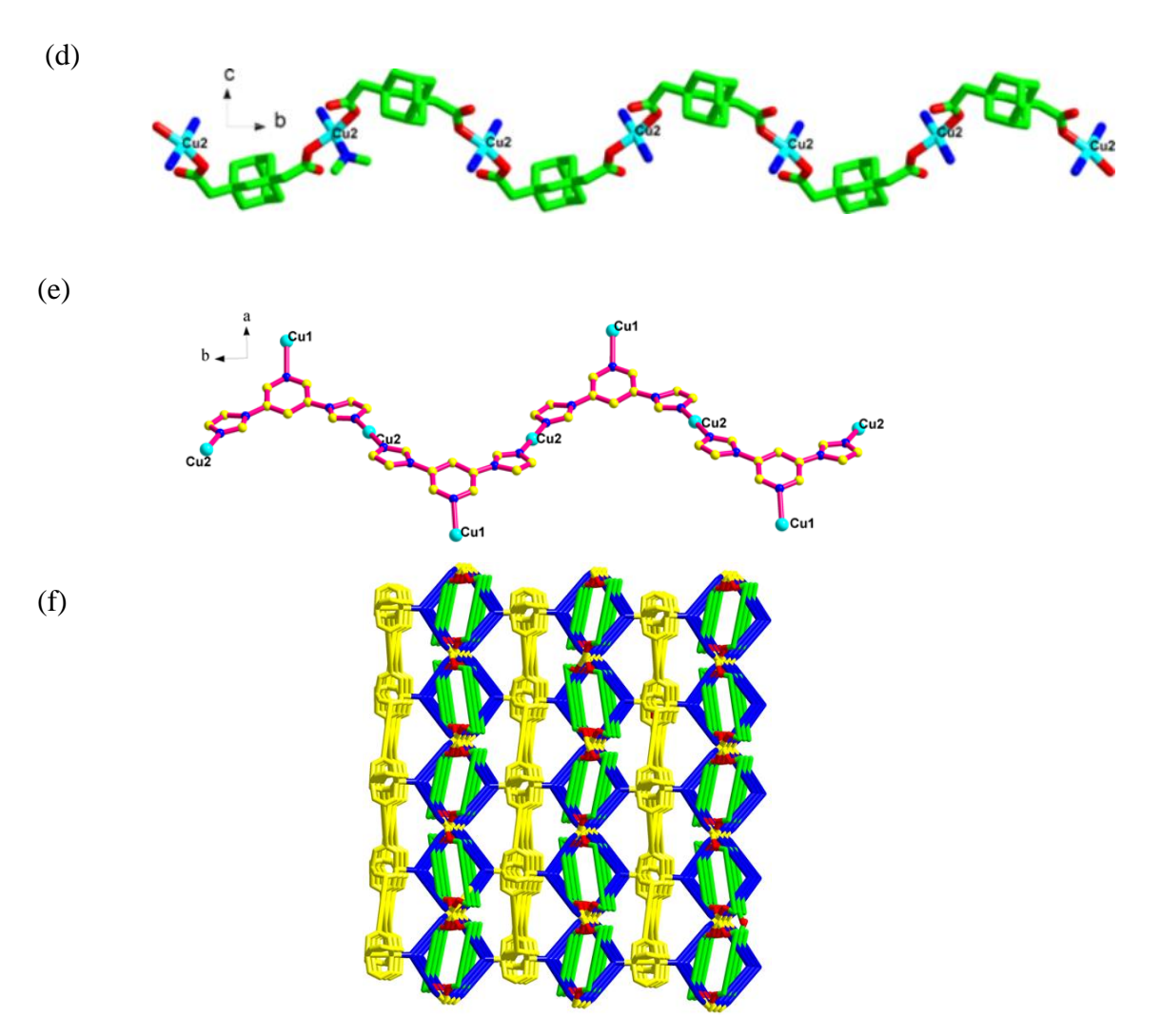


Figure 5.1.Crystal structure of compound $\{Cu_2(ADA)_2(biip)\}_n.4nH_2O$ (1): (a) asymmetric unit; hydrogen atoms are omitted for clarity, (b) conformations of the type I and II ADA^2 -ligands, (c) 2D sheets, formed by the connectivity of paddle wheel $\{Cu_2(COO)_4\}$ and type I ADA^2 - ligand, (d) 1D chain constructed by the connectivity of Cu2 metal centres with type IIADA 2 - ligand, (e) connectivity of copper atoms with the biip linkers and (f) 3D topological representation of 1 in its crystal structure.

with a separation of 9.398Å by the acid ligand having the dihedral angle of 49.62° between two acetate groups. The biip ligand is coordinated to copper metal centres along the crystallographic c axis to form 1D zigzag chain as shown in Figure 5.1e. Interestingly, the connectivity of 2D metal acid sheets and 1D infinite chains through the biip linkers results in the formation of 3D network. In this structure, two nitrogen atoms of imidazole rings from biip ligand coordinated to paddle wheel copper atoms and other nitrogen atom of pyridine moiety from biip is connected to the Cu2 metal centre (Figure 5.1e). Finally, the overall connectivity of acid ligands and biip linkers with the copper metal atoms leads to the formation of extended 3D framework (Figure 5.1f) in the crystals of compound 1.

Compound $\{[(Co)(sdba)(biip)]_2\}_n.6nH_2O(2)$

Single crystal X-ray diffraction analysis of compound **2** reveals that the compound crystallizes in the triclinic space symmetry P-1. As shown in Figure 5.2a, the basic unit consists of two crystallografically independent Co(II) ions, two sdba²⁻ anions, two biip linkers and six lattice water molecules.Co1 and Co2 are four coordinated with distorted tetrahedral geometry composed of two oxygen atoms from two sdba²⁻ (bond distances:Co1-O = 1.962 & 2.012Å and Co2-O = 1.976 & 2.006 Å) and two nitrogen atoms from two biip linkers with bond lengths of Co1-N = 2.026 & 2.028 Å and Co2-N = 2.023 & 2.034 Å. The bond angles are in the range of 96.59 to 124.87° and 95.65 to 127.02° around the metal centres, Co1(II) and Co2(II) respectively. As shown in Figure 5.2b, the carboxylate groups of sdba²⁻ ligands adopts mono dentate μ_1 - η^1 : η^0 coordination mode and these carboxylate groups are coordinated to Co1(II) and Co2(II) with a separation of 13.398Å to result in the formation of

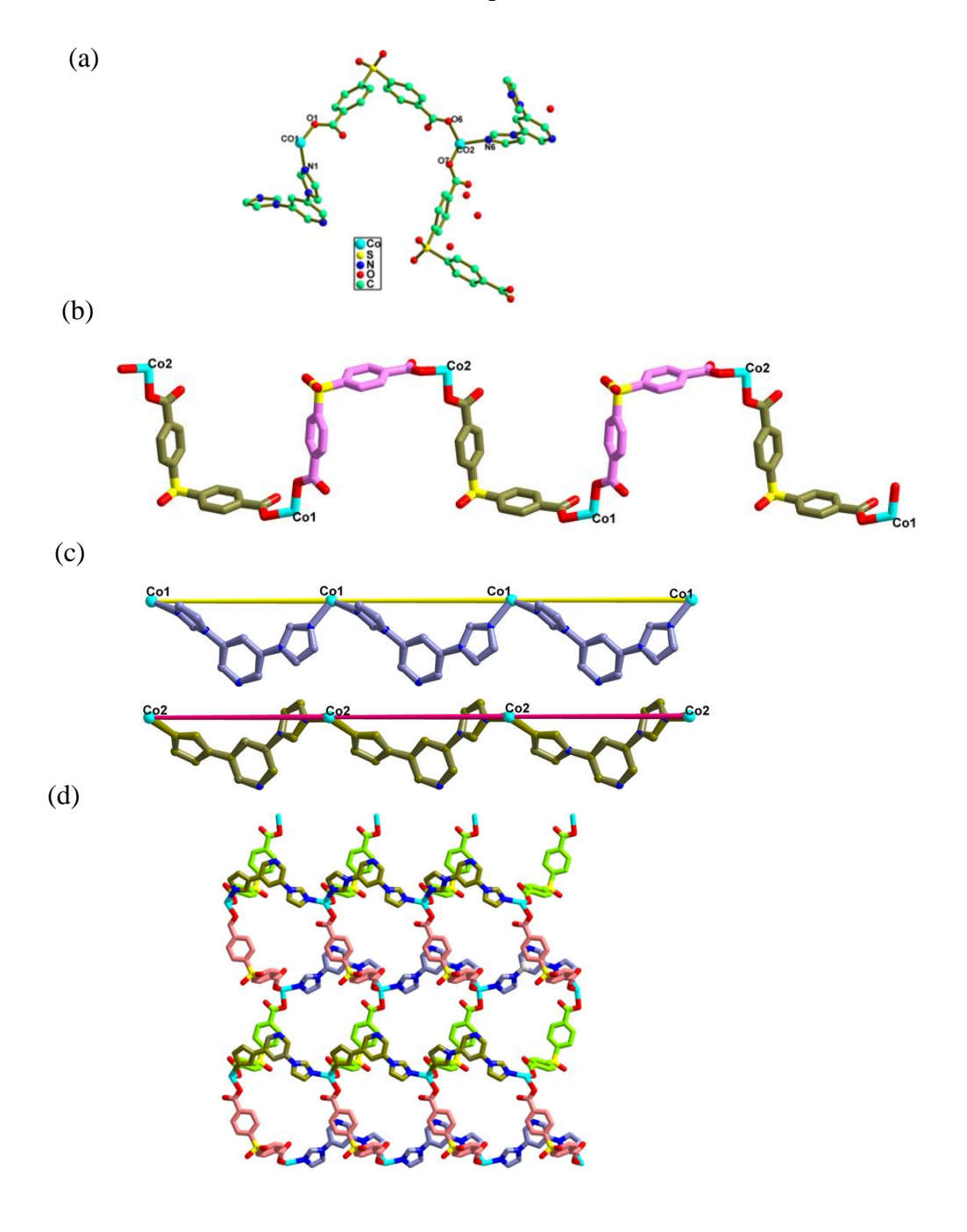
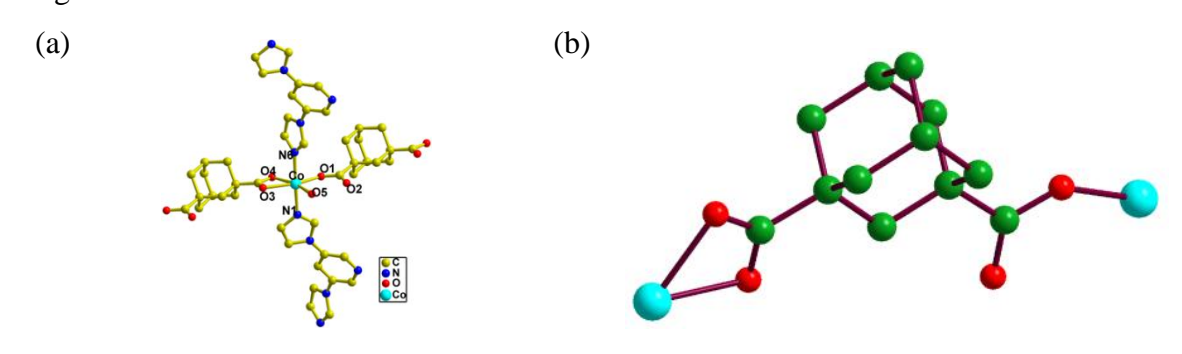


Figure 5.2.Crystal structure of compound $\{[(Co)(sdba)(biip)]_2\}_n.6nH_2O$ (2): (a) the basic unit, (b)1D square-wave like chain constructed by the coordination of $sdba^{2-}$ with the cobalt atoms, (c) 1D chains formed by the coordination of Co1(II) and Co2(II) with biip linkers and (d) 2D structure, formed by the connectivity of $sdba^{2-}$ ligand and biip linker with the cobalt(II) metal centres.

1D square-wave like chain. The rigid biip ligand coordinates to crystallographically independent metal ions, Co1(II) and Co2(II), leading to formation of two metal linker chains as shown in Figure 5.2c. In the crystal structure of compound **2**, overall connectivity of the ligands with the metal ions results in formation of 2D structure (Figure 5.2d).

Compound $\{Co(ADC)(biip)(H_2O)\}_n(3)$

The asymmetric unit in the crystal structure of compound $\{Co(ADC)(biip)(H_2O)\}_n(3)$ consists of one cobalt atom, one ADC²⁻, one biip linker and one coordinated water molecule. A single crystal X-ray diffraction study reveals that the compound 3 crystallizes in the monoclinic space group 'P2(1)/n'. As exposed in Figure 5.3a, the cobalt centre has distorted octahedral geometry, surrounded by three oxygen atoms from two different ADC²⁻ ligands, one oxygen atom from coordinated water molecule and two nitrogen atoms from two bijp linkers to form a [CoN₂O₄] moiety that acts as a secondary building unit (SBU). In the crystal structure, Co-O coordination bond distances are in range of 2.017 to 2.181Å and Co-N bond distances are 2.116 and 2.148Å. The bond angles around the Co(II) metal centre are in the range of 60.32 to 175.23°. One carboxylate group of acid ligand adopts bidentate μ_1 - η^1 : η^1 coordination mode and another carboxylate group adopt mono dentate μ_1 - η^1 : η^0 coordination mode as shown in Figure 5.3b. These carboxylate groups are connected to Co(II) metal centre along crystallographic b axis to results in the formation of 1D linear chain (Figure 5.3c). The cobalt metal centres are separated by the acid ligands with distance of 10.223Å. The 1D chains are further connected by the bijp linkers leading to the formation 2D sheets as shown in Figure 5.3d.





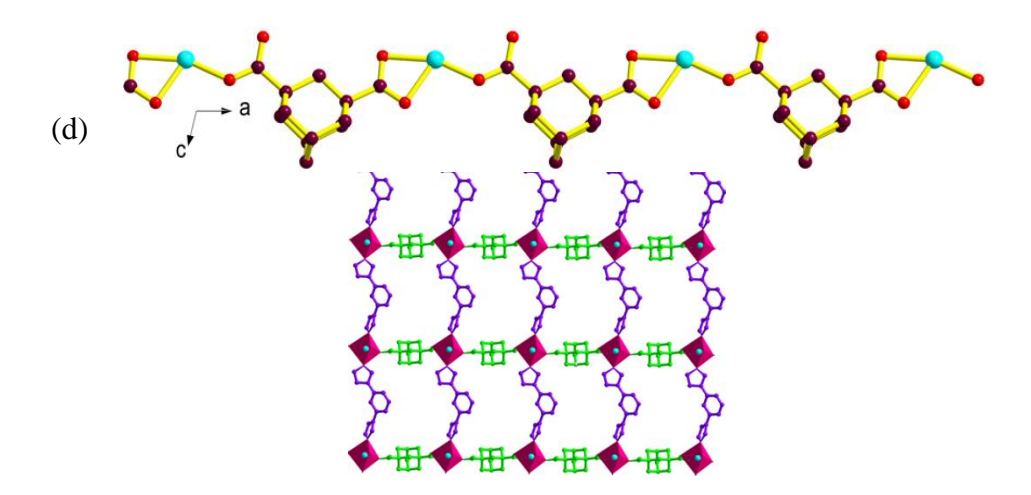
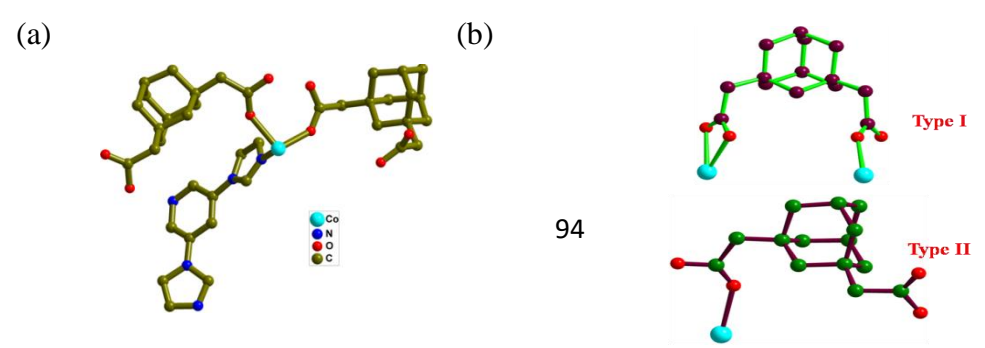


Figure 5.3.Crystal structure of compound $\{Co(ADC)(biip)(H_2O)\}_n$ (3): (a) the molecular structure of compound 3, (b) coordination modes of ADC^2 ligand, (c) 1D linear chain constructed by the coordination of ADC^2 with the cobalt atoms along crystallographic 'b' axis, and (d) 2D network formed by the connectivity of ADC^{2-1} ligand and biip with the cobalt metal centres.

Compound $\{(Co)(ADAH)_2(biip)\}_n$ (4)

The study single crystal X-ray analysis reveals that the compound $\{(Co)(ADAH)_2(biip)\}_n(4)$ crystallizes in triclinic space group 'P-1'. In the crystal structure, the relevant asymmetric unit contains Co(II) metal ion, two ADAH ligands (type I and type II) as shown in Figure 5.4a. In the crystal structure, Co(II) is situated in a special position and thereby the full molecule has a Co(II) center, coordinated by four carboxylates from four ADAH ligands (each ADAH has one uncoordinated hanging carboxyl group) and two nitrogen atoms of imidazole rings from two biip linkers, completing an octahedral geometry around the Co(II) center; this acts as a secondary building unit in the crystal structure. Co-O bond distances are in the range of 2.008 to 2.241Å, Co-N bond distances are 2.074 and 2.104Å. As shown in Figure 5.4b, one carboxylate group of type I ADAH adopts monodentate μ_1 - η^1 : η^1 coordination form and another carboxylate also shows monodentate μ_1 - $\eta^1:\eta^0$ mode, and type II ADAH exhibits monodentate $\mu_1-\eta^1:\eta^0$ coordination type. These type I and type II ADAH ligands are connected to Co(II) metal ion; interestingly, the connectivity of Co(II) ion and type I ADAH ligand, leads to the formation of 20-membered {Co₂(ADAH)₂} macrocycle ring (Figure 5.4c). The biip linkers are coordinated to cobalt metal ion to form another macrocycle {Co₂(biip)₂} ring (Figure 5.4d).



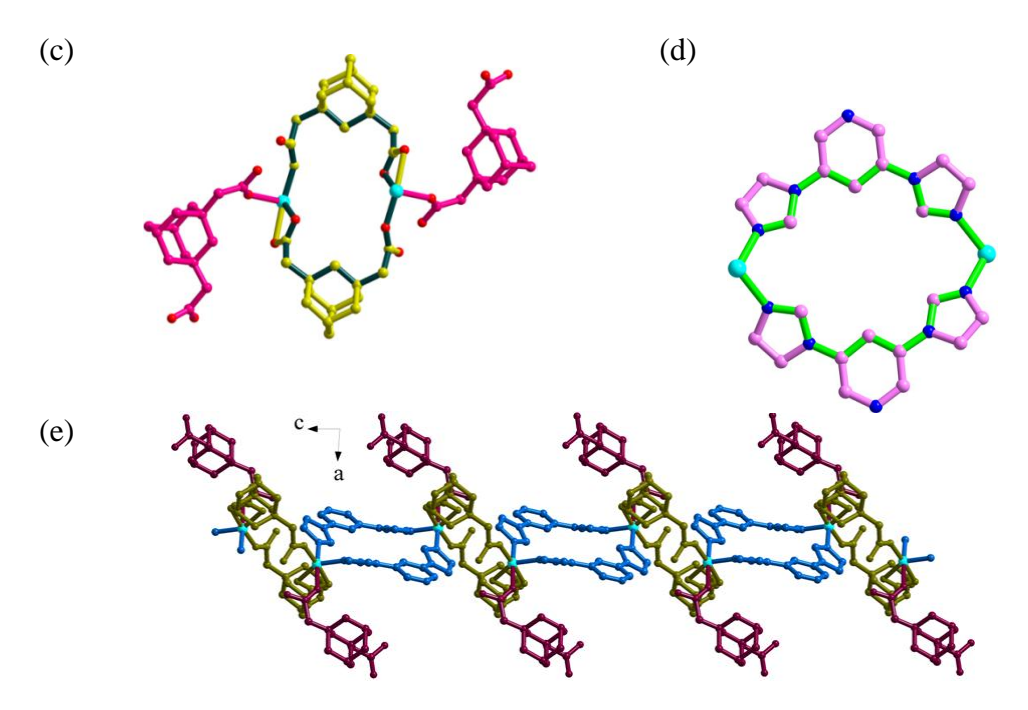
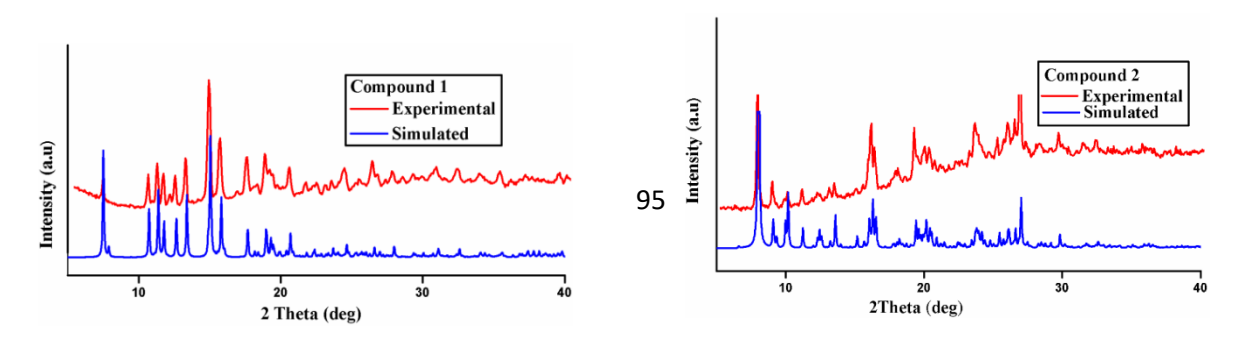


Figure 5.4.Crystal structure of compound $\{(Co)(ADA)_2(biip)\}_n$ (4): (a) The asymmetric unit in the crystal structure, (b) Conformations of acid ligand ADA^{2-} in compound 4, (c) Metal-acid macrocycle $\{Co_2(ADA)_2\}$ ring is generated by the bridging of ADA^{2-} ligands with cobalt metal centres, (d) Representation of macrocycle $\{Co_2(biip)_2\}$ ring, formed by the connectivity of two biip linkers bridged with the Co(II) centres and (e) 1D structure, connectivity of two macrocycle $\{Co_2(ADA)_2\}, \{Co_2(biip)_2\}$ rings through the Co(II) metal ion.

The central Co(II) metal atom is separated by ADAH⁻ and biip ligands with the distance of 10.212 and 6.401Å, respectively. These two macrocycle rings, in the crystal structure, are connected through the cobalt(II) ion resulting in the formation of 1D chain, in which these macrocycles are arranged alternatively as shown in Figure 5.4e.

5.3.3. PXRD Studies and Thermogravimetric Analysis

The X-ray powder diffraction studies have been recorded for compounds 1–4 to ensure the phase purity. Similar diffraction patterns for the simulated data (calculated from single crystal data for all compounds) and observed the data prove the bulk homogeneity of the synthesized crystalline solid materials. All major peaks of the experimental PXRD patterns of compounds 1–4 matches well that of stimulated PXRD patterns, confirming the bulk phase purity of the synthesised compounds as shown in Figure 5.5.



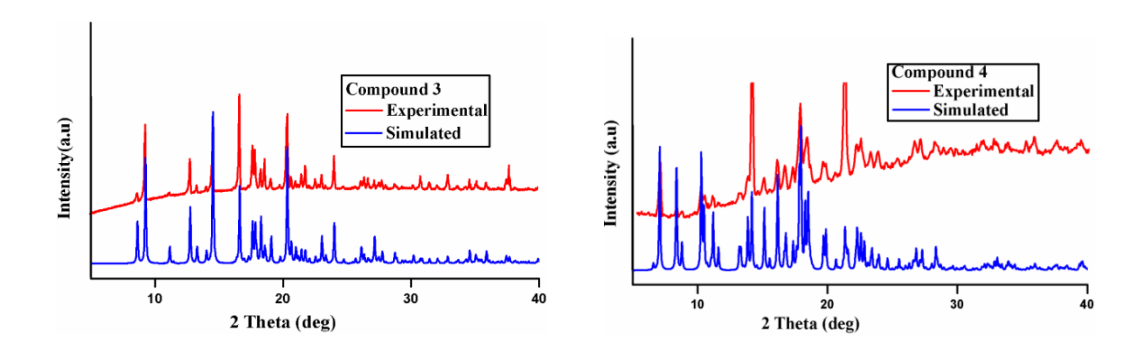
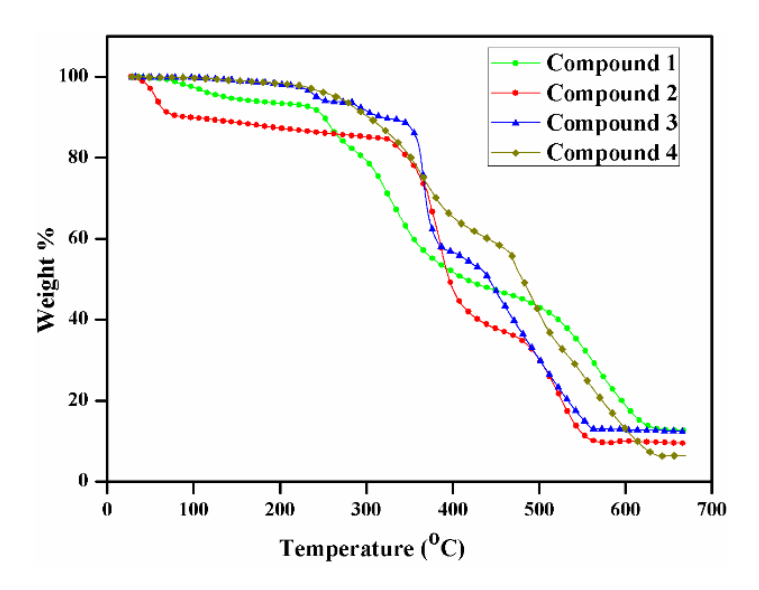


Figure 5. 5. Powder X-ray diffraction patterns of the compounds 1-4.

Thermogravimetric analysis (TGA) plots have been recorded under the flowing of N₂ in the temperature range 30–700 °C for the crystalline compounds 1–4 (Figure 5.6). Compound 1 exhibits thermal stability up to 220 °C with the weight loss of four lattice water molecules (calcd. 7.91%, found 7.26%) and then it undergoes continuous weight loss up to 700°C indicating the decomposition of the organic part i.e., ADA²⁻ and biip. The remaining mass (calcd. 15.14%) above 600 °C is in accordance with the copper oxide (12.62%). TGA curve of compound 2 displays a weight loss of 8.694% (calcd. 8.60%) in region 40-80 °C corresponding to the loss of six lattice water molecules and the relevant crystals remain stable up to 320°C; then the framework collapses in two steps. In the first step, ligand H₂sdba decomposes with a weight loss of 53.86% (calcd. 53.32%) in the temperature range of 330–460 °C and in the second step, bijp moieties come out with weight loss of 27.94% in the range of 480–576 °C; the remaining weight of 9.37% is in accordance with the mass of CoO residue (calcd. 5.96%). The increase in weight designates the partial decomposition at this temperature and complete decomposition at temperatures more than 700 °C. The thermogravimetric curve of compound 3 shows the stability up to 225 °C and then it undergoes continuous weight loss in the temperature range of 230–560°C indicating towards the decomposition of the organic part i.e. sdba²⁻ and biip. The remaining weight is 12.92% according with the CoO residue (12.32%). Compound 4 also follows the same trend as compound 3 and it displays the stability up to 220 °C and then it undergoes a significant continuous weight loss in the temperature range of 220-640 °C attributed to the consecutive loss of ADAH and biip ligands. The remaining weight is in accordance with the CoO residue of 6.26%.



5.3.4. Electronic Properties

Electronic absorption (solid state diffuse reflectance) spectra of compounds **1-4** are recorded at room temperature along with the free ligands as shown in Figure 5.7 The absorption peaks at 692, 499, 232 nm (compound **1**); at 686, 562, 400, 250 nm (compound **2**); at 518, 280 nm (compound **3**) and at 530, 290, 243 nm (compound 4) are observed in the respective spectra. The lower energy bands are attributed to d-d transitions of Cu(II) metal ions in compound **1** and Co(II) metal ions in compounds **2–4**. In all the relevant spectra, the higher energy bands are due to Π – Π * transitions from phenyl groups and n– Π *transitions from imidazolyl moieties, which are analogous with the electronic spectra of the respective free ligands.

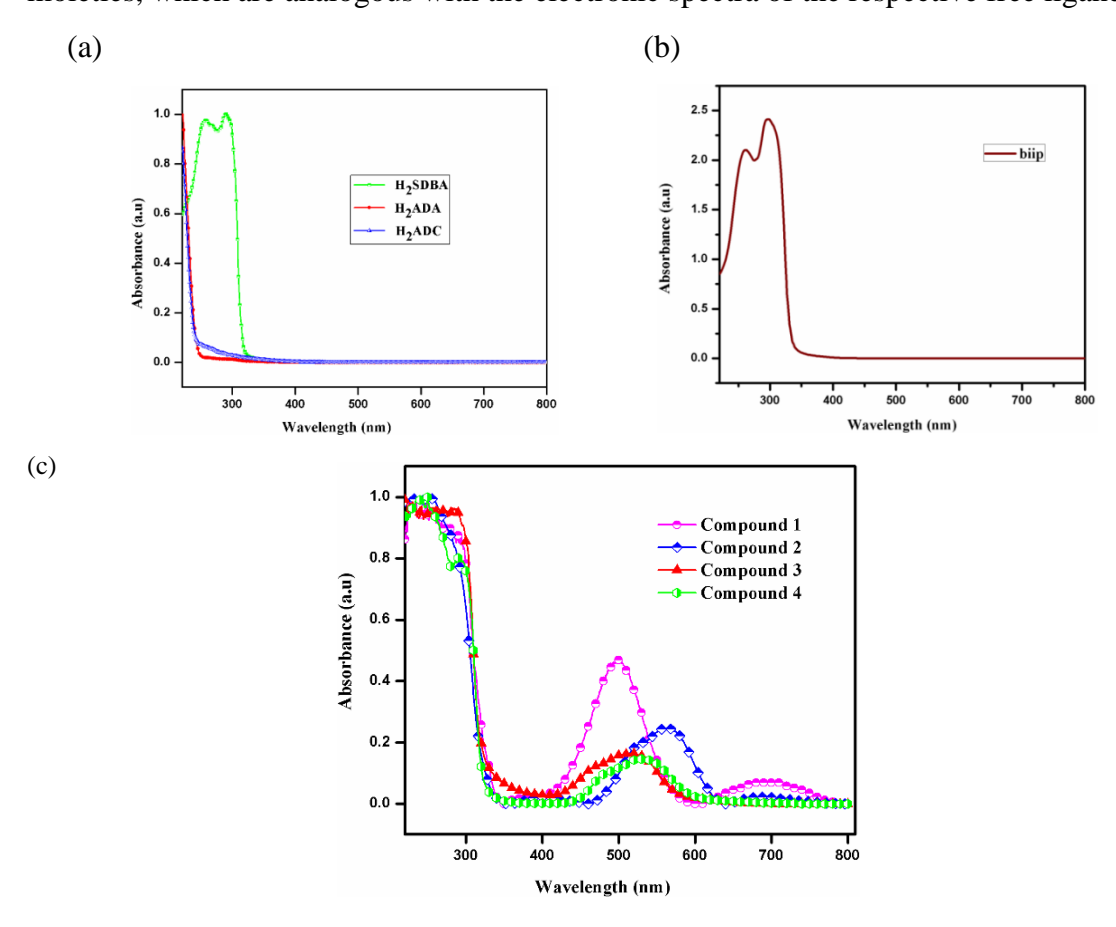


Figure 5.7. Solid state diffuse reflectance (electronic absorption) spectra of the ligands (a) H_2SDBA , H_2ADA , H_2ADC , (b) biip, and (c) compounds **1–4**.

5.4. Conclusion

In summary, we have synthesized four new coordination polymeric compounds $\{Cu_2(ADA)_2(biip)\}_n.4nH_2O$ (1), $\{[(Co)(sdba)(biip)]_2\}_n.4nH_2O$ (2), $\{Co(ADC)(biip)(H_2O)\}_n$ (3) and $\{(Co)(ADAH)_2(biip)\}_n$ (4) by using angular dicarboxylic acids, $H_2ADA = 1,3$ adamantanediacetic acid, H₂ADC = 1,3-adamantanedicarboxylic acid, H₂sdba (4,4'thiodibenzoic acid), and an auxiliary linker, biip {3,5-di(1H-imidazol-1- yl)pyridine}. The compound 1 is a 3D network, formed by the connectivity of two different 2D- and 1Dmetal-acid chains that are further coordinated by the biip linkers. Compound 2 is twodimensional polymer;in this case, square wave-like metal-acid chains are connected by the biip ligand. Compound 3 is also a two-dimensional coordination polymer. In the crystal structure of compound 4, a chainlike arrangement is formed by the connectivity of 20membered metal-acid {Co₂(ADA)₂} ring and another 20-membered metal-N-linker {Co₂(biip)₂} ring through the cobalt(II) resulting in the one-dimensional coordination polymer. The bijp linker plays an important role in the construction of compounds 1-4; in case of compound 1, both the pyridyl nitrogen and imidazol nitrogen are involved, whereas in compounds 2-4, only imidazol nitrogen is participated in the coordination. All the compounds 1-4 are insoluble in common solvents including water. All the compounds are well characterized by single crystal X-ray diffraction analysis, IR spectroscopy, thermogravimetric (TG) and elemental analysis.

 $\textbf{Table 5.1:} \ \textbf{Crystal data and structural refinement parameters for compounds 1-4}$

	1	2	3	4
Empirical formula	C ₃₉ H ₅₃ Cu ₂ N ₅ O ₁₂	$C_{50}H_{46}Co_2N_{10}O_{18}S_2$	C ₂₃ H ₂₅ CoN ₅ O ₅	C ₃₉ H ₄₅ CoN ₅ O ₈
Formula weight	910.95	1256.95	510.41	770.73
$T(K) / \lambda(\mathring{A})$	293(2)/ 0.71073	297(2)/ 0.71073	297(2)/ 0.71073	293(2)/ 0.71073
Crystal system	Monoclinic	Triclinic	Monoclinic	Triclinic
Space group	P 21/c	P -1	P 21/n	P -1
a (Å)	14.4564(3)	11.3698(7)	10.2230(6)	10.5979
b (Å)	18.7051(4)	13.8535(7)	13.1251(7)	12.6971
c (Å)	15.6698(4)	19.4645(12)	16.8036(10)	13.649
α (°)	90.00	89.617(2)	90	79.73
β (°)	104.644(2)	88.479(2)	103.558(2)	85.386
γ (°)	90.00	75.053(2)	90	86.800
Volume (Å ³)	4099.60(16)	2961.1(3)	2191.8(2)	1799.7(7)
Z , ρ_{calcd} (g cm ⁻³)	4, 1.463	2, 1.396	4, 1.547	2, 1.422
μ (mm ⁻¹), $F(000)$	1.105/ 1872	0.707/1268	0.830 /1060	0.538/810
Goodness- of-fit on F ²	1.101	1.139	1.072	0.914
$R1/wR2[I > 2\sigma(I)]$	0.0731/0.2060	0.0661/0.1987	0.0319/0.0755	0.1529/0.3376
R1/wR2 (all data)	0.1074/0.2351	0.0720/0.2032	0.0403/0.0797	0.4000/0.4874
Largest diff	1.422 /-1.087	1.125 /-0.722	0.475 /-0.283	0.976/-0.645
peak/ hole (e Å ⁻³)				

References

- 1. O.M. Yaghi, H. Li, J. Am. Chem. Soc. 117 (1995) 10401.
- 2. Y. He, F. Chen, B. Li, G. Qian, W. Zhou, B. Chen, Coord. Chem. Rev. 373 (2018) 167.
- 3. B. Wang, L.H. Xie, X. Wang, X.M. Liu, J. Li, J.R. Li, Green Energy Environ. 3 (2018) 191.
- 4. J. R. Li, J. Sculley and H. C. Zhou, Chem. Rev. 112 (2012) 869.
- 5.Y. Pan, Y. Qian, X. Zheng, S.Q. Chu, Y. Yang, C. Ding, X. Wang, S.H. Yu, H.L. Jiang, Natl. Sci. Rev. 8 (2021) nwaa224.
- 6. Y. Wen, J. Zhang, Q. Xu, X.T. Wu, Q.L. Zhu, Coord. Chem. Rev. 376 (2018) 248.
- 7. Q.-L. Zhu, Q. Xu, Chem. Soc. Rev. 43 (2014) 5468.
- 8. L. Wang, Y. Han, X. Feng, J. Zhou, P. Qi, B. Wang, Coord. Chem. Rev. 307 (2016) 361.
- 9. P. Horcajada, R. Gref, T. Baati, P.K. Allan, G. Maurin, P. Couvreur, G. Ferey, R.E. Morris, C. Serre, Chem. Rev. 112 (2012) 1232.
- 10. S. Sundriyal, H. Kaur, S.K. Bhardwaj, S. Mishra, K. H. Kim, A. Deep, Coord. Chem. Rev. 369 (2018) 15.
- 11. C. Vaitsis, G. Sourkouni, C. Argirusis, Ultrason. Sonochem. 52 (2019) 106.
- 12. P. Kumar, V. Bansal, K. H. Kim, E.E. Kwon, J. Ind. Eng. Chem. 62 (2018) 130.
- 13. F. Rouhani, F.R. Masuleh, A. Morsali, J. Am. Chem. Soc. 141 (2019) 11173.
- 14. R. Haldar, L. Heinke, C. Woll, Adv. Mater. 32 (2020) No. e1905227
- 15. A.M. Rice, C.R. Martin, V.A. Galitskiy, A.A. Berseneva, G.A. Leith, N.B. Shustova,. Chem. Rev. 120 (2020) 8790.
- 16. Y. Zhao, H. Zeng, X.W. Zhu, W. Lu, D. Li, Chem. Soc. Rev. 50 (2021) 4484.
- 17. Y. Zhao, J. Wang, W. Zhu, L. Liu, R. Pei, Nanoscale. 13 (2021) 4505.
- 18. K. Vikrant, V. Kumar, Y.S. Ok, K.H. Kim, A. Deep, TrAC, Trends Anal. Chem. 105 (2018) 263.
- 19. M.H. Yap, K.L. Fow, G.Z. Chen, Green Energy Environ., 2 (2017) 218.
- 20. G.I. Dzhardimalieva, I.E. Uflyand, RSC Adv. 7 (2017) 42242.
- 21. (a) F. Dai, J. Dou, H. He, X. Zhao, D. Sun, Inorg. Chem. 49 (2010) 4117;
 - (b) G. Li,; J. Lu,; X. Li,; H. Yang,; B. Xu,; R. Cao, CrystEngComm 12 (2010) 3780.
- 22. (a) S. Horike, S. Shimomura. S. Kitagawa, Nat. Chem. 1 (2009) 695;
- (b) N.C. Burtch, T.D. Heinen, D. Bennett, Dubbeldam, M.D. Allendorf, Adv. Mater. 30 (2018) 1704124;
 - (c) S.M.J. Rogge, M. Waroquier, V. Van Speybroeck, Acc. Chem. Res. 51 (2018) 138.

- 23. (a) A. Schneemann, V. Bon, I. Schwedler, I. Senkovska, S. Kaskel, R.A. Fischer, Chem. Soc. Rev. 43 (2014) 6062;
 - (b) S. Horike, S. Shimomura, S. Kitagawa, Nat. Chem. 1 (2009) 695.
- 24. (a) H.-L. Jiang, Q. Xu, Chem. Commun. 47 (2011) 3351;
- (b) F.A.A. Paz, J. Klinowski, S.M.F. Vilela, J.P.C. Tome, J.A.S. Cavaleiro, J. Rocha, Chem. Soc. Rev. 41 (2012) 1088;
- (c) D. Feng, Z.-Y. Gu, J.-R. Li, H.-L. Jiang, Z. Wei, H.-C. Zhou, Angew. Chem., Int. Ed. 51 (2012) 10307;
- (d) D. Feng, W.-C. Chung, Z. Wei, Z.-Y. Gu, H.-L. Jiang, Y.-P. Chen, D.J. Darensbourg, H.-C. Zhou, J. Am. Chem. Soc. 135 (2013) 17105.
- 25. L. Luo, Y. Zhao, Y. Lu, T. Okamura, W.-Y. Sun, Polyhedron 38 (2012) 88.
- 26. Bruker SMART, Version 5.625, SHELXTL, Version 6.12; Bruker AXS Inc.: Madison, Wisconsin, USA, (2000).
- 27. G. M. Sheldrick, Program for Refinement of Crystal Structures; University of Göttingen, Germany, (1997).
- 28. G. M. Sheldrick, Acta Crystallogr., Sect. A: Found. Crystallogr. 64 (2008) 112.
- 29. G. M. Sheldrick, Acta Crystallogr., Sect. C: Struct. Chem. 71 (2015) 3.

Concluding Remarks and Future Scope of the Present Work

Concluding Remarks

This thesis deals with a series of coordination polymers consisting of diverse transition metal ions and a variety of organic ligands. The metal ions include Cu(II), Cd(II) and Co(II) and organic ligands include different bent carboxylic acids, for example [3,3'methylenebis(oxy)dibenzoic acid (3-H₂mboba), 2,2'-(1,3 phenylene)diacetic acid (1,3-H₂pda) and 4,4'-(perfluoropropane-2,2-diyl)dibenzoic acid (H₂hfipbb)]; ditopic V-shaped ligands i.e., H₂oba (4,4'-oxydibenzoic acid), H₂sdba (4,4'-thiodibenzoic acid), H₂hfipbb {4,4'-(perfluoropropane-2,2-diyl)dibenzoic acid} and other flexible carboxylates, H₃tci = tris(2-carboxyethyl)isocyanurate, 1,3-adamantanediacetic acid (H_2ADA) , 1.3adamantanedicarboxylic acid (H₂ADC) and 4,4'-thiodibenzoic acid (H₂sdba). Besides the carboxylates (which get deprotonated during the formation of coordination polymers), the neutral N,N donors have also been employed; some representative N,N linkers are [1,2bis((1H-imidazol-1yl)methyl)benzene] (1,2-bix), N,N'-(1,4-phenylenebis(methylene)) dipyridin-3-amine (px3ampy) and 4,4'-bis((1H-imidazol-1-yl)methyl)biphenyl (bpbix), {3,5-di(1H-imidazol-1-yl)pyridine} (biip), 1,4-bis(triazol-1-yl-methyl)benzene (btx), etc. that act as secondary ligands.

Chapter 2, the first working chapter, describes diverse metallomacrocycles that are constructed from three different dicarboxlylic acids and three different N,N linkers. These metallomacrocycles are of diverse sizes, ranging from 24-membered $\{Co_2(1,2-bix)_2\}$ ring to 28-membered $\{Co_2(3-mboba)_2\}$ ring through bigger 47-membered mixed ligand macrocycle $\{Co_3(hfipbb)(bpbix)_2\}$. Since the relevant compounds having extended structures, formed from these diverse macrocycles, are not soluble in common solvents including water, the system has potential to act as solid hosts to encapsulate the small guest molecules into the cavities of these macrocyles in gas—solid / solid—liquid interface reactions. This implies that this system has potential to function as a solid-state sensor, where the molecules to be sensed can be in vapor state, for example, methanol molecule.

One compound in this chapter, compound $\{Co_2(1,3\text{-pda})(px3ampy)(H_2O)_2\}_n$ contains Co(II)-coordinated water molecule; this can act as the active site for electrocatalytic water oxidation as proposed in the following scheme 1.

Scheme 1. Proposed electrochemical water oxidation scheme (L stands for coordination from coordination polymer)

Chapter 3 has described an unusual interpenetration of 1D chains of a coordination polymer (CP-A) into the 2D layers of another coordination polymer (CP-B) giving rise to an overall three-dimensional inorganic-organic hybrid material. The gas (N_2) adsorption studies of this material are demonstrated. CO_2 adsorption can further be performed to study its CO_2 capture capacity.

Chapter 4 has depicted three coordination polymers, that are again insoluble in common solvents including water. One of these compounds, $\{Cu_2(tci)(btx)_{0.5}(\mu_3-OH)(H_2O)\}_n$ has copper-water coordination and a hydroxyl bridging group. This compound has potential to exhibit electrocatalytic hydrogen evolution reaction (HER). Finally, **chapter 5** has described synthesis and structural characterization four coordination polymers. One of these compounds, $\{Co(ADC)(biip)(H_2O)\}_n$ is again characterized by Co(II)-OH₂ coordination. According to the scheme 1 (shown above), this compound has potential to exhibit electrochemical water oxidation. In this chapter, compound $\{Cu_2(ADA)_2(biip)\}_n$.4nH₂O is three-dimensional network containing material. The gas adsorption studies can be performed on this system.

List of Publications

1. A 'two-in-one' crystal having two different dimensionality in the extended structures: A series of cadmium(II) coordination polymers from V-shaped organic linkers.

Mukara Ramathulasamma, Suresh Bommakanti, Samar K. Das, *Polyhedron*, **2021**, *210*, Article No. 115508.

2. Metallo-macrocycles from a library of flexible linkers: 1D cobalt(II) coordination polymers and a supramolecular pipe,

Paulami Manna, **Mukara Ramathulasamma**, Suresh Bommakanti, Samar K. Das, *Polyhedron*, **2018**, *151*, 394-400.

 Diverse coordination architectures based on a flexible multidentate carboxylate ligand and N-donor linkers: synthesis, structure, supramolecular chemistry and related properties,

Mukara Ramathulasamma, Suresh Bommakanti and Samar K. Das*, Under review in *Polyhedron*.

4. Coordination Polymers from Angular Dicarboxylate- and Imidazol-Ligands: Synthesis, Structure and Supramolecular Chemistry,

Mukara Ramathulasamma and Samar K. Das*, manuscript to be submitted

Posters and Presentations

1. Mukara Ramathulasamma and Samar K. Das.

Diverse coordination architectures based on a flexible multidentate carboxylate ligand and different N-donor linkers: synthesis, structure and properties.

Oral and poster presentation in "CHEMFEST-2017" held at University of Hyderabad, Hyderabad, during 3-4 March, 2017.

2. Mukara Ramathulasamma and Samar K. Das.

A 'two-in-one' crystal having two different dimensionality in the extended structures: A series of cadmium(II) coordination polymers from V-shaped organic linkers.

<u>Poster presentation</u> in "**CPCE-2020**" held at NIT–Jamshedpur, Jharkhand and Virtual National Conference, during 9-10 October, 2020.

Diverse Coordination Motifs Leading to Supramolecular Architectures

by Mukara Ramathulasamma

Submission date: 15-Sep-2022 10:45AM (UTC+0530)

Submission ID: 1900249929

File name: 12CHPH06_phd_thesis_for_plagiarism_check.pdf (6.42M)

Word count: 22896 Character count: 117544

Diverse Coordination Motifs Leading to Supramolecular Architectures

ORIGINALITY REPORT

51%

20%

INTERNET SOURCES

51%

PUBLICATIONS

11%

STUDENT PAPERS

PRIMARY SOURCES

- Mukara Ramathulasamma, Suresh
 Bommakanti, Samar K. Das. "A 'two-in-one'
 crystal having two different dimensionality in
 the extended structures: a series of
 cadmium(II) coordination polymers from Vshaped organic linkers", Polyhedron, 2021
 School of Chemistry
 University of Hyderabad
 Jerobad-500 046, INDIA.
- Paulami Manna, Mukara Ramathulasamma,
 Suresh Bommakanti, Samar K. Das. "Metallomacrocycles from a library of flexible linkers:

 1D cobalt (II) coordination polymers and a
 supramolecular pipe", Polyhedron, 2018 of Chemistry
 University of Hyderabad
 Skdas@uohyd.ac.in
- Submitted to University of Hyderabad,
 Hyderabad
 Student Paper

pubs.rsc.org

2%

Paulami Manna, Bharat Kumar Tripuramallu, Samar K. Das. "Influential Role of Geometrical

15/9/2012

Prof. Samar K. Das School of Chemistry University of Hyderabad '/derabad-500 046., INDIA. skdas@uohyd.ac.in Disparity of Linker and Metal Ionic Radii in Elucidating the Structural Diversity of Coordination Polymers Based on Angular Dicarboxylate and Bis-pyridyl Ligands", Crystal Growth & Design, 2013

Publication

- Paulami Manna, Samar K. Das. "Perceptive % 6 Approach in Assessing Rigidity versus Synthesis, Structure, and Magnetism ar Crystal School of Chemisis School of Chemisis of Hyderabad University of Hyderabad
- Paulami Manna, Bharat Kumar Tripuramallu, Samar K. Das. "Synthesis, Structural Characterization, and Magnetic Properties of a New Series of Coordination Polymers: Importance of Steric Hindrance at the Coordination Sphere", Crystal Growth & Prof. Samar K. Das Design, 2012 School of Chemistry University of Hyderabad ''/derabad-500 046., INDIA. Publication
- skdas@uohyd.ac.in Gulzhian I. Dzhardimalieva, Igor E. Uflyand. <1% "Chemistry of Polymeric Metal Chelates", Springer Science and Business Media LLC, 2018 Publication
- Mukara Ramathulasamma, Suresh Bommakanti, Samar K. Das. "A 'two-in-one' Prof. Samar K. Das School of Chemistry University of Hyderabad yderabad-500 046., INDIA.

skdas@uohyd.ac.in

crystal having two different dimensionality in the extended structures: A series of cadmium(II) coordination polymers from Vshaped organic linkers", Polyhedron, 2021 Publication

<1% www.researchgate.net 10 Internet Source Fang Wang, Xuemin Jing, Bing Zheng, 11 Guanghua Li, Guang Zeng, Qisheng Huo, Yunling Liu. "Four Cd-Based Metal-Organic Frameworks with Structural Varieties Derived from the Replacement of Organic Linkers", Crystal Growth & Design, 2013 "Applications of Metal-Organic Frameworks <1% 12 and Their Derived Materials", Wiley, 2020 Publication Norbert Stock, Shyam Biswas. "Synthesis of <1% 13 Metal-Organic Frameworks (MOFs): Routes to Various MOF Topologies, Morphologies, and Composites", Chemical Reviews, 2011 Publication Arijit Halder, Biswajit Bhattacharya, Rajdip <1% Dey, Dilip Kumar Maity, Debajyoti Ghoshal. "Reversible Phase Transformation in Three Dynamic Mixed-Ligand Metal-Organic Frameworks: Synthesis, Structure, and

Sorption Study", Crystal Growth & Design, 2016

Publication

- Chandan Dey, Tanay Kundu, Bishnu P. Biswal, 15 Arijit Mallick, Rahul Banerjee. "Crystalline metal-organic frameworks (MOFs): synthesis, structure and function", Acta Crystallographica Section B Structural Science, Crystal Engineering and Materials, 2013 Publication
- hdl.handle.net 16 Internet Source

<1_%

< 1%

Bharat Kumar Tripuramallu, Sandip Mukherjee, Samar K. Das. "Mechanistic Aspects for the Formation of Copper Dimer Bridged by Phosphonic Acid and Extending Its Dimensionality by Organic and Inorganic Linkers: Synthesis, Structural Characterization, Magnetic Properties, and Theoretical Studies", Crystal Growth & Design, 2012

Paulami Manna, Mukara Ramathulasamma, 18 macrocycles from a library of flexible linkers: on Paper 1D cobalt(II) coordination polymers and a supramolecular pipe", Polyhedron, 2018 SK DM Publication

Prof. Samar K. Das

Publication

School of Chemistry University of Hyderabad 'yderabad-500 046., INDIA. skdas@uohyd.ac.in

Vedichi Madhu, Samar K. Das. "Neutral 20 coordination polymers based on a metalmono(dithiolene) complex: synthesis, crystal structure and supramolecular chemistry of [Zn(dmit)(4,4'-bpy)]n, [Zn(dmit)(4,4'-bpe)]n and [Zn(dmit)(bix)]n (4,4'-bpy = 4,4'-bipyridine, 4,4'bpe = trans-1,2-bis(4-pyridyl)ethene, bix = 1,4bis(imidazole-1-ylmethyl)-benzene", Dalton

Publication

Transactions, 2011

Wang, X.. "A series of Cd(II) complexes with 21 @p-@p stacking and hydrogen bonding interactions: Structural diversities by varying the ligands", Journal of Solid State Chemistry, 201102

<1%

Publication

Bharat Kumar Tripuramallu, Paulami Manna, Samala Nagaprasad Reddy, Samar K. Das. " Factors Affecting the Conformational Modulation of Flexible Ligands in the Self-**Assembly Process of Coordination Polymers:** Synthesis, Structural Characterization, Magnetic Properties, and Theoretical Studies of [Co(pda)(bix)], [Ni(pda)(bix)(HO)], [Cu(pda) (bix) (H O)] \cdot 8 H O, [Co (μ -OH)(pda)(ptz)] \cdot H O,

<1%

[Co(hfipbb)(bix)], and [Co(2,6-pydc)(bix)] ·4 H O", Crystal Growth & Design, 2011

Publication

pubs.acs.org	<1%
"Handbook on Synthesis Strategies for Advanced Materials", Springer Science and Business Media LLC, 2021 Publication	<1%
Lu Zhao, Feng Guo. "Tuning Structural Topologies of Two Cadmium(II) Coordination Polymers via Isomeric Dipyridyl Ligands: Syntheses, Crystal Structures, and Luminescent Properties", Zeitschrift für anorganische und allgemeine Chemie, 2014 Publication	<1%
baadalsg.inflibnet.ac.in Internet Source	<1%
digitalcommons.wku.edu Internet Source	<1%
patents.justia.com Internet Source	<1%
Submitted to Indian Institute of Science Education and Research (IISER) Bhopal Student Paper	<1%
	"Handbook on Synthesis Strategies for Advanced Materials", Springer Science and Business Media LLC, 2021 Publication Lu Zhao, Feng Guo. "Tuning Structural Topologies of Two Cadmium(II) Coordination Polymers via Isomeric Dipyridyl Ligands: Syntheses, Crystal Structures, and Luminescent Properties", Zeitschrift für anorganische und allgemeine Chemie, 2014 Publication baadalsg.inflibnet.ac.in Internet Source digitalcommons.wku.edu Internet Source Submitted to Indian Institute of Science Education and Research (IISER) Bhopal

Mürsel Arıcı, Okan Zafer Yeşilel, Necmi Dege.
"Three Co(II) coordination polymers
constructed from 2,5-di(4-pyridyl)thiazolo[5,4-d]thiazole and V-shaped dicarboxylic acids:
Syntheses, characterizations, structural diversity and optical properties", Polyhedron, 2019

<1%

Publication

Ying Zhao, Xin-Hong Chang, Guang-Zhen Liu, Lu-Fang Ma, Li-Ya Wang. "Five Mn(II) Coordination Polymers Based on 2,3',5,5'-Biphenyl Tetracarboxylic Acid: Syntheses, Structures, and Magnetic Properties", Crystal Growth & Design, 2015

<1%

Publication

Liang, Lingling, Ronglan Zhang, Jianshe Zhao, Chiyang Liu, and Ng Seik Weng. "Two actinide-organic frameworks constructed by a tripodal flexible ligand: occurrence of infinite {(UO2)O2(OH)3}4n and hexanuclear {Th6O4(OH)4} motifs", Journal of Solid State Chemistry, 2016.

<1%

Publication

Paulami Manna, Bharat Kumar Tripuramallu, Suresh Bommakanti, Samar K. Das.
"Synthesis, characterization and magnetism of metal–organic compounds: role of the positions of the coordinating groups of a

<1%

meso-flexible ligand in placing anisotropy to exhibit spin-canting behaviour", Dalton Transactions, 2015

Publication

- Rashmi A. Agarwal, Arshad Aijaz, Carolina
 Sañudo, Qiang Xu, Parimal K. Bharadwaj. "Gas
 Adsorption and Magnetic Properties in
 Isostructural Ni(II), Mn(II), and Co(II)
 Coordination Polymers", Crystal Growth &
 Design, 2013
 Publication
- www.frontiersin.org
 Internet Source

 "Advanced Structural Chemistry", Wiley, 2021
 Publication

 Guo-Bi Li, Jun-Min Liu, Yue-Peng Cai, Cheng-Yong Su. "Structural Diversity of a Series of Mn(II), Cd(II), and Co(II) Complexes with Pyridine Donor Diimide Ligands", Crystal Growth & Design, 2011
 Publication

 C1 %

<1%

Bei Lv, Xiaofang Wang, Huai-Ming Hu, Yi-Fan Zhao, Meng-Lin Yang, Ganglin Xue. "Synthesis, structure and luminescent sensor of zinc coordination polymers based on a new functionalized bipyridyl carboxylate ligand", Inorganica Chimica Acta, 2016

Jiamei Yu, Lin-Hua Xie, Jian-Rong Li, Yuguang <1% Ma, Jorge M. Seminario, Perla B. Balbuena. " CO Capture and Separations Using MOFs:

Computational and Experimental Studies ", Chemical Reviews, 2017

Publication

Naik, Indravath Krishna, Rudraditya Sarkar, 51 and Samar K. Das. "Bis(quinoxalinedithiolato)nickel(III) Complexes [Bu4N] [NillI(6,7-qdt)2] and [Ph4P][NillI(Ph26,7qdt)2]·CHCl3 (6,7-qdt = Quinoxaline-6,7dithiolate; Ph26,7-qdt = Diphenylquinoxaline-6,7-dithiolate): Synthesis, Spectroscopy, Electrochemistry, DFT Calcula: Bis(quinoxaline-dithiolato)nickel(III) Complexes", European Journal of Inorganic Chemistry, 2015. Publication

<1%

www.science.gov 52 Internet Source

Suresh Bommakanti, Uppari Venkataramudu, 53 Samar K. Das. "Functional Coordination Polymers from a Bifunctional Ligand: A Quantitative Transmetalation via Single Crystal to Single Crystal Transformation", Crystal Growth & Design, 2018 Publication

<1_%

Zhao-Feng Wu, Bin Tan, William P. Lustig, Ever 54 Velasco, Hao Wang, Xiao-Ying Huang, Jing Li. "Magnesium based coordination polymers: Syntheses, structures, properties and

<1%

applications", Coordination Chemistry Reviews, 2019

Publication

scholar.sun.ac.za

Exclude quotes

Exclude matches 14 words

Exclude bibliography On-



SCHOOL OF CHEMISTRY

UNIVERSITY OF HYDERABAD, HYDERABAD - 500046

Ph.D COURSE WORK RESULTS

Name of the Scholar: M. Ramathulasamma

Name of the Supervisor: Prof. S.K. Das

Reg. No.: 12CHPH06

Sl. No.	Course No.	Title of the Course	Number of Credits	Grade
1	CY-801	Research Proposal	3	A
2	CY-806	Instrumental Methods B	3	В
3	CY-810	Basic Concepts in Coordination Chemistry	3	C
4	CY-820	Main Group and Inner Transition Elements	3	В

Final Result: Passed

Date: 07.03.2017

Dean

School of Chemistry

Dean

SCHOOL OF CHEMISTRY

University of Hyderabad Hyderabic if 0 046.